Development of gadolinium doped ceria (GDC) electrolytes and effects of lutetium (Lu) addition for intermediate temperature solid oxide fuel cell (IT-SOFC) applications

By

Muzammal Zulfqar

Reg. #: NUST201463531MCES64114F

Session 2014-2016

Supervised by

Dr. Zuhair S. Khan

A Thesis Submitted to the Centre for Energy Systems in partial fulfillment of the requirements for the degree of MASTERS of SCIENCE in ENERGY SYSTEMS ENGINEERING

US-Pakistan Center for Advance Studies in Energy (USPCAS-E)

National University of Sciences and Technology (NUST)

H-12, Islamabad 44000, Pakistan

March 2017

Certificate

This is to certify that work in this thesis has been carried out by **Mr. Muzammal Zulfqar** and completed under my supervision in Advanced Energy Materials and Fuel Cells laboratory, Centre for Energy Systems, National University of Sciences and Technology, H-12, Islamabad, Pakistan.

Supervisor: _____

Dr. Zuhair S. Khan
USPCAS-E
NUST, Islamabad

GEC member # 1: _____

Dr. Muhammad Bilal Khan
USPCAS-E
NUST, Islamabad

GEC member # 2: _____

Dr. Naseem Iqbal
USPCAS-E
NUST, Islamabad

GEC member # 3: _____

Dr. Nadia Shahzad
USPCAS-E
NUST, Islamabad

HoD-CES _____

Dr. Zuhair S. Khan
USPCAS-E
NUST, Islamabad

Principal/ Dean _____

Dr. Muhammad Bilal Khan
USPCAS-E
NUST, Islamabad

Abstract

Solid oxide fuel cells (SOFCs) have attracted a great attention due to its higher conversion efficiency, high waste heat utilization, greater fuel flexibility and the ability of environmental friendship. Yttria stabilized zirconia (YSZ) is the common material used as an electrolyte for high temperature solid oxide fuel cells (SOFC). Due to high operating temperature, various design issues arise. Therefore, low to intermediate temperature solid oxide fuel cells (SOFCs) are actively being developed. Ceria based materials are among the best options for intermediate temperature SOFC (500-800˚C).

In the present study, successful synthesis of gadolinium doped ceria (GDC) electrolyte material with a formula $Ce_{1-x}Gd_xO_{2-x/2}$ (x=0.15) was carried out by two different techniques namely sol-gel and co-precipitation. Both techniques have the advantages of high phase purity, homogeneity and low processing temperatures along with strong control on crystallite size. The synthesized materials were characterized by X-ray Diffraction, Scanning Electron Microscopy with EDX etc. We have detected a cubic fluorite structure for both synthesized compounds. The co-precipitation synthesis resulted in better control on crystallite size in comparison to that by sol-gel route. The average particle size was found to be in the range of 40-70 nm. The electrical conductivity of the GDC was measured in the temperature range of 220-660 ˚C in air by using two probe LCR meter. GDC synthesized by sol-gel method was found to have highest conductivity value of 2.45×10^{-4} S/cm at 600 ˚C with activation energy of 0.31 keV.

Moreover, the effects of lutetium (Lu) addition on structure, morphology and electrical properties of gadolinium doped ceria (GDC) electrolyte were investigated. Gd and Lu co-doped ceria $Ce_{0.85}Gd_{0.15-x}Lu_xO_{2-\delta}$ (at x = 0.00, 0.05, 0.075, 0.10 and 0.15) electrolytes were synthesized by solid state reaction method. All the synthesized materials were found to be single phase with cubic fluorite structure. The most intense peak crystallite size was calculated by Scherrer equation for all samples. The elastic strain present in the $Ce_{0.85}Gd_{0.10}Lu_{0.05}O_{2-\delta}$ sample is found to be negligible as compared to singly doped Gd and Lu samples. The grain sizes were examined by SEM images and it is found to be in the range of 30-60 nm. The electrical conductivity as a function of temperature and compositions were measured in air in the temperature range of 200 to 600°C and found to be linearly rising with the

increase in temperature. The electrical conductivity of samples varies with the increase in dopant (Lu) content. The maximum conductivity was observed to be 0.0217 S/cm at 600°C for $Ce_{0.85}Gd_{0.10}Lu_{0.05}O_{2-\delta}$ sample, which is slightly higher than that for pure gadolinium doped ceria $Ce_{0.85}Gd_{0.15}O_{2-\delta}$ and quite higher than for pure lutetium doped ceria $Ce_{0.85}Lu_{0.15}O_{2-\delta}$.

Keywords: IT-SOFC; Conductivity; GDC; Ceria; Co-doping.

I dedicated this thesis to my beloved parents, siblings and teachers.

Table of Contents

List of Figures

List of Tables

List of Journals / Conference papers

Journal article:

Muzammal Zulfqar, Zuhair S. Khan*, Effect of lutetium (Lu) as a co-dopant on structural and electrical properties of gadolinium doped ceria (GDC) electrolyte for IT-SOFC applications, under review in Journal of Electroceramics. (Attached to Annexure II).

Conference Papers:

Muzammal Zulfqar, Muhammad Raza Shah, Zuhair S. Khan*, "Investigations on Gadolinium doped Ceria (GDC) electrolyte prepared via sol-gel and co-precipitation routes for intermediate temperature solid oxide fuel cell (IT-SOFC) applications", 4th International Conference on Energy, Environment and Sustainable Development 2016 (EESD 2016). (Attached to Annexure I).

Muhammad Raza Shah, Muzammal Zulfqar, Zuhair S. Khan* "Inorganic-Organic Nano composite hybrid electrolyte membrane based on Titania and Polystyrene for High Temperature PEM Fuel Cell", 4th International Conference on Energy, Environment and Sustainable Development 2016 (EESD 2016).

List of abbreviations

ITSOFC	Intermediate temperature solid oxide fuel cell
LTSOFC	Low temperature solid oxide fuel cell
PEMFC	Polymer electrolyte membrane fuel cell
AFC	Alkaline fuel cell
MCFC	Molten carbonate fuel cell
PAFC	Phosphoric acid fuel cell
GDC	Gadolinium doped ceria
YSZ	Yttria stabilized zirconia
LGDC	Lutetium gadolinium doped ceria
DC	Direct current
LCR	Inductance capacitance resistance
XRD	X – ray diffraction
SEM	Scanning electron microscopy

Chapter 1
Introduction

1.1 Background

As energy is the most important constituent for social and economic development, it is important to know about the production and the utilization of energy. From the beginning until now, fossil fuels like wood, coal, petroleum and natural gas are the main energy sources in different sectors mainly heating and transportation [1]. According to World Energy Council (WEC), the world population will be increased to approximately 8.1 billion in 2020 [2]. As the population increases day by day, so there is a need to make strong efforts to meet increasing energy demands. Thus research has been focused on clean and high efficient energy conversion systems. Conventional energy conversion methods like internal combustion engines and steam turbines have serious drawbacks including high level of pollution and low efficiency due to Carnot limitation [3].

To use fuel directly in internal combustion engine (ICE) have two main disadvantages. One is pollution and the other is low efficiency. Internal combustion engine causes air pollution by emitting various gases like carbon dioxide (CO_2) and nitrogen oxide (NOx) etc. due to incomplete combustion of carbonaceous fuel [4]. From ICE's we cannot get directly electrical energy, due to this it has low efficiency. ICE gives electrical energy in 4 steps, initially from fuel we get chemical energy, then chemical energy converted into heat energy, then heat energy converted into mechanical energy and at the end mechanical energy converted into electrical energy [5]. At every conversion step, there is a loss of energy. To tackle these problems, there is a need of a system or a device which has high efficiency and less pollution. Fuel cell is a device which fulfill these requirements, because it converts chemical energy directly into electrical energy without going through any intermediate steps [6]. Fuel cells particularly solid oxide fuel cell (SOFC) has an electrical efficiency of 55-60 %, due to not involving any intermediate conversion steps [5]. Fuel cells give us a clean energy, when we use pure hydrogen as a fuel and oxygen as an oxidant. Furthermore, fuel cell is a noise free system because it has not any mechanical parts. Thus, fuel cells have significant advantages over conventional energy conversion systems.

1.2 Fuel Cell

Fuel cell is an electrochemical device that converts chemical energy of a fuel directly into electrical energy. In 1839, Sir William Groove operated the first H_2-O_2 fuel cell at room temperature using liquid electrolyte. Sir William fuel cell had three components, anode, cathode and electrolyte. He used dilute sulfuric acid as an electrolyte, hydrogen as a fuel and air as an oxidant. It was Sir William who demonstrated that, electricity can be generated from a chemical reaction by harnessing the electrons [7]. In 1889, Ludwig Mond and Charles Langer named this technique as a fuel cell. In the same year, Nernst used stabilized zirconia as a solid electrolyte to make filament for electrical glowers [8]. Stabilized zirconia after doping with yttrium is still common as a solid electrolyte for solid oxide fuel cells (SOFC). In 1937, Baur and Preis operated the first ceramic fuel cell at 1000 ˚C [9]. Initially space applications are the main use of a fuel cell but it got boost in the mid of 20^{th} century when fuel cell used for transportation and power applications. At the start of 21^{st} century, fuel cells are commercialized and used in electrical vehicles as well as in power applications [5].

1.2.1 Working

A fuel cell consists of mainly three components anode, cathode and electrolyte as shown in fig 1.1. The electrolyte is sandwiched between two porous electrodes namely anode and cathode. The fuel is continuously fed through anode and oxidant through cathode. The presence of an electrolyte avoids the direct mixing of fuel and oxidant. The reaction takes place at triple phase boundary (TPB) where the electrolyte, gas and electrode are interface. At anode, oxidation takes place whereas at cathode reduction occurs [10]. Due to oxidation at anode free electrons are produced which travels through an external wire towards cathode where reduction takes place. Ions are travel through an electrolyte. The main function of a fuel cell is to harness the electrons to get electrical energy. Fuel cell is like a factory and it generates electrical energy as long as the fuel is supplied to it, but it also depends on

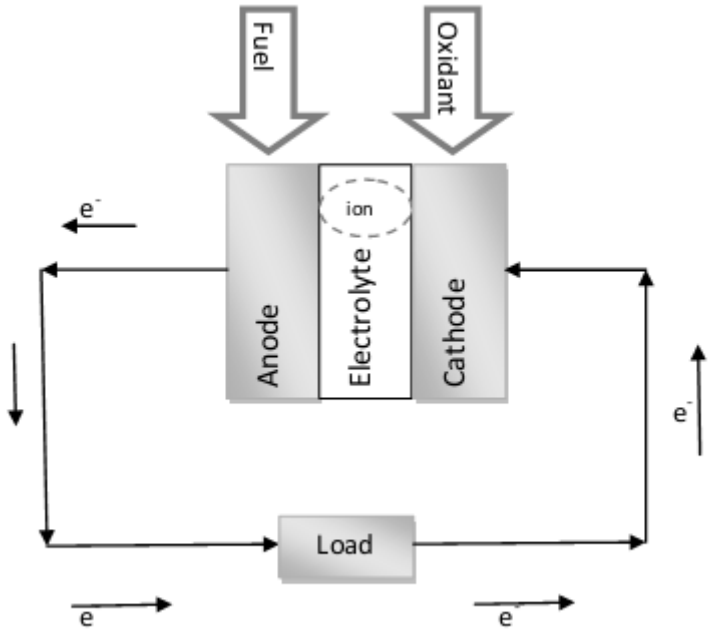

Figure 1. 1: Schematic of fuel cell operation.

the durability of materials [5]. For example, if the fuel cell is solid oxide fuel cell, then at cathode, O^{2-} ions are produced which travels through electrolyte. The electrochemical half reactions are

$$\text{Anode} \quad : \quad 2H_2 + 2O^{-2} \rightarrow 2H_2O + 4e^- \quad \ldots\ldots\ldots\ldots\ldots\ldots 1.1$$

$$\text{Cathode:} \quad O_2 + 4e^- \rightarrow 2O^{-2} \quad \ldots\ldots\ldots\ldots\ldots\ldots 1.2$$

The amount of electricity generated depends upon the reaction surface area, larger the reaction area the greater electricity will be produced. A single cell produces small amount of current. To obtain larger current, a number of cells attached serially using bipolar plates normally referred to as stacking [11].

1.3 Types of fuel cell

After the fabrication of first fuel cell in 1839 by Sir William, various attempts have been made to synthesize different types of fuel cells depending upon fuel and operating temperature. There are five major types of fuel cell which are differentiated by one another on the basis of their electrolyte and working temperature.

1. Polymer Electrolyte membrane fuel cell (PEMFC)
2. Alkaline fuel cell (AFC)
3. Phosphoric acid fuel cell (PAFC)

4. Molten carbonate fuel cell (MCFC)
5. Solid oxide fuel cell (SOFC)

On the basis of their temperature, fuel cells can be divided into two major categories; low temperature and high temperature fuel cell. Molten carbonate and solid oxide fuel cells are high temperature whereas polymer electrolyte membrane fuel cell, alkaline fuel cell and phosphoric acid fuel cell are low temperature fuel cells. All the fuel cells are working on same electrochemical principle [12]. The properties and comparison of all five fuel cells are given in table 1.

For low temperature fuel cell the operating temperature is too low, so direct oxidation of hydro carbon fuel like natural gas cannot occur, therefore methanol and hydrogen are the only fuels for low temperature fuel cells. Low temperature fuel cells used for small scale applications like fuel cell cars and laptops etc. In high temperature fuel cell, natural gas can also be used as a fuel. High temperature fuel cells are used for large scale applications like power generation etc. From table 1.1 we can see that all fuel cells have advantages and disadvantages and can be used for different purposes. Among all, solid oxide fuel cell (SOFC) has distinct advantages like solid electrolyte and high electrical efficiency, so here we discuss solid oxide fuel cell (SOFC) in details.

1.4 Solid Oxide Fuel Cell

Solid oxide fuel cell is a very promising technology for power generation due to its high electrical efficiency and low emission of gases like CO_2, NO_x and SO_x. It has solid ceramic electrolyte which is sandwiched between two porous electrodes. O^{2-} ions are the charge carrier that travels through cathode to anode. It is operated in the temperature range of 600-1000 ˚C. Due to solid electrolyte, corrosion issues are not important. It has phosphoric acid fuel cell, very long life time expectancy (40000 - 80000 h). Due to high

Table 1. 1 Properties of fuel cells [5, 10 and 12]

Properties	**PEMFC**	**PAFC**	**AFC**	**MCFC**	**SOFC**
Electrolyte	Polymer membrane	Liquid H_3PO_4 (immobilized)	Liquid KOH (immobilized)	molten carbonate	Ceramics (YSZ),(GDC)
Electrodes	Carbon	Carbon	Platinum	Nickel and NiO	Ceramic based
Operating Temperature	80 ˚C	200 ˚C	60-260 ˚C	650 ˚C	600-1000 ˚C
Charge Carrier	H^+	H+	OH^-	CO_3^{2-}	O^{2-}
Catalyst	Platinum	Platinum	Platinum	Electrode material	Electrode material
Interconnect	Metal	Graphite	Metal	Stainless steel or Nickel	Nickel, ceramic or Steel
Fuel Compatibility	H_2, Methanol	H_2	H_2	H_2, CH_4	H_2, CH_4, CO
CO Tolerance	Poison (<50 ppm)	Poison (<1%)	Poison (<50 ppm)	Fuel	Fuel
Advantages	Good start - stop properties,	Long term performance, Low cost	Low cost electrolyte,	Fuel flexibility,	Fuel flexibility,
Disadvantages	Expensive platinum catalyst,	Expensive platinum catalyst,	Must use pure fuel,	Corrosive molten carbonate	Sealing issues,
Electrical Efficiency	30 – 40 %	40 %	50 %	45 – 50 %	50 – 60 %

PEMFC: polymer electrolyte membrane fuel cell, AFC: alkaline fuel cell, PAFC:
MCFC: molten carbonate fuel cell, SOFC: solid oxide fuel cell

temperature, it has the advantages of fuel flexibility and gives the high quality heat as byproduct which can use in co-generation applications.

SOFC has many advantages but it also has disadvantages, due to high operating temperature the materials cost is very high, which is the main reason for

commercialization of SOFC. One strategy of cost reduction is to develop low temperature operating materials [6, 11]. This thesis has been focused on the development of low operating temperature electrolyte materials.

1.4.1 Operating Principle of SOFC

In SOFC, a fuel is applied at anode and oxidant at the cathode as shown in Fig 1.2. At cathode, oxidant is electro-reduced and produced O^{2-} ions, which travels through electrolyte towards anode to form a complete reaction.

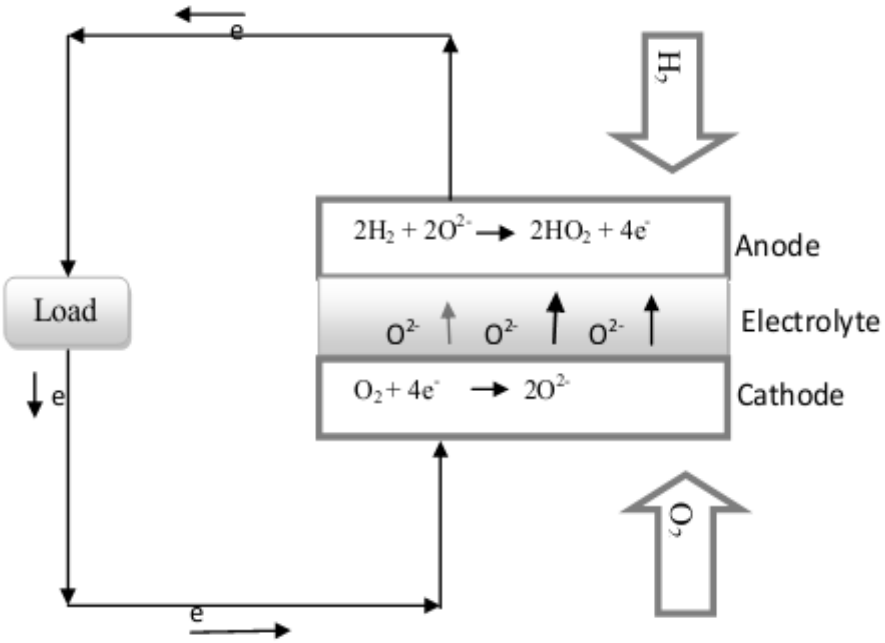

Figure 1. 2: Schematic of an oxide ion conducting solid oxide fuel cell.

The electrochemical half reactions are

Anode : $2H_2 + 2O^{-2} \rightarrow 2H_2O + 4e^-$ ……1.3

Cathode: $O_2 + 4e^- \rightarrow 2O^{-2}$ ……1.4

In SOFC, water is produced at anode rather than at cathode. If we use hydrogen as fuel then the only product is water received at anode. There are four major steps involved in the working of SOFC to generate electrical energy.

1. Reactant delivery at electrodes
2. Electrochemical reaction
3. Transportation or conduction
4. Product removal

First of all, reactant (fuel and oxidant) supplied at both electrodes. It is most important step to produce electricity. A fuel cell can generate electricity as well as fuel is

supplied to it. As the reactant supplied to electrodes, electrochemical reaction starts, which produces ions and electrons. Ions conduct through an electrolyte, whereas electrons conduct through external wire. When the reaction is complete, the last step is to remove the products which are at anode in case of SOFC [5].

The open circuit voltage of a fuel cell can be calculated using Nernst equation,

$$E = E_o - (RT / 2F) \times \ln (p_{oc} / p_{oa}) \qquad (1.5)$$

Where,

E = open circuit voltage

E_o= reversible voltage at standard pressure and temperature

R = Universal gas constant

F = Faraday constant

p_{oc} is the partial pressure of oxygen at cathode and p_{oa} is the partial pressure of fuel at anode.

E_o can be calculated using following equation

$$E_o = \Delta G / 2F \qquad (1.6)$$

Where,

ΔG = Gibbs free energy

The real efficiency of a fuel cell can be calculated as

$$E_{real} = E_{thermo} \times E_{fuel} \times E_{voltage} \qquad (1.7)$$

$$E_{real} = (\Delta G / \Delta H_{HHV}) \times (V / E) \times (1 / \gamma) \qquad (1.8)$$

Where $\gamma = (V_{fuel} / inF)$

If a fuel cell is working on pure hydrogen and oxygen, then the thermodynamically predicted voltage is 1. But the actual value is less than 1 due to polarization losses. There are three types of polarization losses occur, namely anode polarization η_a, cathode polarization η_c and resistance polarization η_r.

$$\eta = \eta_a + \eta_c + \eta_r \qquad (1.9)$$

The polarization depends on cell design, electrode and electrolyte materials and also on operating temperature [5, 8].

1.5 SOFC materials

Synthesized materials must possess standard properties of solid oxide fuel cell. Both the electrodes should have porous so that flow of gases will maximum and also have high electrical conductivity. Electrolyte should be dense so that only ions are passes.

Materials should have close thermal expansion behavior so that thermal stress will be minimized. All the materials should have chemical, mechanical and thermal compatibility at operating temperature [13]. A brief description of anode, electrolyte and cathode is given below.

1.5.1 Anode

A promising SOFC anode material should have electrical conductivity of 100 S / cm or higher [13]. Ni – YSZ cermet is a very common material for SOFC anode. It has very high electro catalytic activity and also high current collection capability. The electrical conductivity of Ni – YSZ cermet is in the range of 10^2 S/cm. But nickel toxicity, redox instability and carbon deposition are the drawbacks of this material [6]. Cu replaces Ni as an anode material because it is inactive to carbon deposition. But, the melting point of Cu is very low (1083 ˚C) as compared to Ni, so it is not possible to sintering at high temperature. Cu – CeO_2 composite is very promising anode material in the temperature range of 700 – 1000 ˚C. In this anode material, Ceria acts as oxidation catalyst, whereas Cu gives electronic conductivity [14]. Perovskite based anodes like $SrLaTiO_3$ were also developed to minimize sulfur poisoning. Every type of anode has its own advantages and disadvantages, but $SrMgMoO_{6-\&}$ and La doped $SrMgMoO_{6-\&}$ anode shows very promising power density and improved sulfur and carbon tolerance [15].

1.5.2 Electrolyte

An electrolyte which is also called the heart of a fuel cell, conduct oxide ions from cathode to anode and completes an electrochemical reaction. Metal oxides which have large inter ionic open structure like ZrO_2, CeO_2, Bi_2O_3 and $LaGaO_3$ based peovskites are used as an electrolyte material for SOFC. A promising electrolyte material for SOFC should have oxide ion conductivity of 0.1 S / cm and low electronic conductivity $<10^{-3}$ [17]. YSZ is the state of art material for SOFC electrolyte which operates at 1000 ˚C. At high operating temperature, there are various issues like sealing and long start up time etc [13]. To overcome these problems, Ceria based materials are used for development of SOFC electrolyte. Pure ceria has low ionic conductivity but it can be increased by doping with some rare earth or alkaline earth materials [14]. Among all rare earth elements SDC and GDC showed highest ionic conductivity. In alkaline earth metals, calcium doped ceria showed prominent results. Both alkaline earth and rare earth were also used as co-dopants with ceria for SOFC

electrolyte [15]. This research is focused on the development of low temperature solid oxide fuel cell electrolyte, so a detail discussion on low temperature electrolyte will be discussed in chapter 2.

1.5.3 Cathode

The cathode should have high electronic conductivity nearly 100 S / cm and stability in oxidizing atmosphere to give better performance [14]. Noble metals were used as cathode material, but they are unsuitable due to their cost and durability. LSM is very common material used for cathode that operates at 1000 ˚C. At low operating temperature, its resistance becomes very high. Two phase cathode is also important which is developed by combining ionic conducting material with electronic conducting material. LSM – YSZ composite is an example of two phase cathode material, which operates relatively low temperature [13]. $La_{0.70}Sr_{0.30}$ $CoO_{3-\delta}$ (LSC) is a very promising cathode material and has high electronic and ionic conductivity over a long temperature range. But LSC showed high ohmic resistance when it reacts with ZrO_2 electrolyte. To prevent this reaction a CeO_2 interface layer placed between LSC cathode and ZrO_2 electrolyte [15]. Another composite cathode $Sm_{0.5}Sr_{0.5}Co_3O_4$ showed promising results at 600 ˚C [16]. Researchers are trying to find a suitable cathode material which operates at low temperature and gives maximum active sites for electrochemical reaction.

1.5.4 Interconnects

A single SOFC produces a small current. To produce larger current SOFCs are attached in series with the help of interconnects. The main function of interconnect material is to provide connections between the anode of one cell and to the cathode of other neighboring cell and so on. Due to very high operating temperature, high stable interconnect materials must be used. Ceramic and metallic type materials are used for high and intermediate temperatures, respectively. In ceramic, Sr doped $LaCrO_3$ is a common material used for interconnects [6]. Doped lanthanum chromite is a very promising material, but high cost is the major issue for commercializing it. Chromium based alloys are used for interconnect materials due to their low oxidation resistance [19]. Iron based alloys are used for planer type intermediate temperature SOFC. Iron based alloys are preferred over chromium based alloys due to high ductility and low cost [20].

1.6 Current issues in SOFC materials

Every component in SOFC has its own challenges, scientists and researchers are trying to overcome these problems. Ni-YSZ cermet is commonly used as an anode material for SOFC, but it causes Ni grain agglomeration, carbon deposition, sulfur poisoning and Ni toxicity [18]. Similarly, surface diffusion and charge transfer at triple phase boundary are the major issues for SOFC anode [13]. Various efforts are made to overcome these Ni based anode material issues, but still there is a lot of remaining to resolve. Similarly, YSZ is the common material for electrolyte operating at 800 – 1000 ˚C causes many problems. Various attempts have been made to develop new electrolyte materials that operate at low temperature. For example, ceria based electrolytes are operated at low temperature, but ease of O^{2-} conduction, lattice strain, grain boundary conductivity and durability are still main issues to resolve [14]. For cathode, initially noble metals were used, but due to high cost and low stability, their uses become negligible. LSM is the state of art material for SOFC cathode, but its operating temperature was very high, which results in high electrode resistance at lower temperature. Existence of overpotential and geometry of active surfaces are the current challenges of SOFC cathode [15]. Chemical inaptness in both oxidizing and reducing environments and matching the coefficient of thermal expansion (CTE) in interconnects are also the main issues in SOFC technology [14]. In this thesis, we are trying to resolve the electrolyte problems by developing ceria based electrolytes for intermediate temperature solid oxide fuel cell.

Summary

Internal combustion engine (ICE) converts chemical energy of fuel into electrical energy through various intermediate steps. At every conversion step, there is a loss of energy. Whereas, fuel cell is a device that converts chemical energy of a fuel directly into electrical energy without going any intermediate steps. Due to direct conversion fuel cell efficiency is very high as compared to combustion engine. Fuel cell gives clean energy when we use pure hydrogen and oxygen as reactants. There are five major types of fuel cells namely alkaline fuel cell (AFC), polymer electrolyte membrane fuel cell (PEMFC), phosphoric acid fuel cell (PAFC), molten carbonate fuel cell (MCFC) and solid oxide fuel cell (SOFC). Fuel cell working temperature depends on the type of electrolyte. Usually fuel cells are categorized into two main types on the basis of their temperature. AFC, PEMFC and PAFC are termed as low temperature fuel cell, whereas, MCFC and SOFC are termed as high temperature fuel cell. Every fuel cell has mainly three parts namely anode, cathode and electrolyte. There are four major steps to follow for every fuel cell to generate electricity such as reactant delivery at electrodes, electrochemical reaction, transportation or conduction and product removal. Solid oxide fuel cell (SOFC) is one of the promising type of fuel cell that gives 55-60 % electrical efficiency which is higher than any other types of fuel cell. SOFC is used for high power applications due to its high efficiency and working temperature.

References

[1] Lucia, Umberto. "Overview on fuel cells." Renewable and Sustainable Energy Reviews 30 (2014): 164-169.

[2] https://www.worldenergy.org/work-programme/strategic-insight/survey-of-energy-resources-and-technologies/2013.

[3] Gupta, Ram B., ed. Hydrogen fuel: production, transport, and storage. Crc Press, 2008.

[4] http://www.newworldencyclopedia.org/entry/Internal_combustion_engine

[5] O'hayre, Ryan, et al. Fuel cell fundamentals. John Wiley & Sons, 2016.

[6] Nesaraj, A. Samson. "Recent developments in solid oxide fuel cell technology-a review." Journal of Scientific & Industrial Research 69.3 (2010): 169-176.

[7] Grove, William Robert. "XXIV. On voltaic series and the combination of gases by platinum." The London and Edinburgh philosophical magazine and journal of science 14.86 (1839): 127-130.

[8] Merewether, Edward Allen. Alternative Sources of Energy: An Introduction to Fuel Cells. US Department of the Interior, US Geological Survey, 2003.

[9] Minh, Nguyen Quang, and Takehiko Takahashi. Science and technology of ceramic fuel cells. Elsevier, 1995.

[10] Appleby, A. John. "Fuel cell handbook." (1988).

[11] Yaqub, Azra, et al. "Preparation via a solution method of La 0.2 Sr 0.25 Ca 0.45 TiO 3 and its characterization for anode supported solid oxide fuel cells." Journal of Materials Chemistry A 1.45 (2013): 14189-14197.

[12] Larminie, James, Andrew Dicks, and Maurice S. McDonald. Fuel cell systems explained. Vol. 2. Chichester, UK: J. Wiley, 2003.

[13] Kawamoto, Hiroshi. "Research and development trends in solid oxide fuel cell materials." QUARTELY REVIW 6 (2008).

[14] Mahato, Neelima, et al. "Progress in material selection for solid oxide fuel cell technology: A review." Progress in Materials Science 72 (2015): 141-337.

[15] Tsipis, Ekaterina V., and Vladislav V. Kharton. "Electrode materials and reaction mechanisms in solid oxide fuel cells: a brief review. III. Recent

trends and selected methodological aspects." Journal of Solid State Electrochemistry 15.5 (2011): 1007-1040.

[16] Sun, Chunwen, Rob Hui, and Justin Roller. "Cathode materials for solid oxide fuel cells: a review." J Solid State Electrochem 14.7 (2009): 1125-1144.

[17] Rękas, M. "Electrolytes for Intermediate Temperature Solid Oxide Fuel Cells." Archives of Metallurgy and Materials 60.2 (2015): 891-896.

[18] Kuhn, Melanie, and Teko W. Napporn. "Single-chamber solid oxide fuel cell technology—from its origins to today's state of the art." Energies 3.1 (2010): 57-134.

[19] Zhu, Wei Zhong, and S. C. Deevi. "Development of interconnect materials for solid oxide fuel cells." Materials Science and Engineering: A 348.1 (2003): 227-243.

[20] Fontana, Sebastian, et al. "Metallic interconnects for SOFC: Characterization of corrosion resistance and conductivity evaluation at operating temperature of differently coated alloys." Journal of Power Sources171.2 (2007): 652-662.

Chapter 2
Ceria based electrolytes for SOFCs

Electrolyte is considered as the heart of a fuel cell, which transport oxide ions from cathode to anode and thus completes the electrochemical half reaction. The main objective of this research is to design a low temperature electrolyte for solid oxide fuel cell (SOFC), so in this chapter we discuss about various types of electrolytes mainly doped ceria electrolytes for SOFCs. The function of an electrolyte is to transmit oxygen ions from one electrode to other (cathode to anode in case of SOFC) [1]. The requirement for a good SOFC electrolyte has oxygen ionic conductivity of 0.1(S/cm). Electrolyte must be fully dense and properly connected with fuel and air electrode [2]. It has negligible electronic conductivity and high ionic conductivity. Electrolyte should not react with electrode materials under operating conditions [22].

2.1 Electrolyte types

There are various types of electrolytes used for SOFCs, but YSZ, Bismuth oxide and Lanthanum gallate are the best known. We discuss here briefly all of these types of electrolytes. Doped ceria is also known as the best electrolyte for low to intermediate temperature solid oxide fuel cell. This thesis is focused on doped ceria electrolyte mainly Gadolinium doped ceria (GDC) and ceria based co-dopant electrolytes. In this chapter, we discuss doped ceria and ceria based co-dopant electrolytes in details.

2.1.1 Yttria Stabilized Zirconia (YSZ)

For SOFC electrolyte, the area of research is focused on cubic fluorite structured oxide, as it has comparatively open structure. The group IVB oxides such as ZrO_2, CeO_2 are the most successful fluorite structure oxides electrolyte when it is doped with some alkaline earth or rare earth oxides [3]. ZrO_2 based electrolyte is the first practical electrolyte, mostly doped with Yttria (Y), which fulfill the requirement of SOFC electrolyte at high temperature. Yttria stabilized Zirconia (YSZ) electrolyte work at 1000 °C or above to achieve better ionic conductivity [4]. Various approaches have been made to enhance the ionic conductivity of YSZ at low temperatures. At 1000 °C, the ionic conductivity of 8YSZ is 0.178S/cm, but at 800 °C, it reduces to 0.052 (S/cm) [8]. By using dispersants the electrical conductivity can be increased. For example, terpineol and lecithin are highly effective dispersants

and electrical conductivity of 8YSZ increased from 0.1 μS/cm to 0.4 S/cm at 1000 ˚C [23]. To lowering the temperature of YSZ electrolyte, reducing the thickness of YSZ membrane required [4]. There are various practical issues and limitations to reducing the size of YSZ electrolyte. At a certain thickness, YSZ works at best, but further reducing the layer has no advantage. Practically, it is difficult to produce a layer which is less than 1μm, without producing cracks in it. When cracks created, then there is cross mixing of gases occur, which lower the power density of fuel cell [5].

2.1.2 Bismuth oxide (Bi_2O_3)

Instead of decreasing the width of the electrolyte, there are other materials that operate at low or intermediate temperatures like Bismuth oxide etc. [4]. Bismuth oxide (Bi_2O_3) has highly open structure, that's why it has highly oxygen ion conductivity nearly 1 (S/cm) at intermediate temperature (i.e. 750 °C). Bismuth oxide co-doping with Yttria and silver (YSB composite) gives the maximum value of conductivity [22]. YSB gives the electrical conductivity value of 0.070 S/cm at 600 °C which is higher as compared to the GDC (0.017 S/cm at 600 °C) [24]. Similarly triple-doped Bi_2O_3 also showed very promising results at 850 °C. Terbium oxide, dysprosium oxide and holmium oxide triple doped with Bi_2O_3 was synthesized by solid state route. The highest electrical conductivity value found to be 1.02×10^{-2} S/cm at 850 °C [25]. The problem with Bi_2O_3 based electrolyte is the reduction of Bi^{3+} to metallic Bi, when there is comparatively high oxygen partial pressure, which in fact devastated the electrolyte [6]. Other problems with Bi_2O_3 are metastable structure below 600 °C, volatilization and low mechanical strength [22]. It gives maximum electrical conductivity than any electrolyte but there is a need to find a suitable dopant with Bi_2O_3 so that these problems are resolved.

2.1.3 Lanthanum gallate

Another electrolyte material is the lanthanum gallate, which is based on a perovskite lattice (ABO_3), instead of a fluorite based lattice (AO_2). Although, it has less open structure than fluorite structure, but the conductivity of "lanthanum strontium gallium magnesium oxide" (LSGM) is higher than zirconia based electrolyte at 800°C. Similarly, the composite of doped lanthanum gallate (LSGM) and doped ceria (SDC) was synthesized by co-precipitation method. The composite exhibits very small grain boundary response as compared to LSGM and SDC and showed the conductivity

value of 0.026 S/cm at 750 °C [26]. The only problem with lanthanum gallate based electrolyte is its high cost [7].

Table 2. 1 Comparison of electrolytes conductivity [22, 23, 31]

Material	Composition	Operating temperature (˚C)	Conductivity (S/cm)
Yttria stabilized zirconia (YSZ)	8 mol % Y_2O_3-ZrO_2	1000	0.03
Bismuth Oxide	$(Bi_{0.096}Sr_{0.05})_{0.85}Y_{0.15}O_{1.5+\&}$	600	0.070
Lanthanum gallate	$La_{0.9}Sr_{0.1}Ga_{0.8}Mg_{0.2}O_{3-\&}$	750	0.026
Gadolinium doped ceria (GDC)	$Ce_{0.85}Gd_{1.5}O_{2-\&}$	600	0.025

2.2 Doped ceria electrolyte

SOFC working at high temperature causes many issues like sealing, long start up time etc., which results in high cost. The objective is to synthesize a low temperature electrolyte to overcome these problems. Ceria is the best option for low to intermediate temperature SOFC electrolyte, when it is doped with some alkaline earth or rare earth materials. Pure ceria has low ionic conductivity and mechanical strength [10]. But, it can be increased when it is doped with some rare earth or alkaline earth materials [9]. In reducing environment, doped ceria is more stable than bismuth oxide (Bi_2O_3). In fact, doped ceria is the best candidate for low temperature SOFC (500 – 800 °C) [4].

When ceria doped with some rare earth, the ionic conductivity can be increased at specific value, and then further doping, results in decreasing the ionic conductivity. When ceria doped with Lanthanum (La), although the ionic conductivity was not increased too much, but highest parameter values can be achieved and it can be decreases along period [11]. Praseodymium doped ceria (PDC) electrolyte was prepared with three methods i.e. co-precipitation, flux and solid state reaction method. In heat treatment, both time and temperature measured until the powder characteristics (morphology, purity etc.) can be achieved. At 5 mol %, Praseodymium doped ceria (PDC) electrolyte gives better result [12]. Neodymium doped ceria (NDC) electrolyte was prepared by a sol-gel method and their structure and ionic

conductivities measured by x-ray diffraction (XRD) and electrochemical impedance spectroscopy (EIS) respectively. At 15 mol %, NDC electrolyte gives the highest grain boundary conductivity of 2.56 (S/m) at 600 °C [13]. Samarium doped ceria (SDC) electrolyte was synthesized by polyol process. Prepared powders and pellets characterized by XRD, EIS and EDS techniques. Various results showed that, SDC-20 sample gives the highest conductivity of 4.29×10^{-2} (S/cm) at 800 °C [11]. Gadolinium doped ceria (GDC) electrolyte was synthesized by thermal decomposition with various concentrations. All samples have fluorite based structure. At 15 mol %, GDC shows the highest conductivity of value 0.025 (S/cm) at 600 °C [15]. Erbium doped ceria (EDC) electrolyte was prepared by self-propagating reaction method at room temperature (SPRT). According to results, EDS has fluorite structure. EDC-15 shows the highest conductivity of value 1.10×10^{-1} (S/cm) at 700 °C [14]. Lutetium doped ceria (LDC) electrolyte was synthesized by reverse micro emulsion method. Structural and morphological properties were characterized by TEM, XRD and Raman spectroscopy [16]. Ytterbium doped ceria electrolyte synthesized and results were measured by transmission electron microscopy (TEM). The results showed that, by doping ytterbium (Yb), the conductivity can decreases due to trapping the oxygen vacancies [31].

By doping alkaline earth metals in ceria, ionic conductivity can be increased. Calcium (Ca) and Strontium (Sr) co-doped with ceria have highest ionic conductivity at low temperature than singly doped with Ca or Sr [32]. Calcium (Ca) and Magnesium (Mg) co-doped with ceria prepared by auto-combustion method. XRD analysis shows that, the sample has fluorite structure. Ca and Mg co-doped ceria electrolyte gives excellent ionic conductivity of value $2.0 * 10^{-2}$ (S/cm) at 700 °C [33]. Mg and Gd co-doped ceria electrolyte (CGM) was synthesized by sol-gel method. The CGM electrolyte gives high open circuit voltage (OCV) and higher maximum power density (MPD) [34]. Sr doping with GDC electrolyte, results in enhancement of grain growth and also reducing the binding energy of lattice. Sr-GDC electrolyte shows the ionic conductivity value of 0.072 (S/cm) at 700 °C [35]. Silver (Ag) and Strontium (Sr) co-doped with GDC were synthesized by the cation complexation technique. By adding Sr in GDC, grain growth rate increased, while adding Ag, grain conductivity can increased. Using co-additives of Sr and Ag, the activation energy of grain conduction can be decreased [36]. From literature, it can be concluded that gadolinium doped ceria (GDC) and samarium doped ceria (SDC) are the most promising candidates for

intermediate temperature (500-800 ˚C) solid oxide fuel cell (SOFC). As this research is focused on GDC, so here we discuss GDC electrolyte in details.

2.2.1 Gadolinium doped ceria (GDC) electrolyte

The main function of ceria doping with rare earth metals is to increase the conductivity value at low temperature. Whenever we synthesize an electrolyte, there are two parameters that always kept in mind, the first one is suitable dopant and other one is concentration. A suitable dopant can find with the help of ionic radius and concentration can be measured by various experiments. Conductivity value mainly depends on the ionic radius, material that has closed the ionic radius with ceria exhibit high conductivity value [28]. According to literature a smaller mismatch in size between host and dopant ion gives maximum value of conductivity. A critical ionic radius for ceria is 1.038Å. Gadolinium Gd^{3+} has the ionic radius of $r^{3+}_{Gd,VIII} = 1.053$ Å. As the Gd^{3+} ionic radius is very close to critical ionic radius of ceria, so that is the reason GDC gives maximum value of conductivity.

Doping concentration is also very important, because at high doping concentration vacancy-vacancy diffusion occur which reduces the conductivity. At 15 mol % GDC shows the maximum value of conductivity. M.G. Chourishiya et al., [30] prepared GDC electrolyte by solid state method showed the conductivity value of 0.1 S/cm at 1023 K and activation energy Ea of 0.9 eV. Xibao Li et al., [31] synthesized GDC by a citrate-nitrate combustion method showed very promising results at low temperatures.

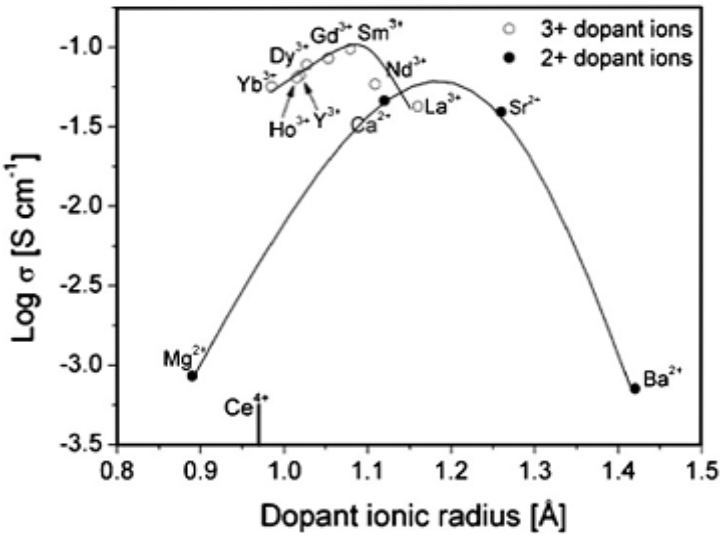

Figure 2. 1 : Ionic conductivity vs. ionic radius [6a]

GDC pellet sintered at 1300 ˚C had relative density of 97 % and conductivity value of 1.27×10^{-2} S/cm at 600 ˚C. The value of lattice parameter increased as the dopant concentration increased [31]. Fernando F. Munoz et al., [32] synthesized GDC by three different methods: template filling, cation complexation and reverse micro emulsion. GDC prepared by template filling method had the largest specific surface area of 97 m^2 g^{-1} and high catalytic activity towards CH_4 oxidation as compared to other two methods [17]. Various techniques have been used to synthesize GDC electrolyte for the sake of high conductivity. In this research, we synthesize GDC electrolyte by three different methods i.e. sol-gel, co-precipitation and solid state methods to analyze the effect of crystal structure, morphology and electrical conductivity.

2.3 Doubly doped ceria electrolytes

According to literature, doubly doped ceria electrolyte gives better performance than singly doped ceria electrolyte. Neodymium doped ceria (NDC) electrolyte co-doped with Lutetium (Lu) was synthesized by solid oxide reaction method. The ionic conductivity was measured by EIS in the temperature range of 250-700 °C. In Lu-NDC, the elastic strain found to be negligible, when compared to NDC or LDC (Lu). At 500 °C, the grain ionic conductivity value of 1.9×10^{-3} (S/cm) was observed [17]. Xuequing sha et al., [3] synthesized lanthanum doped ceria co-doped with Yttrium via sol-gel method. Ionic conductivity was measured in the temperature range of 700-850 °C. The results showed that doubly doped ceria had higher value of conductivity than singly doped ceria electrolyte. Shobit Omar et al., [13] investigated the effect of Neodymium (Nd) on samarium doped ceria (SDC) using solid state method. The ionic conductivity of NSDC composite was found to be 30 % higher than the singly doped SDC or NDC. Form literature it can be concluded that, a co-dopant strategy can lead to increase the ionic conductivity of ceria based electrolyte.

2.3.1 GDC co-dopant electrolytes

As this research is focused on GDC and GDC co-dopant electrolytes, so here we discuss about GDC co-dopant electrolytes. GDC electrolyte co-doped with Praseodymium (Pr) was prepared by Hebb-Wagner polarization technique. The results showed that, the ionic conductivity value of GDC is 5×10^{-4} (S/cm) and the value of GDC co-doped with Pr is 5×10^{-6} (S/cm). So, it can be concluded that gadolinium

and praseodymium co-doped ceria showed high value of conductivity than singly doped GDC and PDC [17]. GDC co-doped with Samarium (Sm) gives the maximum ionic conductivity of value 6.50×10^{-2} (S/cm) at 700 °C [18]. GDC co-doped with five trivalent metals (Sm, Y, Nd, Pr, and La) was prepared by using Pechini method. From these, Sm and Y give better results than others synthesized electrolytes. 3 mol % Sm co-doped with GDC showed very promising results than other co-dopant electrolytes [20]. GDC electrolyte co-doped with (LSGM) was prepared by glycine-nitrate process. The results showed that, GDC-LSGM composite electrolyte gives excellent ionic conductivity [16]. S. Ramesh et al., [8] used sol-gel technique to synthesized GDC-Pr composite electrolyte with this formula Ce_{1-x} $(Gd_{0.5}$ $Pr_{0.5})_x$ O_2 (where x = 0-0.24). Total ionic conductivity was measured by electrochemical impedance spectroscopy (EIS) in the temperature range of 150-700 °C. The GDC-Pr composite showed the conductivity value of 1.059×10^{-2} S/cm at 500 °C with an activation energy 0.62 eV, which is 11 % higher than GDC. According to the best of our knowledge, Lutetium is not co-doped with GDC. In this research study, we synthesize gadolinium and lutetium co-doped ceria (LGDC) electrolytes with three different compositions by solid state method to check the effect of morphology, structure and electrical conductivity.

Objectives of the study

- Synthesis of gadolinium doped ceria electrolytes (GDC) by sol-gel, co-precipitation and solid state reaction methods.
- Synthesis of gadolinium (Gd) and lutetium (Lu) co-doped ceria electrolytes by solid state reaction method.
- Investigation into structural and electrical properties of the prepared ceria based electrolytes.
- Comparative analysis of the physical and electrical properties.

Summary

For SOFC electrolyte, the area of research is focused on cubic fluorite crystal structure as it has comparatively open structure. Yttria stabilized zirconia (YSZ) is one of the first practical electrolyte for SOFC but it has many disadvantages. YSZ works at 1000 ˚C or above to achieve better ionic conductivity. Working at high temperature causes various issues like sealing, long start up time and maintenance problems etc. To overcome these issues, there is a need to develop an electrolyte which works at low temperature. Various attempts have been made to develop an electrolyte which works at low temperature like bismuth oxide etc. Bismuth oxide works at 700 ˚C and gives highest value of conductivity, but the only problem with this, is the reduction of bismuth oxide into metallic bismuth which destroys the whole electrolyte. Ceria is the best option for low to intermediate temperature solid oxide fuel cell. Pure ceria has low ionic conductivity and mechanical strength, but it can be increased by doping with rare earth or alkaline earth materials. Gadolinium doped ceria is one of the most promising electrolyte for SOFC which works at 500 -800 ˚C and gives high value of conductivity. Co-doping strategy is also used for high value of conductivity and mechanical strength. Gadolinium and samarium co-doped with ceria (SGDC) gives the higher value of conductivity than singly doped GDC or SDC.

References

[1] Minh, Nguyen Q. "Ceramic fuel cells." Journal of the American Ceramic Society 76.3 (1993): 563-588.

[2] Badwal, S. P. S., et al. "Review of progress in high temperature solid oxide fuel cells." J. Aust. Cer. Soc 50 (2014): 23-37.

[3] Sha, Xueqing, et al. "Study on La and Y co-doped ceria-based electrolyte materials." Journal of alloys and compounds 428.1 (2007): 59-64.

[4] Ralph, J. M., A. C. Schoeler, and M. Krumpelt. "Materials for lower temperature solid oxide fuel cells." Journal of Materials Science 36.5 (2001): 1161-1172.

[5] Steele, Brian CH. "Ceramic ion conducting membranes." Current Opinion in Solid State and Materials Science 1.5 (1996): 684-691.

[6] Takahashi, Takehiko, and Hiroyasu Iwahara. "Oxide ion conductors based on bismuth oxide." Materials Research Bulletin 13.12 (1978): 1447-1453.

[7] Wolfenstine, J., P. Huang, and A. Petric. "Creep behavior of doped lanthanum gallate versus cubic zirconia." Solid State Ionics 118.3 (1999): 257-259.

[8] Ramesh, S., and KC James Raju. "Preparation and characterization of Ce 1− x (Gd 0.5 Pr 0.5) x O 2 electrolyte for IT-SOFCs." international journal of hydrogen energy 37.13 (2012): 10311-10317.

[9] Steele, Brian CH. "Ceramic ion conducting membranes." Current Opinion in Solid State and Materials Science 1.5 (1996): 684-691.

[10] Mogensen, Mogens, Nigel M. Sammes, and Geoff A. Tompsett. "Physical, chemical and electrochemical properties of pure and doped ceria." Solid State Ionics 129.1 (2000): 63-94.

[11] Dönmez, Göknur, et al. "Polyol Synthesis and Investigation of Ce1− xRExO2− x/2 (RE= Sm, Gd, Nd, La, 0≤ x≤ 0.25) Electrolytes for IT-SOFCs." Journal of the American Ceramic Society 98.2 (2015): 501-509.

[12] Bondioli, Federica, et al. "Nonconventional synthesis of praseodymium-doped ceria by flux method." Chemistry of Materials 12.2 (2000): 324-330.

[13] J. X., Omar, Shobit, Eric D. Wachsman, and Juan C. Nino. "Higher conductivity Sm 3+ and Nd 3+ co-doped ceria-based electrolyte materials." Solid State Ionics 178.37 (2008): 1890-1897.

[14] Stojmenović, M., et al. "Studies on structural, morphological and electrical properties of Ce 1− x Er x O 2− δ (x= 0.05–0.20) as solid electrolyte for IT–SOFC." Materials Chemistry and Physics 153 (2015): 422-431.

[15] Veranitisagul, Chatchai, et al. "Electrolyte materials for solid oxide fuel cells derived from metal complexes: Gadolinia-doped ceria." Ceramics International38.3 (2012): 2403-2409.

[16] Małecka, Małgorzata A., Leszek Kępiński, and Mirosław Mączka. "Structure and phase composition of nanocrystalline Ce 1− xLuxO 2− y." Journal of Solid State Chemistry 181.9 (2008): 2306-2312.

[17] Muñoz, Fernando F., et al. "Effect of preparation method on the properties of nanostructured gadolinia-doped ceria materials for IT-SOFCs." international journal of hydrogen energy 37.19 (2012): 14854-14863.

[18] Li, Xibao, et al. "Synthesis and electrical properties of Ce 1− x Gd x O 2− x/2 (x= 0.05–0.3) solid solutions prepared by a citrate–nitrate combustion method." Ceramics International 38.4 (2012): 3203-3207.

[19] Li, Bin, et al. "Study on GDC-LSGM composite electrolytes for intermediate-temperature solid oxide fuel cells." International Journal of Hydrogen Energy38.26 (2013): 11392-11397.

[20] Kim, Namjin, Byong-Ho Kim, and Dokyol Lee. "Effect of co-dopant addition on properties of gadolinia-doped ceria electrolyte." Journal of Power Sources 90.2 (2000): 139-143.

[21] Omar, Shobit, Eric D. Wachsman, and Juan C. Nino. "A co-doping approach towards enhanced ionic conductivity in fluorite-based electrolytes." Solid State Ionics 177.35 (2006): 3199-3203.

[22] Rękas, M. "Electrolytes for Intermediate Temperature Solid Oxide Fuel Cells." Archives of Metallurgy and Materials 60.2 (2015): 891-896.

[23] Curi, M. O., et al. "Dispersant effects on YSZ electrolyte characteristics for solid oxide fuel cells." Ceramics International 41.5 (2015): 6141-6148.

[24] Xia, C. R., Yuelan Zhang, and Meilin Liu. "Composite cathode based on yttria stabilized bismuth oxide for low-temperature solid oxide fuel cells." (2003).

[25] Gönen, Yunus Emre, Ismail Ermiş, and Mehmet Ari. "Electrical properties of triple-doped bismuth oxide electrolyte for solid oxide fuel cells." Phase Transitions (2016): 1-8.

[26] Mahato, Neelima, et al. "Progress in material selection for solid oxide fuel cell technology: A review." Progress in Materials Science 72 (2015): 141-337.

[27] Hui, Shiqiang Rob, et al. "A brief review of the ionic conductivity enhancement for selected oxide electrolytes." Journal of Power Sources172.2 (2007): 493-502.

[28] Shannon, RD T. "Revised effective ionic radii and systematic studies of interatomic distances in halides and chalcogenides." Acta Crystallographica Section A: Crystal Physics, Diffraction, Theoretical and General Crystallography 32.5 (1976): 751-767.

[29] Chourashiya, M. G., et al. "Studies on structural, morphological and electrical properties of Ce 1− x Gd x O 2−(x/2)." Materials Chemistry and Physics 109.1 (2008): 39-44.

[30] Ye, Fei, et al. "Ionic conductivities and microstructures of ytterbium-doped ceria." Journal of The Electrochemical Society 154.2 (2007): B180-B185.

[31] Jaiswal, Nandini, et al. "Ceria co-doped with calcium (Ca) and strontium (Sr): a potential candidate as a solid electrolyte for intermediate temperature solid oxide fuel cells." Ionics 20.1 (2014): 45-54.

[32] Jaiswal, Nandini, et al. "Effect of Mg and Sr co-doping on the electrical properties of ceria-based electrolyte materials for intermediate temperature solid oxide fuel cells." Journal of Alloys and Compounds 577 (2013): 456-462.

[33] Wang, Feng-Yun, et al. "Study on Gd and Mg co-doped ceria electrolyte for intermediate temperature solid oxide fuel cells." Catalysis Today 97.2 (2004): 189-194.

[34] Roy, Johnson. "The effect of strontium doping on densification and electrical properties of Ce0. 8Gd0. 2O2− δ electrolyte for IT-SOFC application." Ionics18.3 (2012): 291-297.

[35] Horovistiz, A. L., and E. N. S. Muccillo. "Micro structural and electrical characterizations of chemically prepared Ce 0.8 Gd 0.2− x (Ag, Sr) x O 1.9 (0≤ x≤ 0.02)." Solid State Ionics 225 (2012): 428-431.

Chapter 3
Review on synthesis and characterization techniques

There are various routes to synthesize an electrolyte for solid oxide fuel cell. But sol-gel, co-precipitation and conventional solid state are the most promising methods[1]. In this research, we synthesize GDC by sol-gel, co-precipitation and solid state methods. Furthermore, we synthesized lutetium doped ceria and GDC co-doped with Lutetium by solid state reaction method. Here we discuss a brief review on these synthesis methods and characterizations techniques which are used to characterize these electrolytes.

3.1 Wet chemistry route

Wet chemistry route provides a new approach to the preparation of ceramics. The main advantage of this route is allowing a better control in the whole process[2]. Other advantages include homogeneous distribution of precursors, low processing temperature and high purity etc.[3]. Sol-gel, co-precipitation and hydrothermal etc. are the major examples of wet chemistry route. A brief review of sol-gel and co-precipitation is given below.

3.1.1 Sol-gel method

Sol-gel synthesis defines as the synthesis of an inorganic network by a chemical reaction in a solution at low temperature. In other words, a conversion from liquid (solution) into a solid (gel) is called sol-gel synthesis. The word sol-gel consists of two words sol and gel. Sol means dispersions of colloidal solid particles in a liquid. Gel is a continuously interconnected, porous and rigid network which formed after various processes[3]. Preparation of a sample by sol-gel method involves following steps[4].

i. Complexation
ii. Hydrolysis and polycondensation
iii. Gelation
iv. Aging
v. Drying
vi. Densification

Molarity plays an important role in synthesizing a sample. Initially after calculation when the material (precursor) added into water, complexation process starts. The precursor reacts with water and form complex OR substituent's. After stirring of few minutes, the complex metals convert into OH substituent by condensation reactions. At the end of first two process OR and OH substituent's convert into only oxide state network. A gel can be formed by heating the sample at hot plate with continuous stirring. Usually a gel formation occurred within 2 to 3 hours at 70-80 ˚C. After gel formation, aging process is very important. A gel consist of porous network, so to avoid cracking, aging must be required. One or two day aging is enough for any kind of samples. After aging the next step is drying. An aged gel still contains pores. So to removing pores, drying is necessary. After drying, the sample still contains chemisorbed hydroxyls that are not removed at low drying temperature. So heating at high temperature is required. For a ceria based electrolyte, 600-1000 ˚C temperature is required for a suitable time. A schematic flow diagram of sol-gel process is shown in Fig. 3.1.

3.1.2 Co-precipitation method

Co-precipitation method is not much different with sol-gel method. In co-precipitation the focus is on precipitates. A co-precipitation method consists of mainly two steps

i. nucleation
ii. and agglomeration of particles[5].

Starting is same as by sol-gel i.e. mixing of metal precursor with solvent. The important step in co-precipitation is nucleation. In this step, the formation of a large number of small particles will occur. The shape and size of precipitates depends upon the aggregation and also on experimental conditions. The nuclei growth depends on the degree of super saturation[6]. F. Haber et al. [5] stated that the growth rate of nuclei depends on two factors; aggregation velocity and orientation velocity. If the material solubility is very high in solvent, then larger aggregates formed. There must be equilibrium with aggregation and orientation velocity. If the super saturation is very high than aggregation velocity dominates, which results in amorphous material.

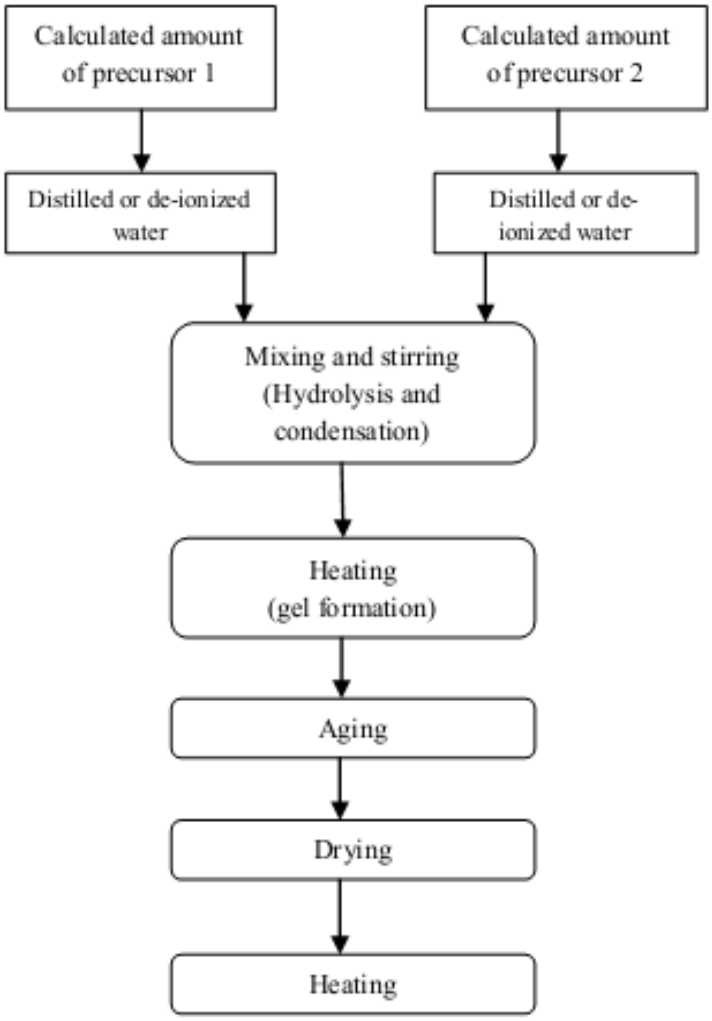

Figure 3. 1. Flow diagram of sol-gel process

Generally, there are three methods used for co-precipitation namely;

i. mixed crystal formation
ii. real co-precipitation
iii. surface adsorption by the precipitate[7].

After precipitate formation, the next step is drying. Then at the end heating at high temperature will be required for removing of chemisorbs hydroxyls. A flow chart of co-precipitation method is shown in Fig. 3.2.

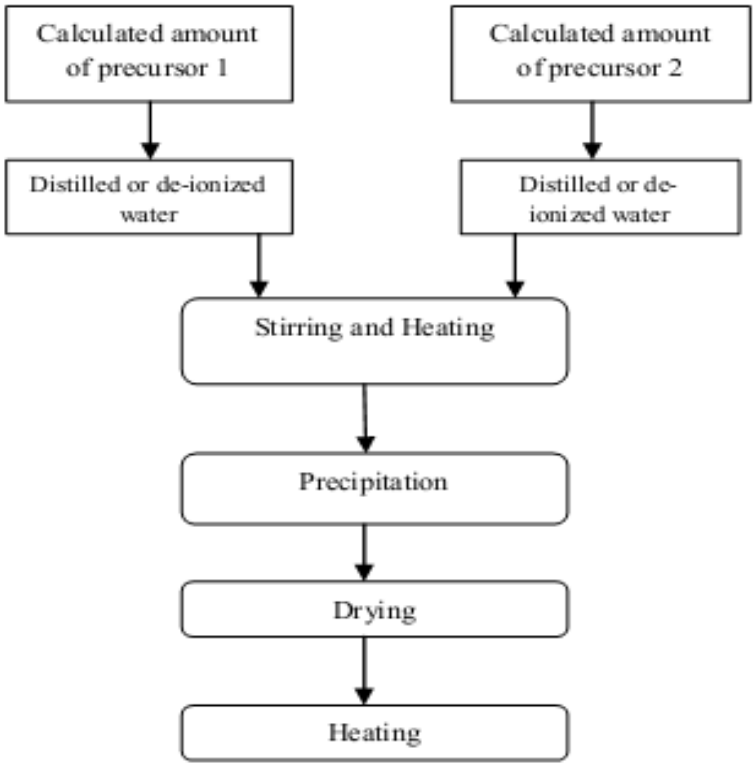

Figure 3. 2. Flow diagram of co-precipitation method

3.2 Solid state method

The simplest and the most used method to synthesize materials is solid state reaction method. In this method solids are mixed and heated at specific temperature for appropriate time to complete a reaction. The first high temperature superconductor was synthesized by this method[8].

According to Fick's first law, small particles can be obtained when the surface contact area is maximum. Tamman's rule stated that a two third of the melting point of the reactant is required to complete a chemical reaction for a specific time[9]. There are many steps to follow for a solid state reaction method.

- First of all, select pure starting materials.
- Used calculated amounts of precursors.
- Grinding is necessary for a homogenizing mixing. For a sample less than 20 g used agate mortar and pestle, where when sample is greater than 20 g use ball mill. Use an appropriate organic solvent in a small amount for a homogenizing mixing.
- By pellitizing powders, the crystallite contact may be increased.
- Reaction temperature can be calculated by Tamman's rule, which we already discussed.

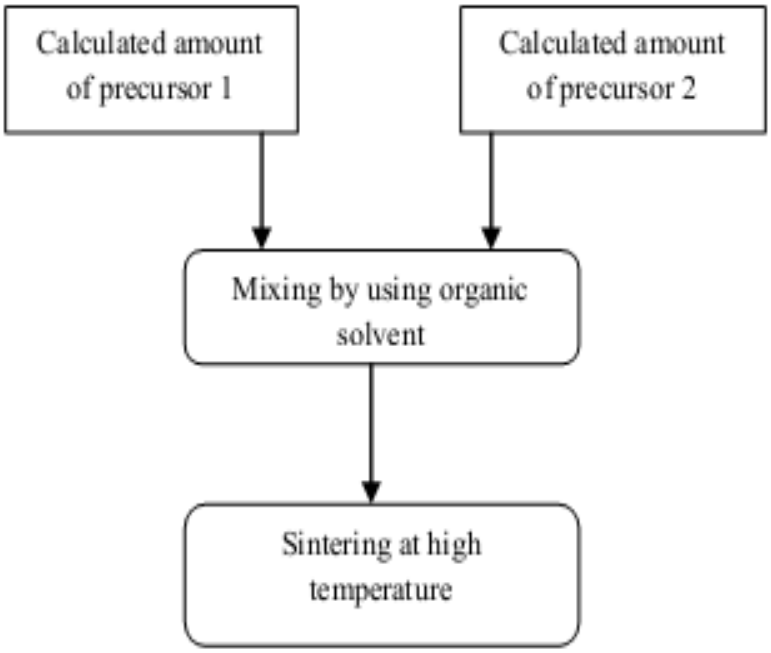

Figure 3. 3 Flow diagram of solid state method

Reaction time depends upon the complete sample reaction[10].

Solid state reaction method has many advantages, but it also has many disadvantages. High purity and high homogeneity is always a problem via solid state method. Due to reaction at high temperature, high energy is required. At high temperature, desired compound may be decomposed. Reaction time is very slow, but it can be increased by increasing the temperature[11]. The flow diagram of solid state method is shown in Fig. 3.3.

3.3 Characterization techniques

There are various techniques which can be used for the characterization of solid oxide fuel cell electrolyte. Here we discussed briefly about X-ray Diffraction (XRD), Scanning electron microscopy (SEM), Energy Dispersive Spectroscopy (EDS) and DC electrical conductivity.

3.3.1 X-ray Diffraction

In 1895, German scientist Roentgen discovered x-rays, but their nature was not known at that time so named as x-rays. X-rays can travel in straight lines like ordinary light and also penetrates in human body, wood and opaque objects etc[12]. X-rays are electromagnetic rays with very shorter wavelength of 1Å. X-rays exist between

gamma and ultraviolet rays in the spectrum. Electrons are usually used for the production of x-rays spectrum. When electrons bombarded on a metal target, most of the kinetic energy of electrons converted into heat and a in a very short amount (less than 1%) x-rays are produced. Diffraction strongly depends upon the phase relation of two or more than two waves[13].

X-ray Diffraction is a versatile, non destructive tool that is used for the identification of phases and crystallographic structure in a compound. It is also used for the determination of crystallite size, lattice parameter and lattice strain etc. XRD works on the principle of Bragg's law[14].

In 1913, Sir W.H. Bragg and his son Sir W. L Bragg described the phenomenon of X-ray reflection. They stated that there are two most important geometrical factors on which XRD based namely;

i. The incident beam which is always coplanar with reflected beam.
ii. And the angle between diffracted and transmitted beam is always 2θ.

We may write

$$n\lambda / 2d = \sin\theta \qquad (3.1)$$

It can be written as

$$n\lambda = 2d \sin\theta \qquad (3.2)$$

Where:

n is the number of incident x-ray beams, λ is the wavelength of x-ray beams, d is the distance between atomic layers and θ is the angle of incidence. Fig.3.4 explains how Bragg's law can work. 1 is first incident x-ray beam and 2 is second x-ray beam whereas 1' and 2'are reflected beam respectively. 'd' is the distance between two atomic layers[12].

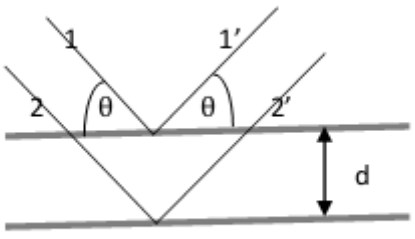

Figure 3. 4. Description of Bragg's law

The crystallite size 'D' can be calculated from XRD spectrum using Scherer equation;

$$D = 0.9 \times \lambda / B \times \cos \theta \qquad (3.3)$$

Where;

B is the full width at half maximum intensity, λ is the wavelength of x-rays and θ is the diffraction angle[15].

3.3.2 Scanning Electron Microscopy

Microscopy is a technique which is used for viewing objects that are not seen with naked eye. There are various types of microscopy exist which are different from one another on the basis of their magnification and resolution power. Optical, electron and scanning probe microscopy are usually used to view the samples[16]. Optical and electron microscopy both are working on the same principle of diffraction and reflection whereas scanning probe microscopy works on the interaction of scanning probe[17].

Scanning electron microscopy (SEM) is a very powerful tool to study the surface morphology of samples. SEM has magnification up to ~ 300,000X and resolution from 10 nm to 1μm. In SEM, initially electrons being excited by rapid scanning, then these excited electrons interact with cathode ray tube (CRT).

Magnetic lens are used to holding the CRT[18]. The controlled electron beam when interact with specimen produces a various types of signals which are used for imaging[17]. When incident electrons collided with specimen, it can produce a variety of signals including auger electrons, secondary electrons, backscattered electrons and x-rays.

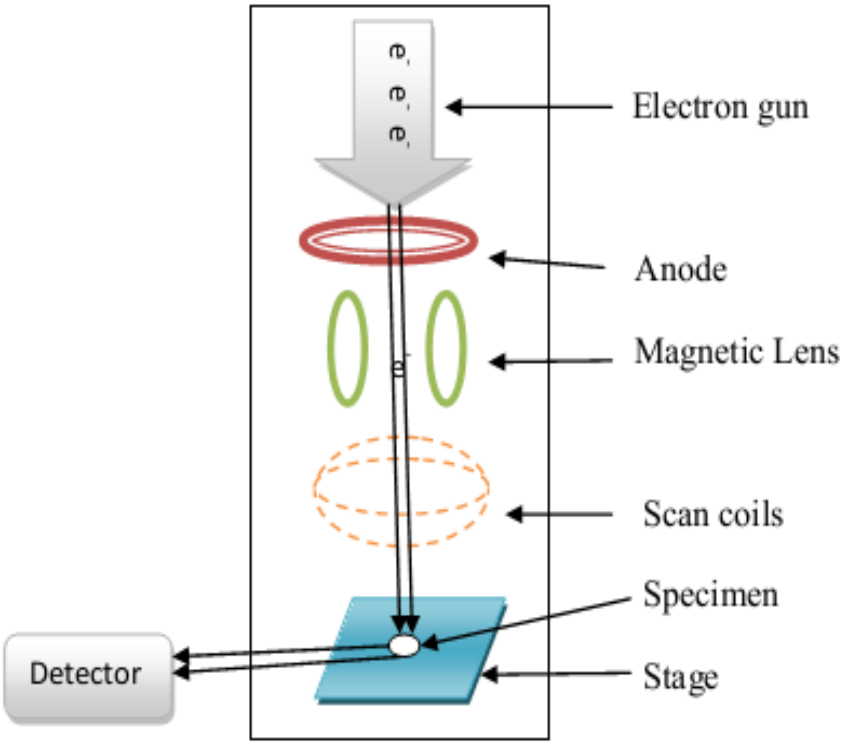

Figure 3. 5 Schematic of Scanning Electron Microscopy (SEM)

There are five major steps for sample preparation to carry out the SEM analysis which are given below[19]

i. Sectioning
ii. Mounting
iii. Grinding
iv. Polishing
v. Etching (if necessary)

3.3.2.1 Particle surface interaction

When the excited beam of electrons hit the specimen, they penetrate it into it and secondary electrons, auger electrons, backscattered electrons, visible light and x-rays are produced containing valuable information in it. Secondary electrons are mainly originated from topography; these are low energy electrons with high resolution. Backscattered electrons are high energy electrons originated from bulk of the sample and are dependent on their atomic number. For x-rays chemistry, long enough time is required. Auger electrons contain surface compositional information.

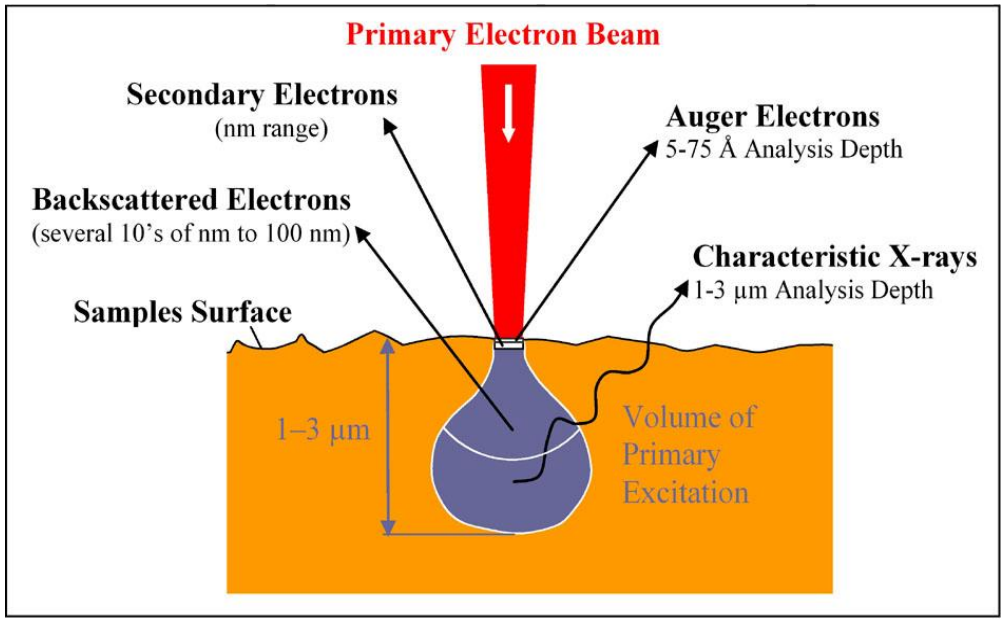

Figure 3. 6 Electron beam – sample interaction [23]

3.3.3 Energy Dispersive Spectroscopy

Energy dispersive spectroscopy (EDS) is an elemental analysis technique for chemical characterization and works on the same principle as SEM. EDS is always attached with SEM and TEM. It is also called energy dispersive x-rays analysis or x-rays spectroscopy analysis. When excited electrons bombarded a metal target, a low wavelength and high energy electrons converted into x-rays including meaningful information. Each element has specific energy value which can be detected by EDS[20].

3.3.4 DC Electrical Measurement

DC conductivity can be measured using two probe LCR meter (Wayne Kerr precision analyzer 6440B). The basic function is to calculate the conductivity by measuring resistivity of the sample. Pellets with suitable dimensions are formed for resistance measurement. Pellet is placed in a ceramic rod with the help of two copper plates. The two copper plates are connected with two probe LCR meter. The ceramic rod with pellet is placed in a furnace for heating treatment. Initially the electrons are in low energy state at to room temperature and LCR meter shows very high resistance. As the temperature increases, the resistance value decreases. We measured the value of resistance at desired temperature range[21].

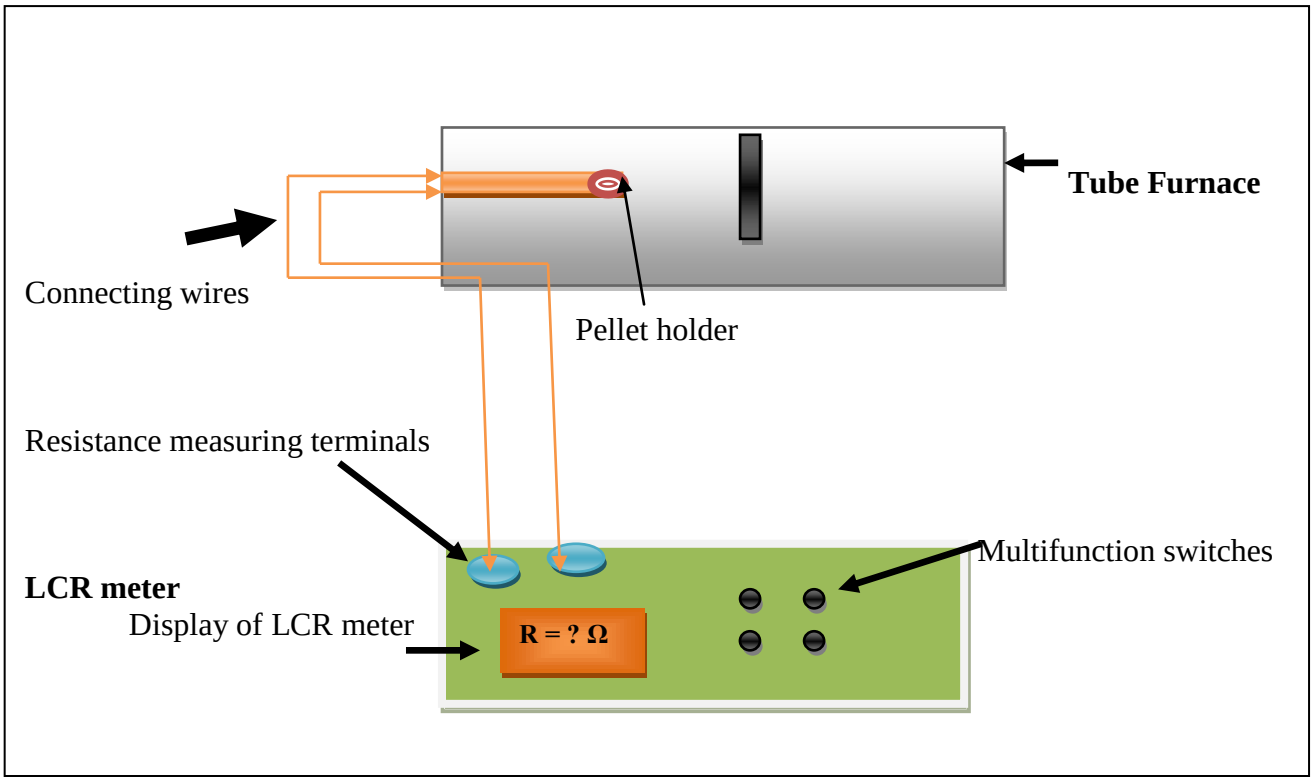

Figure 3. 8 Schematic of DC conductivity

.

Summary

In this chapter, a brief review of synthesis techniques mainly sol-gel, co-precipitation and solid state is presented for the synthesis of electrolytes. Various routes have been used for the preparation of SOFC electrolyte, but sol-gel, co-precipitation and solid state are mostly used. Wet chemistry route (sol-gel and co-precipitation) is used for atomic mixing and homogeneous distribution of particles. Solid state method is used due to its simplicity and low cost precursors. XRD is used to identify the structure, phase, lattice parameter and crystallite size whereas SEM with EDS is used for morphological and elemental analysis. XRD works on the principle of Bragg's law. Bragg's law states that, when x-rays are bombarded on metal target, an electronic cloud produced and moved as an electromagnetic wave. X-rays are detected by detector and a diffractrogram is recorded which has meaningful information. In SEM, a focused electron beam is targeted on the sample, which results in excitation of electrons. Various types of signals are produced such as auger electrons, backscattered electrons etc. containing meaningful information. Two probe Wayne Kerr (precision component analyzer 64440B) LCR meter is used to measure the DC electrical conductivity. DC resistance is measured at different temperature ranges. Resistivity is measured with DC resistance and sample dimension and from resistivity, we measured DC conductivity.

References

[1] L. De Chimie, D. M. Condensde, C. Ua, M. Curie, P. Jussieu, and P. Cedex, "Sol-gel C hemistry of Transition Metal Oxides J . Livage , M . Henry and C. Sanche z," 1989.

[2] H. Schmidt, "Chemistry of Material Preparation by the Sol-gel process. H. Schmid Fraunhofer-lnstitut ffw Silicatforschun~ Wi~rzburg~ Fed. Rep. Germany," vol. 100, pp. 51–64, 1988.

[3] S. Glaswerke, "I. Introduction," vol. 48, pp. 11–16, 1982.

[4] L. L. Hench and J. K. West, "The sol-gel process," Chem. Rev., vol. 90, no. 1, pp. 33–72, 1990.

[5] I. Kolthoff, "Theory of Coprecipitation. The Formation and Properties of Crystalline Precipitates," J. Phys. Chem., vol. 36, no. 3, pp. 860–881, 1932.

[6] K. Sinkó, "Influence of chemical conditions on the nanoporous structure of silicate aerogels," Materials (Basel)., vol. 3, no. 1, pp. 704–740, 2010.

[7] M. I. Khalil, "Co-precipitation in aqueous solution synthesis of magnetite nanoparticles using iron(III) salts as precursors," Arab. J. Chem., vol. 8, no. 2, pp. 279–284, 2015.

[8] P. Methods, "Chapter 3: Preparative Methods," pp. 1–21.

[9] R. Kumar, D. Prasad, and N. Brahme, "ScienceDirect Comparison of photoluminescence properties of Gd 2 O 3 phosphor synthesized by combustion and solid state reaction method," J. Radiat. Res. Appl. Sci., vol. 7, no. 4, pp. 550–559, 2014.

[10] C. Growth, "Solid State Reactions Film deposition Sol-gel method."

[11] Y. J. Leng, S. H. Chan, S. P. Jiang, and K. A. Khor, "Low-temperature SOFC with thin film GDC electrolyte prepared in situ by solid-state reaction," Solid State Ionics, vol. 170, no. 1–2, pp. 9–15, 2004.

[12] M. Cohen, "X-ray Diffraction Addison- Weseley Metallurgy Series."

[13] X. D. S. Uses, "X-ray Diffraction (XRD) X-ray Diffraction Calibration Procedures."

[14] S. a Speakman and D. Ph, "Introduction to X-Ray Powder Diffraction Data Analysis An X-ray diffraction pattern is a plot of the intensity of X-rays scattered at different angles by a sample," Mater. Sci.

[15] M. G. Chourashiya, J. Y. Patil, S. H. Pawar, and L. D. Jadhav, "Studies

on structural, morphological and electrical properties of Ce1-xGdxO2-(x/2)," Mater. Chem. Phys., vol. 109, no. 1, pp. 39–44, 2008.

[16] J. Mertz, "Optical Microscopy," pp. 37–67, 2010.

[17] J. Paluszynski and W. Slowko, "Three dimensional surface reconstruction in s canning e lectron m icroscopy," vol. 52, no. 1990, pp. 1–2, 1999.

[18] U. of Utah, "Lecture 3 :Brief Overview of Traditional Microscopes," pp. 1–50, 2009.

[19] M. Olivier, "Fuel Cell Characterization," 2008.

[20] "Fuel Cell Fundamentals - Ryan O'Hayre .pdf." .

[21] Keithley, "Low Level Measurements Handbook," Book, p. vi, I-5, 2016.

[22] D. Of and T. H. E. Experimental, "Two Probe Method For Resistivity Measurement of Insulators at Different Temperatures (Ambient to 200 o C)," Power, 2000.

[23] https://www.google.com.scanning+electron+microscopy&biw.

Chapter 4
Experimentation

4.1 Background

A number of experiments were performed to carry out the specific objectives mentioned in chapter 2. The details of following experiments are presented in this chapter.

I. Synthesis of gadolinium doped ceria $Ce_{1-x}Gd_xO_{1.5}$ (x=0.15) electrolytes by sol-gel and co-precipitation methods.

II. Synthesis of gadolinium and lutetium doped ceria $Ce_{0.85}Gd_{0.15-x}Lu_xO_{1.5}$ (x = 0.00, 0.05, 0.075, 0.10 and 0.15) electrolytes by solid oxide reaction method.

In this research, gadolinium doped ceria electrolytes with a chemical formula $Ce_{1-x}Gd_xO_{1.5}$ (x=0.15) were synthesized by two different techniques namely sol-gel and co-precipitation with same composition. Moreover, gadolinium and lutetium doped ceria electrolytes with a chemical formula $Ce_{0.85}Gd_{0.15-x}Lu_xO_{1.5}$ (x = 0.00, 0.05, 0.075, 0.10 and 0.15) were synthesized by solid state reaction method. The synthesized materials were then characterized by XRD, SEM with EDS and LCR meter.

4.1.1 Materials

A list of equipment used for these experiments is as follows;

List of equipment

- Muffle furnace
- Hydraulic press
- Drying oven
- pH meter
- Weight balance
- Magnetic stirrer

Chemicals

- Cerium nitrate hexahydrate ($Ce(NO_3)_3.6H_2O$)
- Gadolinium nitrate hexahydrate ($Gd(NO_3)_3.6H_2O$)
- Cerium oxide (Ce_2O_3)
- Gadolinium oxide (Gd_2O_3)

- Lutetium Oxide (Lu_2O_3)
- Anhydrous citric acid ($C_6H_8O_7$)
- Ammonia solution (NH_4OH, 25 %)
- De-ionized water
- Acetone (for washing)

4.2 Synthesis of gadolinium doped ceria (GDC) electrolyte

Gadolinium doped ceria with a chemical formula $Ce_{1-x}Gd_xO_{1.5}$ (x=0.15) was synthesized by wet chemistry including sol-gel and co-precipitate routes.

4.2.1 Synthesis by sol-gel method

The sample with a general formula of $Ce_{1-x}Gd_xO_{1.5}$ (x=0.15) was synthesized by sol-gel method as shown in Fig.4.1. The precursor of cerium nitrate hexahydrate and gadolinium nitrate hexahydrate were used as starting materials. Stoichiometric amounts of Gd $(NO_3)_3.6H_2O$ and Ce $(NO_3)_3.6H_2O$ were dissolved in de-ionized water separately. Then Gd $(NO_3)_3.6H_2O$ was added in Ce $(NO_3)_3.6H_2O$ drop wise with continuous stirring. Stoichiometric amount of anhydrous citric acid was also dissolved in de-ionized water. The composition of total oxide to citric acid was 1:1. For better results, both solutions were mixed drop wise in a separate beaker with continuous stirring. To get homogenizing mixture, the sample was stirred for 10 hours. After complete mixing, the temperature was raised to 80˚C with continuous stirring to remove extra water and to form a gel. As the temperature increases, the solution become more viscous and after 4 hours a transparent gel was formed. Then put beaker in a dry place for 24 hours. Because, during aging polycondensation continues which increase the thickness and decrease porosity [5]. The gel was then dried in an oven at 120 ˚C for several hours for complete drying. After drying, the sample was ground using agate mortar to get a fine powder. The fine powder was than calcined at 600 ˚C for 4 h.

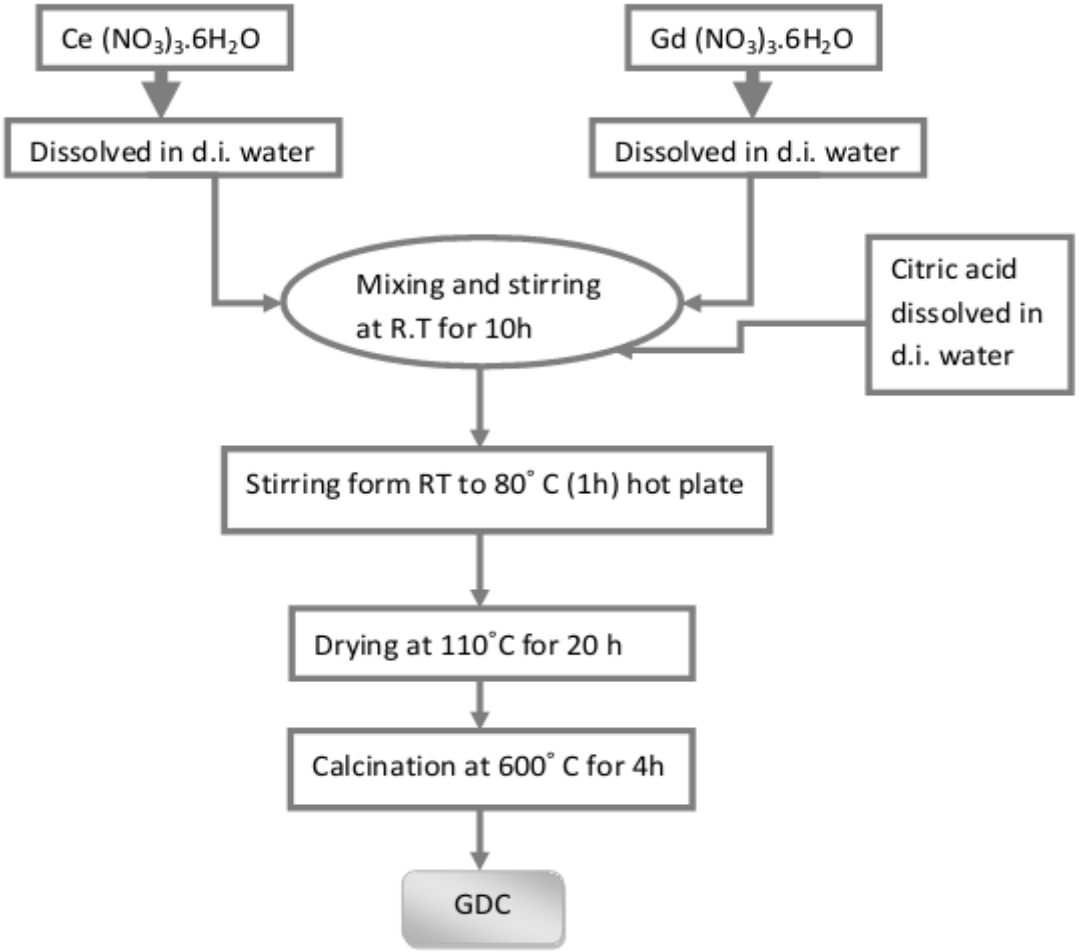

Figure 4. 1. Synthesis of GDC by sol-gel method

After calcination, the sample was ground using agate mortar and pestle for characterizations.

4.2.2 Synthesis by co-precipitation method

The ceramic electrolyte with the formula of $Ce_{1-x}Gd_xO_{1.5}$ (x=0.15) was synthesized by co-precipitation method as shown in Fig.4.2. The precursor of Cerium nitrate hexahydrate and gadolinium nitrate hexahydrate were used. Stoichiometric amounts of gadolinium nitrate hexahydrate and cerium nitrate hexahydrate were dissolved in de-ionized water separately. The concentration of the precursor solution was 1M. Then mix both the solution in a separate beaker with continuous stirring at hot plate.

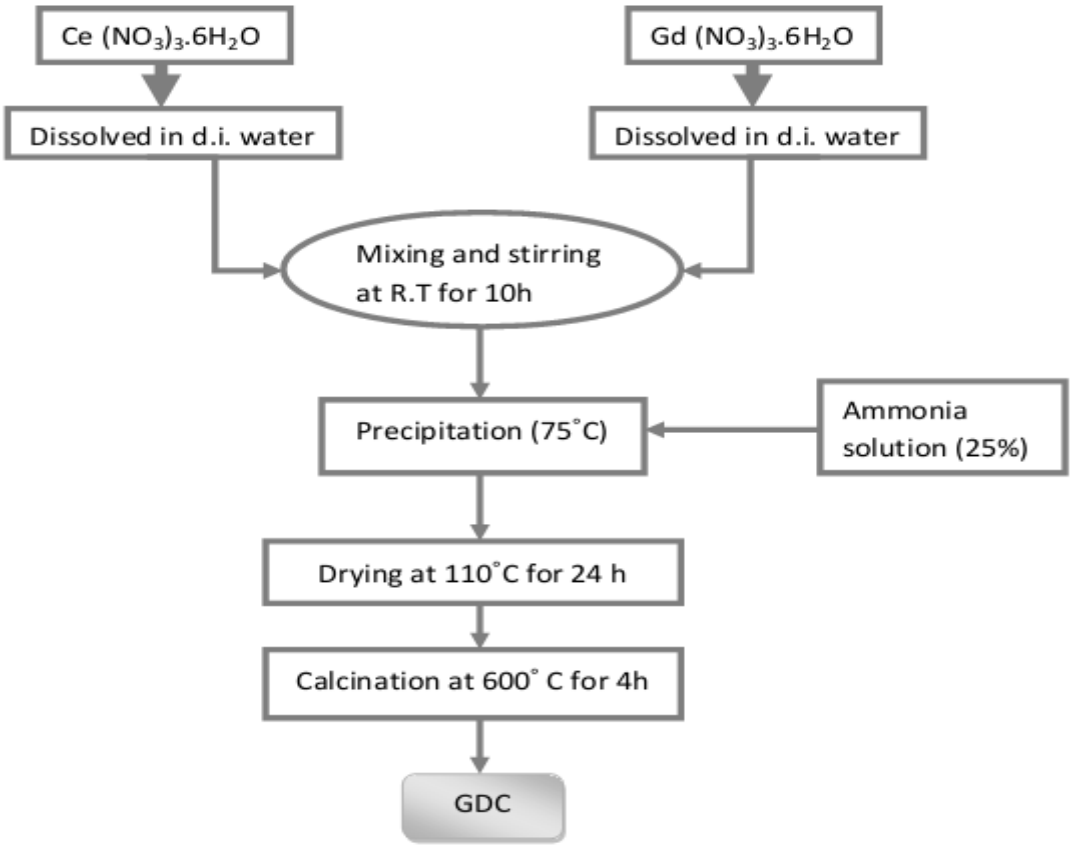

Figure 4. 2 GDC synthesized by co-precipitation method

After homogenizing mixing, added ammonium hydroxide drop wise in the solution with continuous stirring, until precipitation occurred. After precipitation raise the temperature to 200˚C to dry the slurry type sample with continuous stirring at hot plate. Pale yellow matter was obtained after complete drying. Then ground the sample by using agate mortar and pestle to obtain a fine powder. The fine powder was calcined at 600 ˚C for 4 hours.

4.3 Synthesis of gadolinium and lutetium co-doped ceria (LGDC) electrolytes

Co-doped ceria electrolytes of gadolinium (Gd) and lutetium (Lu) with a chemical formula of $Ce_{0.85}Gd_{0.15-x}Lu_xO_{1.5}$ (x = 0.00, 0.05, 0.075, 0.10 and o.15) were synthesized by solid state reaction method. Cerium oxide (Ce_2O_3), gadolinium oxide (Gd_2O_3) and lutetium oxide (Lu_2O_3) were used as starting materials. The calculated amounts of all of these materials were ground using agate mortar and pestle. An appropriate amount of ethanol was also added for homogenizing mixture. After well mixing, the samples were dried at 120 ˚C for 8 hours, so that ethanol evaporates. After complete drying, again ground the samples to remove pores. The samples were

sintered at 1200 ˚C for 4 hours in a muffle furnace to complete a chemical reaction. The sintering temperature was calculated by Tamman's rule. The sample was allowed to cool at room temperature in the same muffle furnace.

The obtained samples were ground using agate mortar and pestle for XRD and SEM analysis. For conductivity measurement, a pellet was synthesized with a thickness of 2 mm and a diameter of 10 mm using hydraulic press. The flow chart of synthesis of LGDC is shown in Fig.4.5.

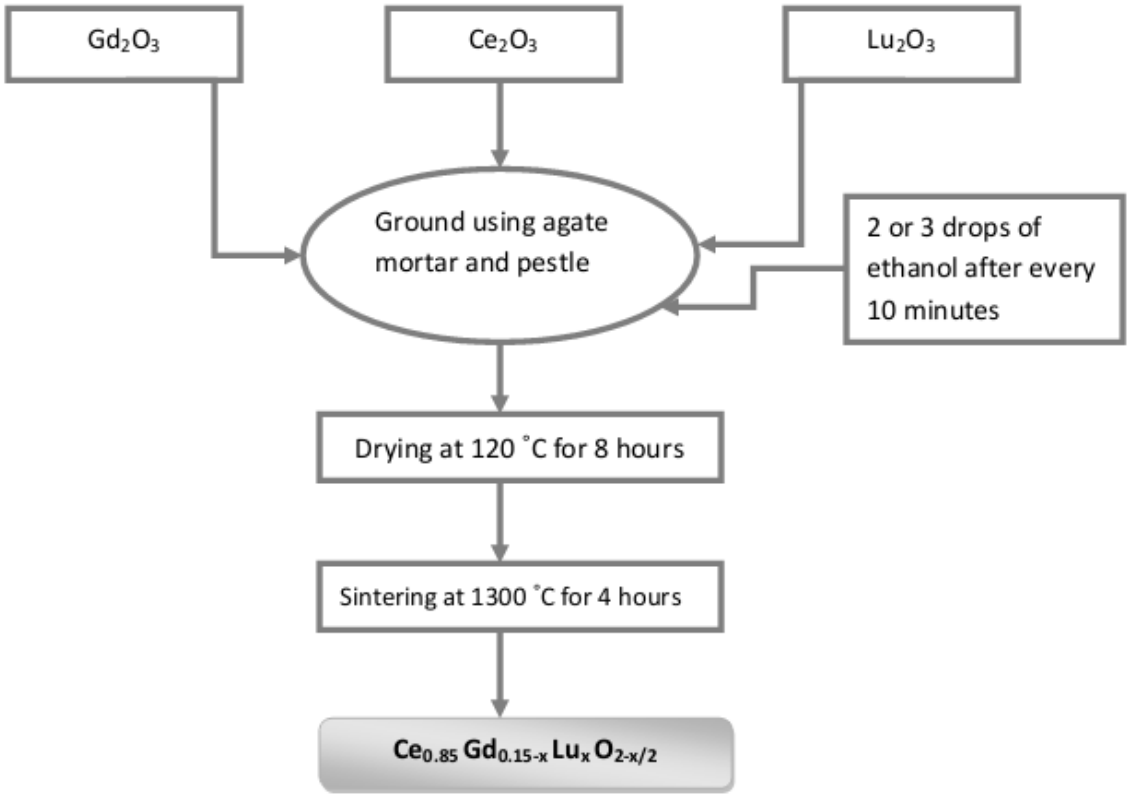

Figure 4. 3 Synthesis of LGDC by solid state method

4.4 Characterization

After synthesis, the samples were then characterized by different characterization techniques. XRD and SEM were used for structural analyses, whereas LCR meter was used to measure dc conductivity. The parameter details of these techniques are given below.

4.4.1 Structural Analyses

Crystal structure and phase formation of all the samples were analyzed by X-ray Diffraction equipment (STOE Germany). X-ray diffractogram of all the samples were

recorded with computer interface using Cu K_α at λ = 1.5418 Å at scan angle ranging from 20˚ to 80˚ with step size 0.04 / second, the reflection peaks were recorded using accelerated voltage of 20 kV and a current of 5 mA. The crystallite size was calculated with main reflection peak (111) by measuring B (full width half maximum intensity).

The morphology of the samples was observed by scanning electron microscopy (JEOL Analytical SEM). The average grain size was measured from higher magnification SEM images.

4.4.2 DC Electrical Conductivity

DC conductivity was measured by measuring the DC resistance. After measuring resistance value, resistivity ρ value calculated with this formula

$$\rho = (R_{avg} \times A) / L \qquad (4.1)$$

Where ρ is the resistivity, L is the thickness of pellet, A is the area of pellet and R is the resistance of pellet. After measuring resistivity form these parameters we calculate the conductivity form the following relation

$$\rho = 1/ \sigma \qquad (4.2)$$

This can be written as,

$$\sigma = 1/ \rho \qquad (4.3)$$

Fig.4. shows the typical Arrhenius plots of ln (σT) versus 1000/T. The changes in dc conductivity calculated from the bulk resistance and sample dimensions with temperature. The dc conductivity obeys the Arrhenius behavior[22]

$$\sigma_{dc} = \sigma_o \exp (- Ea / kT) \quad (4.4)$$

Where k is the Boltzmann's constant, T is the absolute temperature, σ_o is the pre-exponential factor and Ea is the activation energy. Activation energy can be calculated by finding the slope of Arrhenius line.

Summary

Initially, gadolinium doped ceria (GDC) with chemical formula $Ce_{1-x}Gd_xO_{2-x/2}$ (x=0.15) was synthesized by three different methods; sol-gel, co-precipitation and solid state reaction methods. XRD and SEM with EDS were employed to carry out structural, morphological and elemental analysis respectively. Then lutetium doped ceria with formula $Ce_{1-x}Lu_xO_{2-x/2}$ (x=0.15) was synthesized by solid state reaction method. At the end gadolinium and lutetium co-doped ceria electrolytes $Ce_{0.85}Gd_{0.15-x}Lu_xO_{2-x/2}$ (x=0.05, 0.075, 0.1) were synthesized with three different compositions by solid state method. XRD and SEM were used to analyze the structural and morphological analyses. DC electrical conductivity was measured by two probe method with the help of LCR meter (Wayne Kerr precision component analyzer 6440B).

References

[1] D. Wattanasiriwech and S. Wattanasiriwech, “Effects of Fuel Contents and Surface Modification on the Sol-gel Combustion Ce0.9 Gd0.1O1.95 Nanopowder,” Energy Procedia, vol. 34, pp. 524–533, 2013.

[2] S. Kuharuangrong, “Ionic conductivity of Sm, Gd, Dy and Er-doped ceria,” J. Power Sources, vol. 171, no. 2, pp. 506–510, 2007.

[3] Dikmen, Sibel. "Effect of co-doping with Sm 3+, Bi 3+, La 3+, and Nd 3+ on the electrochemical properties of hydrothermally prepared gadolinium-doped ceria ceramics." Journal of Alloys and Compounds 491.1 (2010): 106-112.

[4] Medvedev, D., et al. "Investigation of the structural and electrical properties of Co-doped BaCe 0.9 Gd 0.1 O 3− δ." Solid State Ionics 182.1 (2011): 41-46.

[5] Hench, Larry L., and Jon K. West. "The sol-gel process." Chemical Reviews90.1 (1990): 33-72.

Chapter 5
Results and Discussion

5.1 Gadolinium doped ceria electrolyte via sol-gel and co-precipitate routes

5.1.1 X-ray Diffraction Analysis

Fig.5.1 shows the XRD pattern of gadolinium doped ceria (GDC) powder synthesized by two different methods, namely sol-gel and co-precipitation. The XRD pattern revealed the formation of cubic $Gd_{0.15}Ce_{0.85}O_{1.5}$ in all samples. All peaks are associated to cubic fluorite crystal structure with the space group Fm-3m (225) (PDF Card No. 75-0161). XRD peaks positioned at 2 theta values of 28.40˚, 32.95˚, 47.28˚, 56.16˚, 58.99˚, 69.32˚, 76.51˚, and 78.95˚ corresponding to (111), (200), (220), (311), (222), (400),

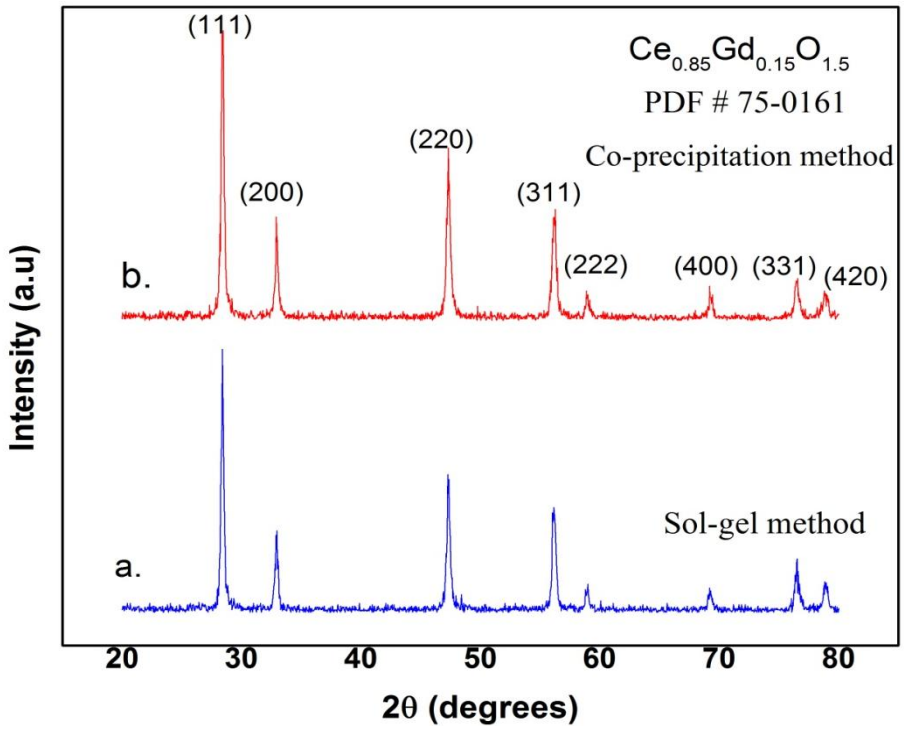

Figure 5. 1 XRD patterns of 15 mol% GDC calcined at 600 ˚C for 4h prepared by sol-gel and co-precipitation methods.

Table 5. 1 Results based on XRD

Method	**Composition**	**Crystallite size (nm)**
Sol-gel	$Gd_{0.15}Ce_{0.85}O_{1.5}$	53
Co-precipitation	$Gd_{0.15}Ce_{0.85}O_{1.5}$	40

(331) and (420) crystallographic planes, matching well according to the PDF # 75-0161. There are no other phases formed in sol-gel and co-precipitation methods. From diffractrogram, it can be seen that the intensity of (111) peak is maximum in all samples. The interplaner spacing d and lattice parameter of all samples are calculated by JADE 6.0 software. The reflection from (111) plane is used to measure the crystallite size D, calculated from the Sherrer equation

$$D = 0.9 \times \lambda \ / B \times \cos(\theta) \qquad (5.1)$$

Where 'θ' is the diffraction angle, 'λ' is the wavelength of X-rays, and B is the full width at half maximum intensity.

Table 1 shows the crystallite size 'D' of GDC prepared by both methods. From table, it can be concluded that, GDC prepared from sol-gel method has crystallite size slightly larger than that of GDC prepared by sol-gel method. There is a good agreement with SEM results of both the samples.

The peaks of sample prepared by co-precipitation are relatively broad as compared to sample prepared by sol-gel, due to small crystallite size. The XRD pattern showed that GDC electrolyte prepared by two different methods have same phase and structure.

5.1.2 Microstructure / Morphology

Fig. 5.2 shows the micrographs of GDC electrolyte synthesized by sol-gel and co-precipitation. SEM micrograph shows the particles are well dispersed and in a round shape. In fig. 2a the particles prepared via sol-gel method have nearly homogeneous size distribution without definite big agglomerate. The particles prepared by co-precipitation have high rate of agglomeration, but all the particles forming agglomeration are highly uniform. The particles size ranges from 50 to 70 nm by sol-

gel and from 40 to 60 by co-precipitation. So by co-precipitation method, the particles are larger, fewer and denser then by sol-gel method[1]. It can also be concluded that the Ostwald's ripening is increased by increasing the pH of the solution[2].

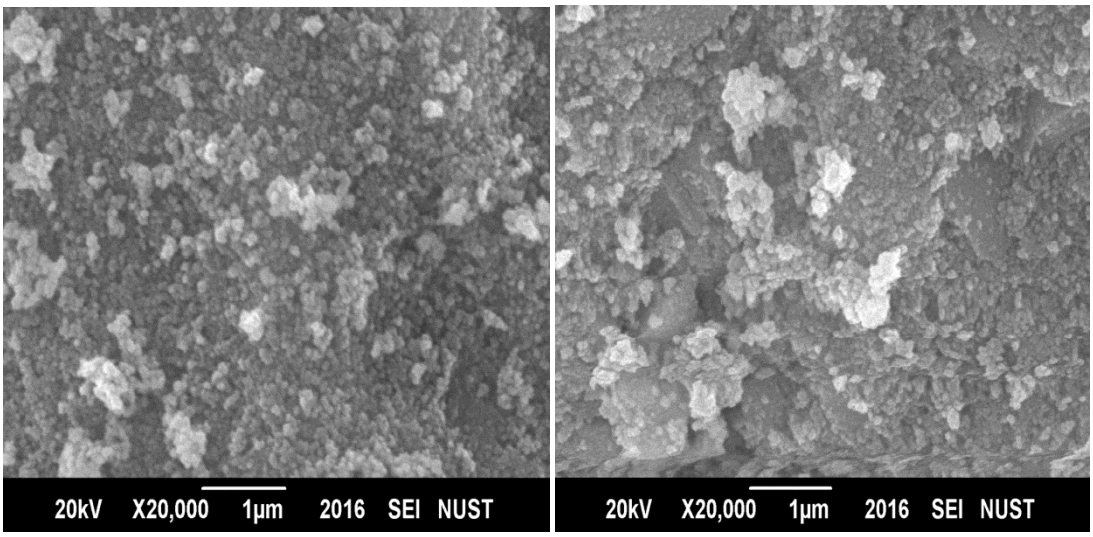

Figure 5. 2 SEM Images of $Gd_{0.15}Ce_{0.85}O_{1.5}$ by sol-gel (a) and by co-precipitation (b)

Fig. 2 shows the EDS analysis of the prepared samples. There is no other element found in EDS analysis except O, Ce and Gd. The intense peaks of Gd, Ce and O are present, which confirms the purity of GDC powders. The atomic percentage of cerium and gadolinium are higher in the sample prepared by co-precipitation method as shown in Fig. 5.3 (a, b).

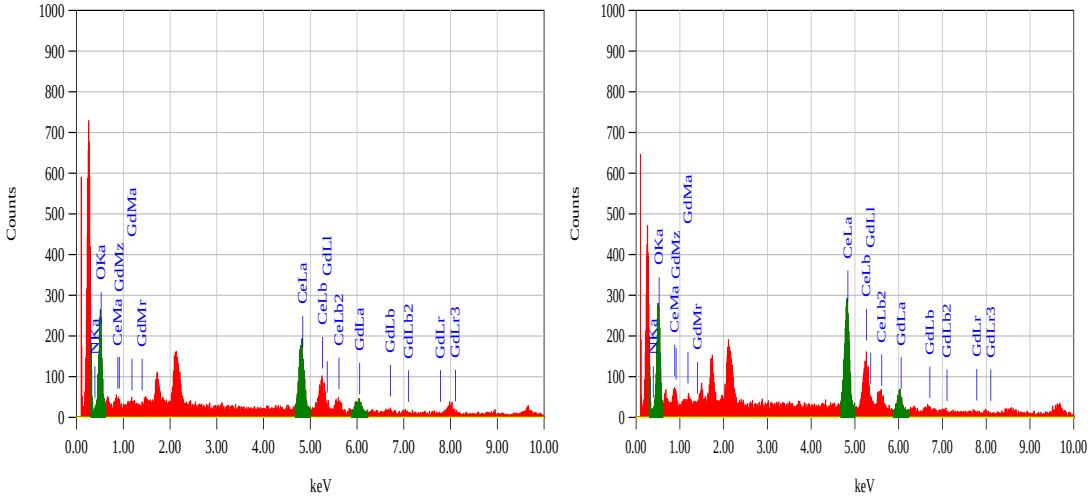

Figure 5. 3 EDS spectra of $Gd_{0.15}Ce_{0.85}O_{1.5}$ by sol-gel (a) and by co-precipitation (b)

5.1.3 DC electrical properties

The DC conductivity was measured by two probe method with LCR meter (Wayne Kerr precision analyzer 6440B) in the temperature range of 200 – 600 ˚C. Fig.4. shows the typical Arrhenius plots of ln (σT) versus 1000/T. The changes in dc conductivity calculated from the bulk resistance and sample dimensions with temperature. The dc conductivity obeys the Arrhenius behaviour

$$\sigma_{dc} = \sigma_o \exp(- Ea / kT)$$

Where k is the Boltzmann's constant, T is the absolute temperature, σ_o is the pre-exponential factor and Ea is the activation energy [3].

Conductivity curve of both the samples consist of two linear parts. Initially the conductivity value is very low form 200 to 280 ˚C in the sample prepared by co-precipitation method. At 280 ˚C, the conductivity value becomes higher, because the electrons move fast due to low resistance. After 280 to 600 ˚C, the conductivity curve is almost linear and it increases with the temperature increases. Similarly, GDC prepared by sol-gel method showed very low conductivity from 200 to 240 ˚C and from 240 to 600 ˚C the conductivity curve is almost linear. GDC prepared by sol-gel method

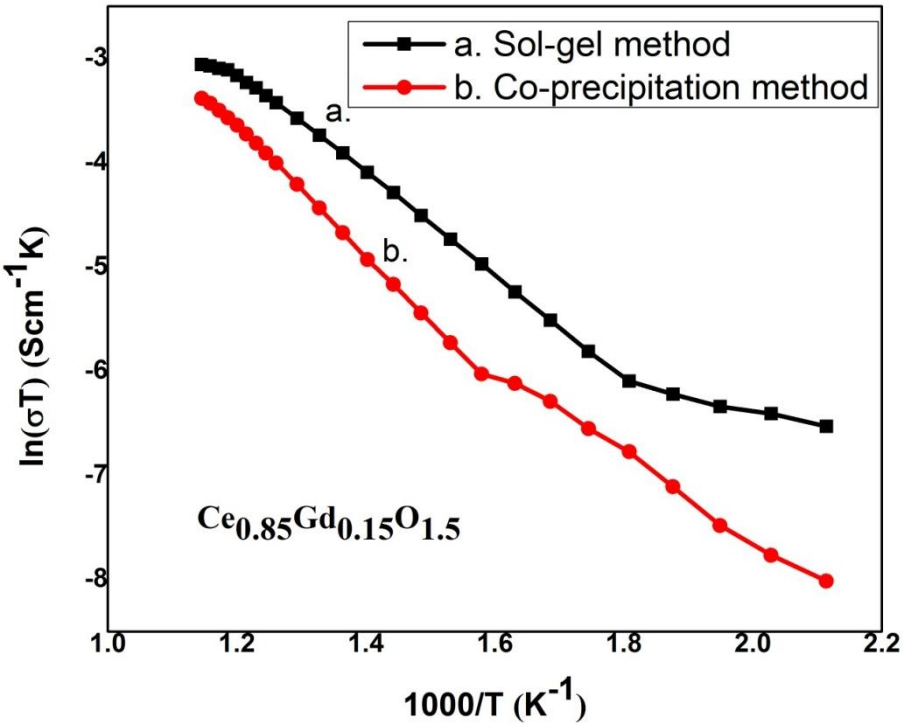

Figure 5. 4 DC conductivity curves of $Gd_{0.15}Ce_{0.85}O_{1.5}$ by sol-gel (a) and by co-precipitation (b)

showed the conductivity value of 0.0217 (S/cm) at 600 ˚C with activation energy Ea value of 0.31 eV. And GDC prepared by co-precipitation showed the conductivity value of 0.0103 (S/cm) at 600 ˚C with activation energy of 0.36 eV slightly lower than by sol-gel method.

5.2 Gadolinium and lutetium co-doped ceria electrolytes

5.2.1 X-ray diffraction analysis

Fig. 5.5 shows the XRD patterns of the as prepared $Ce_{0.85}\ Gd_{0.15-x}\ Lu_x\ O_{2-\delta}$ samples (x = 0, 0.05, 0.075, 0.10 and 0.15) calcined at 1200˚C for 4 hours. All sample peaks are associated to cubic fluorite crystal structure with the space group Fm-3m (225). XRD peaks positioned at 2 theta values corresponding to crystallographic planes, matching well according to the pattern of pure ceria CeO_2 with JCPDS File No. 34-0394. There is no other phase found in all samples. From diffractogram, it can be seen that the intensity of (111) peak is maximum in all samples. The reflection from (111) plane is used to measure the most intense peak crystallite size $D_{(111)}$.

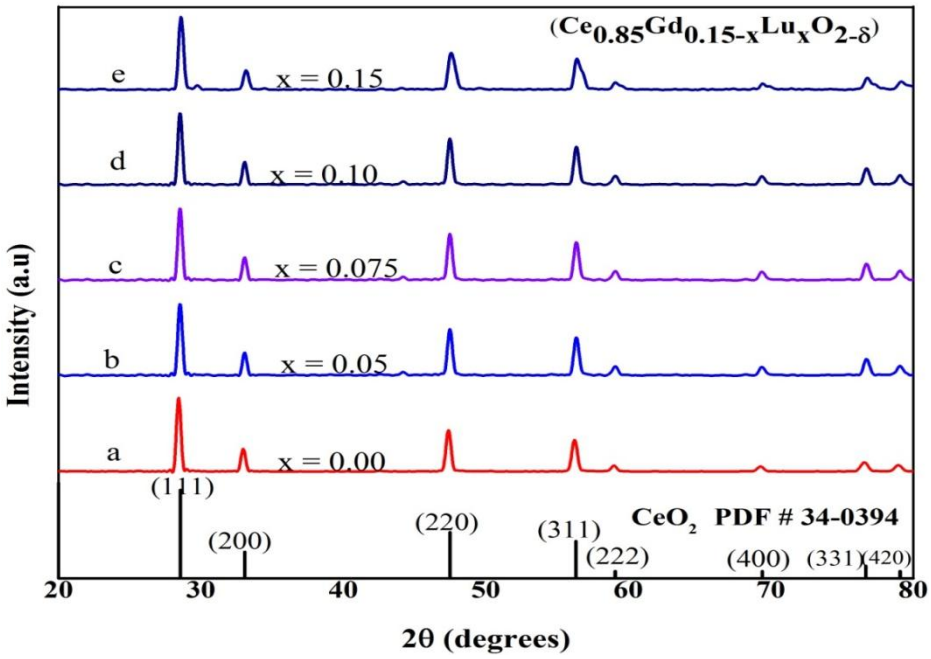

Figure 5. 5 XRD patterns of $Ce_{0.85}Gd_{0.15-x}Lu_xO_{2-\delta}$ samples (x = 0, 0.05, 0.075, 0.10 and 0.15) calcined at 1200˚C for 4hours.

The most intense peak crystallite size $D_{(111)}$ is calculated from Scherrer formula,

$$D = \frac{0.9 \times \lambda}{\beta \times \text{Cos}\theta} \quad \ldots\ldots\ldots\ldots 5.1$$

where D is the crystallite size, λ is the wavelength of x-rays, θ is the diffraction angle and β is the full width at half maximum intensity in radians. The interplaner spacing d and lattice parameter of all the samples are calculated using JADE 6.0 software by fitting the peak data of ceria phase. The crystallite sizes relative to most intense peak are given in Table1. It can be observed from Fig 5.5 that the addition of Lu_2O_3 in GDC samples can cause a small shift in higher angles in ceria peaks which showed the change in lattice parameters. The 2θ values of doped ceria slightly shift towards right with x changes from 0 to 0.15.

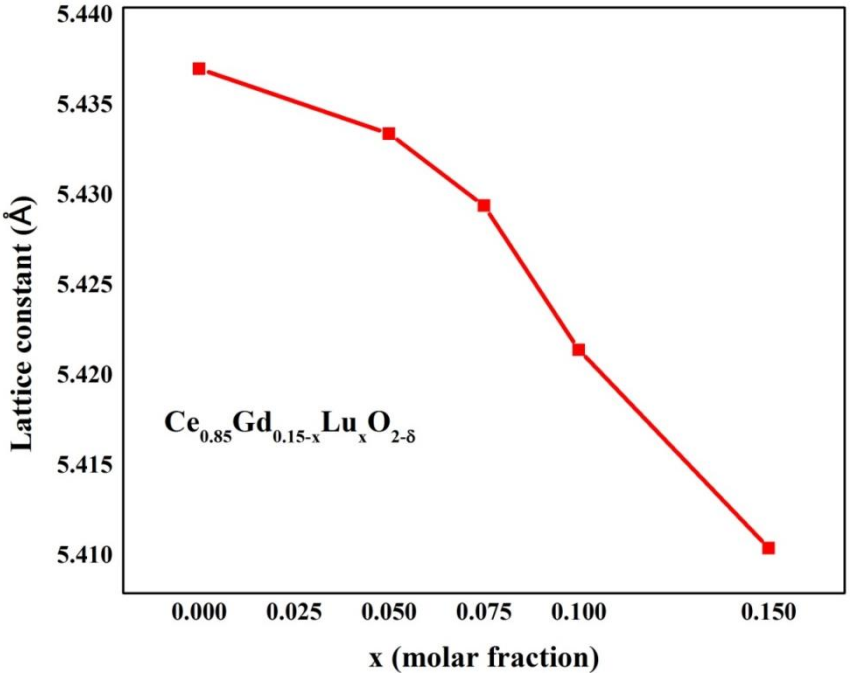

Figure 5. 6 The dependence of lattice constant on the composition of as prepared doped ceria electrolytes.

The relationship between dopant concentration and unit cell parameters is shown in Fig. 5.6. From Fig. 5.6 it can be seen that the cell parameter decreases with the increasing concentration of lutetium as x varies from 0 to 0.15.

Table 5. 2
The most intense peak crystallite size calculated by Scherrer formula and Elastic strain present in the lattice of doped ceria electrolytes.

Doping concentration	Sample ID	Crystallite size $D_{(111)}$ (nm)	Elastic strain (10^{-3})
x = 0.00	$Ce_{0.85}Gd_{0.15}O_{2-\delta}$	47	1.91
x = 0.05	$Ce_{0.85}Gd_{0.10}Lu_{0.05}O_{2-\delta}$	44	0.36
x = 0.075	$Ce_{0.85}Gd_{0.075}Lu_{0.075}O_{2-\delta}$	36	-1.21
x = 0.10	$Ce_{0.85}Gd_{0.05}Lu_{0.10}O_{2-\delta}$	31	-1.68
x = 0.15	$Ce_{0.85}Lu_{0.15}O_{2-\delta}$	37	-2.38

As reported in literature, the critical ionic radius of ceria doping with trivalent metals is 0.1038 nm [4]. The ionic radius of Lu^{3+} (0.085 nm) is smaller whereas the ionic radius of Gd^{3+} (0.1053 nm) is larger than the critical ionic radius of ceria which is

0.1038 nm [5]. Therefore the cell parameter decreases with the increasing concentration of Lutetium as x varies from 0 to 0.15. From Fig. 5.6, it can be seen that the relationship is linear between lattice parameter and the concentration of lutetium, it means that lattice parameter follows Vegard's rule [6], which further confirms that Gd and Lu are co-doped into crystal lattice of ceria.

The effect of dopant concentration on the elastic strain available in cubic fluorite crystal structure of doped ceria samples was calculated by using the following relation [7];

$$\text{Elastic strain} = (a_o - a) / a \quad \ldots\ldots\ldots\ldots\ldots(2)$$

where a_o is the lattice constant of $Ce_{0.85}Gd_{0.15-x}Lu_xO_{2-\delta}$ and a is the lattice constant of pure ceria CeO_2. Table 1 shows the different values of elastic strain present in doped ceria samples of $Ce_{0.85}Gd_{0.15-x}Lu_x O_{2-\delta}$ (x = 0.00, 0.05, 0.075, 0.10 and 0.15). Negative and positive elastic strain is seen as lutetium concentration varies from 0 to 0.15. There is a very small elastic strain present in $Ce_{0.85}Gd_{0.10}Lu_{0.05}O_{2-\delta}$ sample.

5.2.2 Microstructure / Morphology

Fig.5.7 shows the SEM micrographs of the as prepared $Ce_{0.85}Gd_{0.15-x}Lu_xO_{2-\delta}$ (x = 0.00, 0.05, 0.075, 0.10, 0.15) co-doped ceria samples calcined at 1200˚C for 4 hours. SEM images reveal that prepared composites consist of well separated particles without distinct agglomeration and have occasionally irregular shapes. The grain size was measured from higher magnification SEM images. The average grain size of each sample was found to be in the range of 30 to 60 nm which is in good agreement with the results of XRD. Samples a, b and c with low concentration of Lu^{3+} at x = 0, 0.05 and 0.075 respectively, have larger particle size as compared to samples d (x = 0.10) and e (x = 0.15) with higher concentration of Lu^{3+}.

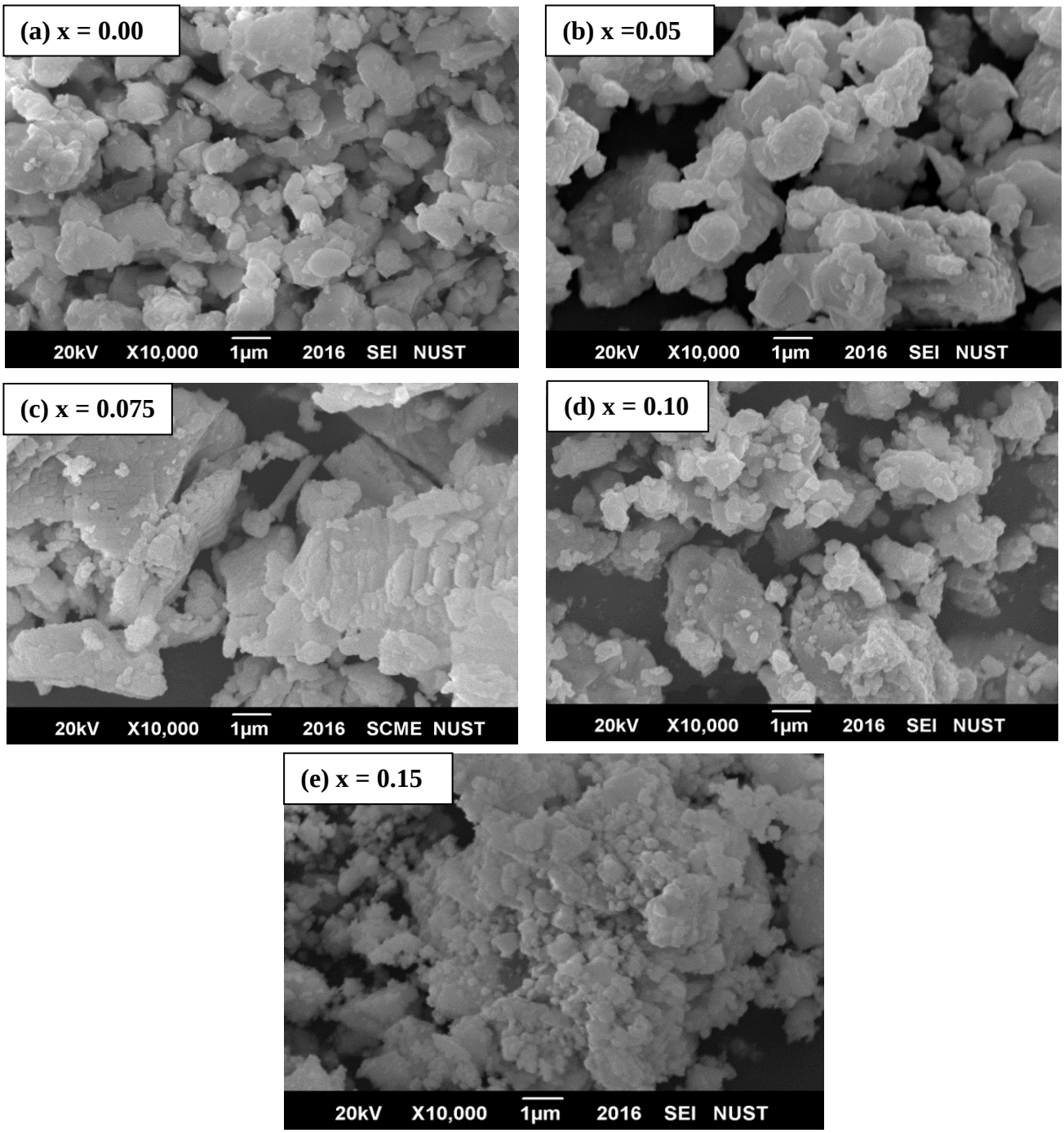

Figure 5. 7 SEM Micrographs of $Ce_{0.85}Gd_{0.15-x}Lu_xO_{2-\delta}$: (a) x = 0, (b) x = 0.05, (c) x = 0.075, (d) x = 0.10 and (e) x= 0.15 calcined at 1200˚C for 4h.

The addition of Lutetium in ceria impedes the crystallite growth of ceria as Lu^{3+} concentration increases from x = 0 to 0.15. This observation is well matched with literature data [8] and [9], and it also testifies with the results of XRD. It can also be clearly shown from SEM images d (x = 0.10) and e (x = 0.15) that the solubility decreases with the increasing concentration of Lutetium. According to Malgorzata et

al. [10] lesser solubility of Lutetium in Ceria at higher concentration may be explained by the segregation of dopant ions at the surface of Ceria crystallites. All samples have dense particles with heterogeneous shapes and sizes. The singly doped $Ce_{0.85}Gd_{0.15}O_{2-\delta}$ (a) and $Ce_{0.85}Lu_{0.15}O_{2-\delta}$ (e) materials have most heterogeneous as compared to co-doped ceria samples (b, c and d).

It is interesting to note that all the particles in the samples are heterogeneously distributed with irregular shapes and without large agglomeration, which further demonstrates that solid state route is the effective way to produced nano sized particles.

5.2.3 DC electrical properties

The dc electrical conductivity was measured as a function of temperature and

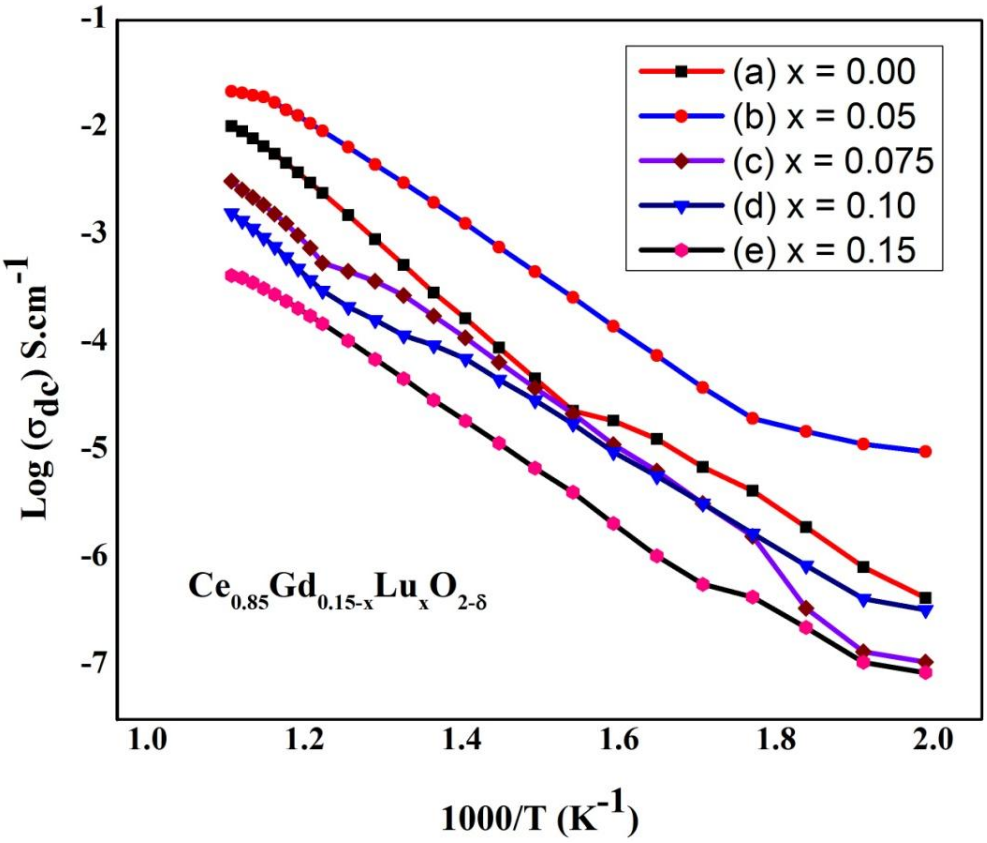

Figure5.8. Arrhenius plots for dc electrical conductivities of $Ce_{0.85}Gd_{0.15-x}Lu_xO_{2-\delta}$ samples (x = 0, 0.05, 0.075, 0.10 and 0.15) sintered at 1400°C for 4 hours.

compositions for as prepared $Ce_{0.85}Gd_{0.15-x}Lu_xO_{2-\delta}$ (x = 0.0, 0.05, 0.075, 0.10 and 0.15) samples. The changes in dc electrical conductivity were measured from the bulk resistance and sample dimensions with temperature. The relationship between the temperature and conductivity obeys the Arrhenius behavior of the form

$$\sigma_{dc} = \sigma_o \exp [- E_a / kT] \quad \ldots\ldots\ldots \quad 5.3$$

where σ_{dc} is the dc conductivity, k is the Boltzman constant, σ_o is the pre-exponential factor, E_a is the activation energy and T is the absolute temperature.

Fig.5.8 shows the typical Arrhenius plots of ln (σ_{dc}) versus 1000/T for $Ce_{0.85}Gd_{0.15-x}Lu_xO_{2-\delta}$ samples (x = 0.0, 0.05, 0.075, 0.10 and 0.15) sintered at 1400 °C for 4 hours. After measuring the resistance of pellets, the resistivity was calculated by using the formula,

$$\rho = RA / L \quad \ldots\ldots\ldots\ldots \quad (5.4)$$

where ρ is the resistivity, L is the thickness, A is the area of pellet and R is the resistance of pellet. The dc conductivity was calculated by using

$$\sigma_{dc} = 1 / \rho \quad \ldots\ldots\ldots\ldots\ldots \quad (5.5)$$

It is obvious form fig that dc conductivity increases with increasing temperature which is the normal characteristics of fluorite structured electrolytes. Initially, at low temperature range the dc conductivity value of all samples is very low and show little deviation from linearity, whereas, at high temperature range the dc conductivity value is high and show linear dependence, which implies that the dc conductivity is dependent on temperature and also follows Arrhenius behavior [11]. It can be seen that the sample $Ce_{0.85}Gd_{0.10}Lu_{0.05}O_{2-\delta}$ showed dc conductivity value of 0.0217 (S/cm) at 600°C, which is slightly high than pure gadolinium doped ceria $Ce_{0.85}Gd_{0.15}O_{2-\delta}$ and very high than pure lutetium doped ceria $Ce_{0.85}Lu_{0.15}O_{2-\delta}$. The calculated values of dc conductivity as a function of temperature and compositions are given in Table 2.

For electrolyte materials it is important to analyze the value of ionic conductivity. Pure ceria has low ionic conductivity [6]. The oxide transference number (also called transport number) for pure ceria was found to be ~ 0.002 in the temperature range of 550-1200°C [12]. In pure ceria, the electronic conductivity is due to small polaron known as defects which is produced due to trapping of electron carrier in between atoms or ions hopping [13]. Gadolinium doped ceria (GDC) has the oxide transference number of 0.880 at 600°C which is very high as compared to pure ceria [14]. A co-doping strategy is used to increase the ionic conductivity and suppress the electronic conductivity of ceria. Various studies have been reported the value of oxide transference number in the range of 0.85 to 0.95 at 600°C for co-doped ceria [15] . So, if we consider the oxide transference number equal to 0.90 then the value of ionic conductivities.

Table 5. 3

DC electrical conductivities and activation energies of $Ce_{0.85}Gd_{0.15-x}Lu_xO_{2-\delta}$ samples

Doping concentration	Sample ID	Dc conductivity σ_{dc} ($S.cm^{-1}$) at 600 ˚C	Activation energy E_a (eV) at 600 ˚C
x = 0	$Ce_{0.85}Gd_{0.15}O_{2-\delta}$	0.01033	0.89
x = 0.05	$Ce_{0.85}Gd_{0.10}Lu_{0.05}O_{2-\delta}$	0.02173	0.68
x = 0.075	$Ce_{0.85}Gd_{0.075}Lu_{0.075}O_{2-\delta}$	0.00318	1.12
x = 0.10	$Ce_{0.85}Gd_{0.05}Lu_{0.10}O_{2-\delta}$	0.00160	1.17
x = 0.15	$Ce_{0.85}Lu_{0.15}O_{2-\delta}$	0.00042	1.59

for $Ce_{0.85}Gd_{0.15-x}Lu_xO_{2-\delta}$ samples (x = 0.00, 0.05, 0.075, 0.10 and 0.15) at 600°C are 9.2×10^{-3} (S/cm), 1.95×10^{-2} (S/cm), 2.86×10^{-3} (S/cm), 1.44×10^{-3} (S/cm) and 3.78×10^{-4} (S/cm) respectively.

The values of activation energies for the prepared samples were calculated from the slopes of the lines in Fig.4 and shown in Table 2. Activation energy is mainly due to defect association enthalpy (ΔH_a) and oxygen migration enthalpy (ΔH_m) [16]. (ΔH_m) is not depends on dopant concentration whereas (ΔH_a) is depends on elastic strain and dopant cation [17]. As there is very low elastic strain found in two samples $Ce_{0.85}Gd_{0.10}Lu_{0.05}O_{2-\delta}$ and $Ce_{0.85}Gd_{0.15}O_{2-\delta}$, so it may be reason for lower activation energy. The other samples have higher elastic strain and higher activation energy as compared to $Ce_{0.85}Gd_{1.0}Lu_{0.05}O_{2-\delta}$ and $Ce_{0.85}Gd_{0.15}O_{2-\delta}$ samples. These results are well matched with literature data [17] and [18]. From these results, it can be concluded that, the ionic conductivity is directly related to lattice distortion. Guan et al. [18] reported that, less distortion in pure ceria lattice causes decrease in activation energy and increased in electrical conductivity. Further, it demonstrates that, a co-dopant strategy can be used to increase electrical conductivity of ceria based electrolytes.

5.3 Relationship between observed elastic strain and electrical characteristics

A material internal strain is consists of elastic and plastic strain. An elastic strain is a type of strain in which the body returned to its original shape when the deforming

force is removed. An elastic strain is produced due to crystal lattice distortion whereas plastic strain is produced due to presence of dislocations [14].

In solid oxide fuel cell, fluorite structured oxide electrolytes are used such as YSZ, GDC, SDC etc. Due to charge compensation effects, oxygen vacancies are created by adding

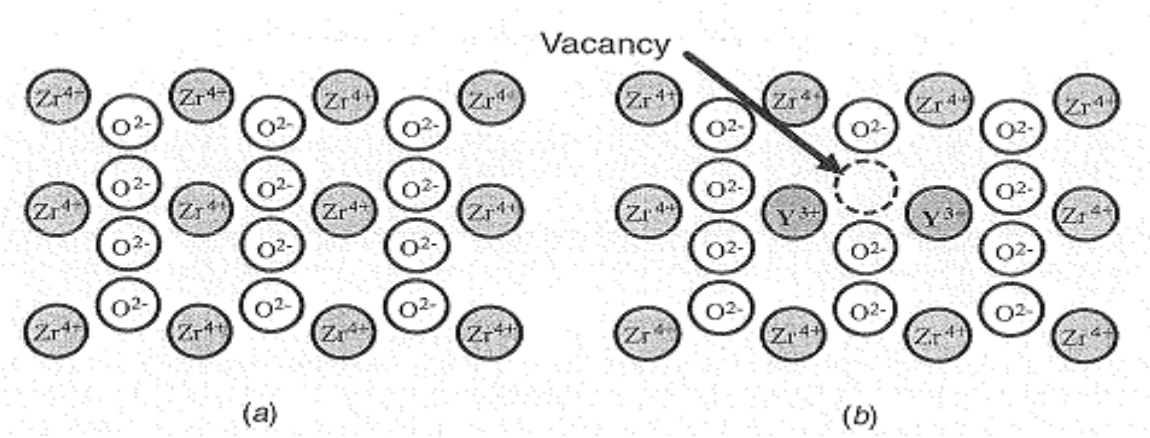

Figure 5. 9 View of the (111) plane in (a) pure zirconia (b) YSZ [15]

yttrium into zirconium as shown in fig. 5.9. An oxygen vacancy is created for every two Y^{3+} ions replacing Zr^{4+} ions. Due to electrostatic attraction between oppositely charged particles, the oxygen vacancies available in the structure are directly related to the acceptor dopant cations [15]. These charges are directly related to ionic radii. According to Kilner and Brook, maximum ionic conductivity can be obtained if there is minimum elastic strain available in the lattice of doped oxide electrolytes [16]. According to Kim, the critical ionic radius of ceria for trivalent dopant cation is 0.1038 nm [17]. Fig.5.10 shows the ionic conductivity of trivalent dopant cations. Gadolinium doped ceria has the highest ionic conductivity among all singly doped ceria electrolytes. This result is well matched with the ionic radius concept, as the ionic radius of Gd^{3+} is very close to the critical ionic radius of ceria.

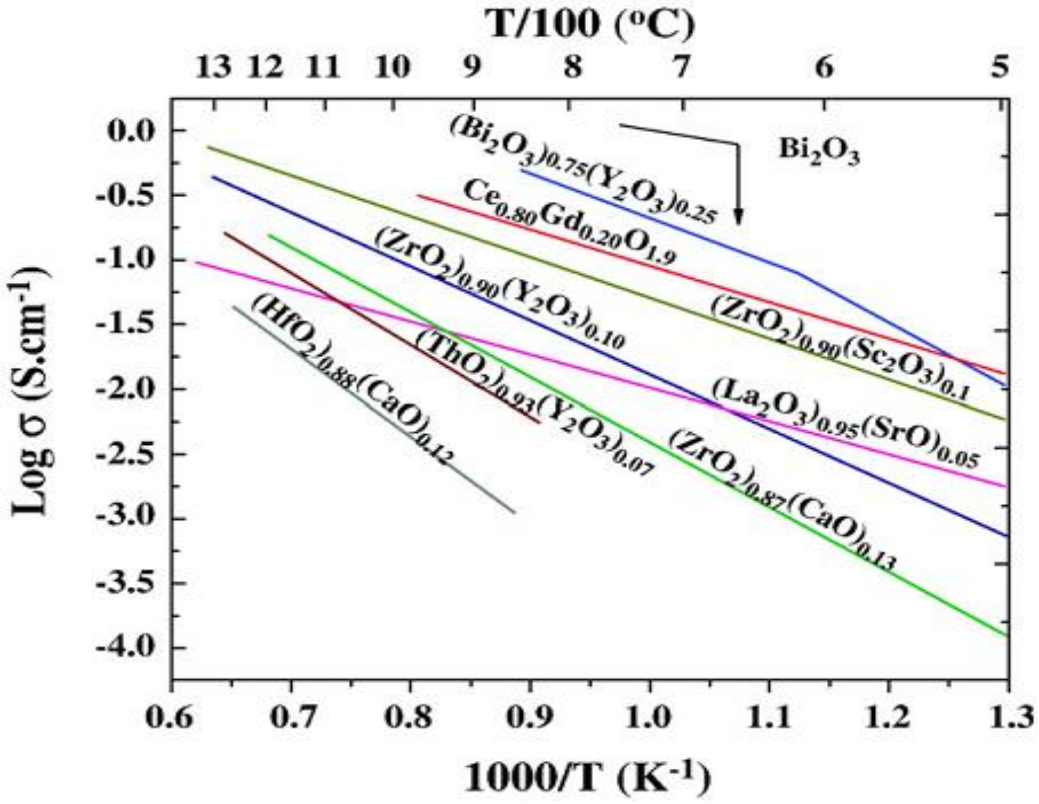

Figure 5. 10. Electrical conductivity of fluorite oxides [3]

Omar et al. [15] investigated the effect of elastic strain on the ionic conductivity of Lu and Nd co-doped ceria $Lu_xNd_yCe_{1-x-y}O_{2-\delta}$ (where x + y = 0.05, 0.10, 0.15 and 0.20) electrolytes. It was found that positive strain which is produced by introducing of larger dopant ion Nd^{3+} was balanced with the negative elastic strain produced by smaller dopant ion Lu^{3+}, and hence the grain ionic conductivity of $Lu_xNd_yCe_{1-x-y}O_{2-\delta}$ is larger than either of singly doped ceria $Lu_xCe_{1-x}O_{2-\delta}$ and $Nd_xCe_{1-x}O_{2-\delta}$ electrolytes [3].

The effect of dopant concentration on the elastic strain available in cubic fluorite crystal structure of doped ceria samples was calculated by using the following relation [18];

$$\text{Elastic strain} = (a_o - a) / a$$

where a_o is the lattice constant of doped ceria samples and a is the lattice constant of pure ceria CeO_2.

In this study, I have analyzed the effects of lutetium addition on gadolinium doped ceria $Ce_{0.85}Gd_{0.15-x}Lu_xO_{2-\delta}$ (x = 0.00, 0.05, 0.075, 0.10 and 0.15) electrolytes. In results, negative and positive elastic strain is seen as lutetium concentration varies from 0 to 0.15. There is a very small elastic strain present in $Ce_{0.85}Gd_{0.10}Lu_{0.05}O_{1.5}$

sample. The sample $Ce_{0.85}Gd_{0.10}Lu_{0.05}O_{1.5}$ gives dc conductivity value of 0.0217 (S/cm) at 600°C, which is slightly high than pure gadolinium doped ceria $Ce_{0.85}Gd_{0.15}O_{1.5}$ and very high than pure lutetium doped ceria $Ce_{0.85}Lu_{0.15}O_{1.5}$.

From results, it can be concluded that there is an inverse relation is seen between observed elastic strain and conductivity.

References

[1] L. L. Hench and J. K. West, “The sol-gel process,” Chem. Rev., vol. 90, no. 1, pp. 33–72, 1990.

[2] C. Frayret, A. Villesuzanne, M. Pouchard, and S. Matar, “Density functional theory calculations,” Int. J. Quantum Chem., vol. 101, no. 6, pp. 826–839, 2005.

[3] S. Omar, E. D. Wachsman, and J. C. Nino, “A co-doping approach towards enhanced ionic conductivity in fluorite-based electrolytes,” Solid State Ionics, vol. 177, no. 35–36, pp. 3199–3203, 2006.

[4] M. Anwar, Z. S. Khan, K. Mustafa, and A. Rana, “Effects of some rare earth and carbonate-based co-dopants on structural and electrical properties of samarium doped ceria (SDC) electrolytes for solid oxide fuel cells,” Int. J. Mod. Phys. B, vol. 29, no. 24, p. 1550179, 2015.

[5] M. Mogensen, N. M. Sammes, and G. A. Tompsett, “Physical, chemical and electrochemical properties of pure and doped ceria,” Solid State Ionics, vol. 129, no. 1, pp. 63–94, 2000.

[6] Y. Tsur and C. a Randall, “Maximum Likelihood Estimation Method,” vol. 66, no. 189376, pp. 2062–2066, 2000.

[7] M. A. Małecka, L. Kepiński, and M. Maczka, “Structure and phase composition of nanocrystalline Ce1-xLuxO2-y,” J. Solid State Chem., vol. 181, no. 9, pp. 2306–2312, 2008.

[8] M. A. Małecka, L. Kepiński, and W. Miśta, “Synthesis, structure and morphology of CeO2 and CeLnOx mixed oxides,” J. Alloys Compd., vol. 451, no. 1–2, pp. 567–570, 2008.

[9] A. Tschope and R. Birringer, “Grain Size Dependence of Electrical Conductivity in Polycrystalline Cerium Oxide,” J. Electroceramics, vol. 7, pp. 169–177, 2001.

[10] C. Milliken, “Properties and Performance of Cationâ€• Doped Ceria Electrolyte Materials in Solid Oxide Fuel Cell Applications,” J. Am. Ceram.Soc., vol. 86, no. 189049, pp. 2479–2486, 2005.

[11] M. Dudek, “Some Structural Aspects of Ionic Conductivity in Co-Doped Ceria-Based Electrolytes,” Arch. Metall. Mater., vol. 58, no. 4, pp. 1355–1359, 2013.

[12] X. W. Wang, J. G. Chen, Y. W. Tian, X. E. Wang, B. H. Zhang, and X. H. Chang, “Lattice strain dependent on ionic conductivity of Ce0.8+xY0.2−2xSrxO1.9 (x=0–0.08) electrolyte,” Solid State Ionics, vol. 296, pp. 85–89, 2016.

[13] X. Guan, H. Zhou, Y. Wang, and J. Zhang, “Preparation and properties of Gd3+ and Y3+ co-doped ceria-based electrolytes for intermediate temperature solid oxide fuel cells,” J. Alloys Compd., vol. 464, no. 1–2, pp. 310–316, 2008.

[14] Kilner, J. A., and R. J. Brook. "A study of oxygen ion conductivity in doped non-stoichiometric oxides." Solid State Ionics 6.3 (1982): 237-252.

[15] Kim, Dae-Joon. "Lattice Parameters, Ionic Conductivities, and Solubility Limits in Fluorite-Structure MO2 Oxide [M= Hf4+, Zr4+, Ce4+, Th4+, U4+] Solid Solutions." Journal of the American Ceramic Society 72.8 (1989): 1415-1421.

[16] Shannon, RD T. "Revised effective ionic radii and systematic studies of interatomic distances in halides and chalcogenides." Acta crystallographica section A: crystal physics, diffraction, theoretical and general crystallography 32.5 (1976): 751-767.

[17] Y. Tsur and C. a Randall, “Maximum Likelihood Estimation Method,” vol. 66, no. 189376, pp. 2062–2066, 2000.

[18] L. Zhang, L. Zhu, and A. V Virkar, “Electronic conductivity measurement of yttria-stabilized zirconia solid electrolytes by a transient technique,” J. Power Sources, vol. 302, pp. 98–106, 2016.

Conclusions

In this study, gadolinium doped ceria (GDC) electrolyte was successfully synthesized by sol-gel and co-precipitation methods. It was found that both the prepared samples have single phase with cubic fluorite structure. The co-precipitation synthesis resulted in better control on crystallite size in comparison to that by sol-gel route. DC conductivity results showed that GDC prepared by sol-gel method has slightly higher value of conductivity and lower activation energy.

Meanwhile, effects of lutetium (Lu) addition on gadolinium doped ceria (GDC) electrolytes were also studied. Gd^{3+} and Lu^{3+} co-doped ceria $Ce_{0.85}Gd_{0.15-x}Lu_x O_{2-\delta}$ samples (x = 0.00, 0.05, 0.075, 0.10 and 0.15) were synthesized by solid state reaction method. All the synthesized materials were found to be single phase with cubic fluorite structure. The reflection from (111) plane was used to measure the most intense peak crystallite sizes. The elastic strain present in the $Ce_{0.85}Gd_{0.10}Lu_{0.05}O_{2-\delta}$ sample is found to be negligible as compared to singly doped Gd^{3+} and Lu^{3+} samples. SEM images reveal that all the samples consist of well separated particles without large agglomeration. The electrical conductivity of co-doped ceria samples were found to be improved as compared to singly doped ceria. Among all, the sample co-doped with 5 mol% Lu^{3+} and 10 mol % Gd, showed the best conductivity performance. It suggests that the co-doping with Gd^{3+} and Lu^{3+} with a suitable ratio that is closed to critical ionic radius of ceria can further improve the conductivity performance.

Recommendations

Gadolinium doped ceria (GDC) is one of the most promising candidate for intermediate temperature solid oxide fuel cells. In this research, GDC with a formula of $Ce_{0.85}Gd_{0.15}O_{1.5}$ (GDC15) was successfully synthesized by sol gel and co-precipitate methods. In the case of yttria stabilized zirconia (YSZ), 8YSZ is the foremost composition for SOFC, but still in GDC there is no standard composition has been achieved. There is a need to synthesize GDC with different composition to achieve standard ratio between cerium and gadolinium. It is suggested that GDC with different compositions GDC5, GDC10, GDC20 and GDC25 etc. should be synthesized and compared to achieve maximum results.

Moreover, we have synthesized Gd and Lu co-doped ceria electrolytes with three different compositions and observed a little bit elastic strain present in the samples, however, by changing Gd and Lu ratio, a free elastic strain sample can be achieved which will definitely a novel work in co-doped ceria electrolytes. The effects of Lutetium (Lu) addition on GDC have been analyzed by dc LCR mater. DC LCR meter measured dc conductivity and we calculated ionic conductivity by theoretical approximations. As Lutetium addition on GDC is a novel approach, so it is suggested that, these electrolytes must be analyzed by Electrochemical Impedance Spectroscopy (EIS) or AC LCR meter to accumulate the frequency response.

Socio-economic aspects of solid oxide fuel cell technology by using GDC and LGDC electrolytes

Solid oxide fuel cell is a high temperature fuel cell working in the temperature range of 800 to 1000 ˚C. Due to operating at high temperature it has various advantages such as fuel flexibility, high efficiency and environmental friendly. Yttria stabilized zirconia (YSZ) is mostly used as an electrolyte for SOFC, which is operated in the temperature range of 800 to 1000 ˚C.

Due to operating at high temperature, various design issues arise such as sealing and reducing lifetime etc. High cost is the major hindrance for a fuel cell to widely deployed, which is produced due to operating at high temperature. Scientists are in a quest to synthesize/design new materials that operate at low to intermediate temperature range (500 – 800 ˚C). Economic feasibility of a fuel cell technology depends on various factors such as abundancy and low cost extraction of raw materials, large scale manufacturing, and large lifetime.

In this study, I have synthesized ceria based electrolytes which are operated at low to intermediate temperature range (500 – 800 ˚C). This is the key difference between zirconia and ceria based electrolytes. In zirconia based electrolytes, YSZ is mostly used whereas, in case of ceria, gadolinium doped ceria (GDC) and samarium doped ceria (SDC) are mostly used as an electrolytes. GDC gives the ionic conductivity value of 0.025 S/cm at 600 ˚C, whereas YSZ gives the same value at 800 ˚C and it is highly reduced at 700 ˚C. If GDC can be used practically in SOFC, the cost of the system may be reduced and in the result the technology may become economically feasible.

According to literature, doubly doped ceria gives the higher conductivity than singly doped ceria electrolytes. Due to this reason, I have checked the effects of lutetium addition on gadolinium doped ceria (LGDC) electrolytes. LGDC gives the higher conductivity value than singly doped GDC and LDC at 600 ˚C.

Solid oxide fuel cells are future energy devices, because they give 90 % efficiency in combined heat and power systems. On the other hand, the whole world is facing global warming, ozone depletion, acid rain and air pollution due to incomplete

combustion of a carbonaceous fuel. Whereas, in a SOFC, hydrogen is mostly used as a fuel and like electricity it is a high quality energy carrier with very high efficiency and nearly zero emission.

Therefore, synthesis and development efforts of novel materials in SOFC technology should be continued as this technology has the potential to be environmental friendly as well as economically feasible.

Annexure I

4th International Conference on Energy, Environment and Sustainable Development 2016 (EESD 2016)

Investigations on Gadolinium doped Ceria (GDC) electrolyte prepared via sol-gel and co-precipitation routes for intermediate temperature solid oxide fuel cell (IT-SOFC) applications

Muzammal Zulfqar, Muhammad Raza Shah, Zuhair S. Khan[1]

US-Pakistan Center for Advance Studies in Energy(USPCAS-E) NUST, Islamabad 44000,Pakistan

Abstract

Yttria Stabilized Zirconia (YSZ) is the common material used as an electrolyte for high temperature solid oxide fuel cells (SOFC). Due to high operating temperature, various design issues arise. Therefore, low to intermediate temperature solid oxide fuel cells (SOFCs) are actively being developed. Ceria based materials are among the best options for intermediate temperature SOFC (500-800˚C). We have carried out successful synthesis of Gadolinium doped Ceria (GDC) electrolyte material with a formula $Ce_{1-x}Gd_xO_{2-x/2}$ (x=0.15) by two different techniques namely sol-gel and co-precipitation. Both techniques have the advantages of high phase purity, homogeneity and low processing temperatures along with strong control on crystallite size. The synthesized materials were characterized by X-ray Diffraction, Scanning Electron Microscopy with EDX etc. We have detected a cubic fluorite structure for both synthesized compounds. The co-precipitation synthesis resulted in better control on crystallite size in comparison to that by sol-gel route. The average particle size was found to be in the range of 40-70 nm. The electrical conductivity of the GDC pellet was measured in the temperature range of 220-660 ˚C in air by using two probe LCR meter. GDC pellet synthesized by sol-gel method was found to has highest conductivity value of 2.17×10^{-4} S/cm at 600 ˚C with activation energy of 0.31 keV.

* Corresponding author. Tel.: +92 51 9085 5276.
E-mail address: zskhan@ces.nust.edu.pk

Annexure I

4th International Conference on Energy, Environment and Sustainable Development 2016 (EESD 2016)

Keywords: IT-SOFC;sol-gel;co-precipitation

1. Introduction

SOFC working at high temperature causes many issues like sealing, long start up time etc., which results in high cost and maintenance problems[1]. There is a need to synthesize a low temperature electrolyte to overcome these problems. Ceria is the best option for low to intermediate temperature SOFC electrolyte. Pure ceria has low ionic conductivity and mechanical strength[2]. But, it can be increased when it is doped with some rare earth or alkaline earth materials[3]. Among various rare earth elements reported as dopant, gadolinium is one of the most suitable dopant[4]. Conductivity value mainly depends on the ionic radius, material that has closed the ionic radius with ceria exhibit high conductivity value[5]. According to literature a smaller mismatch in size between host and dopant ion gives maximum value of conductivity[6]. A critical ionic radius for ceria is 1.038Å. Gadolinium Gd^{3+} has the ionic radius of $r^{3+}_{Gd,\ VIII}$ = 1.053Å. As the Gd^{3+} ionic radius is very close to critical ionic radius of ceria, so GDC gives maximum value of conductivity and it is a suitable dopant for ceria[7]. GDC electrolyte prepared by solid state method showed the conductivity value of 0.1 S/cm at 1023 K and activation energy Ea of 0.9 eV[8]. Similarly GDC synthesized by a citrate-nitrate combustion method showed very promising results at low temperatures. GDC pellet sintered at 1300 ˚C had relative density of 97 % and conductivity value of 1.27×10^{-2} S/cm at 600 ˚C[9]. Numerous techniques have been used for the preparation of GDC electrolyte such as hydrothermal, conventional solid state, co-precipitation, spray and freeze drying and sol-gel[10], [11]. Among various synthesis techniques wet chemistry route mainly sol-gel and co-precipitation shows very promising results with low processing temperature, homogeneity and purity[12].

Annexure I

4th International Conference on Energy, Environment and Sustainable Development 2016 (EESD 2016)

The present study deals with the synthesis of GDC electrolyte by two different methods namely sol-gel and co-precipitation. The detailed analysis of morphological, structural and electrical properties of prepared GDC electrolyte was carried out.

2. Experimentation

2.1. Sol-gel method

The sample with a general formula of $Ce_{1-x}Gd_xO_{2-x/2}$ (x=0.15) was synthesized by sol-gel method. The precursor of cerium nitrate hexahydrate and gadolinium nitrate hexahydrate were used as starting materials. Stoichiometric amounts of Gd $(NO_3)_3.6H_2O$ and Ce $(NO_3)_3.6H_2O$ were dissolved in de-ionized water separately. Then Gd $(NO_3)_3.6H_2O$ was added in Ce $(NO_3)_3.6H_2O$ drop wise with continuous stirring. Stoichiometric amount of anhydrous citric acid was also dissolved in de-ionized water. The composition of total oxide to citric acid was 1:1. For better results, both solutions were mixed drop wise in a separate beaker with continuous stirring. To get homogenizing mixture, the sample was stirred for 10 hours. After complete mixing, the temperature was raised to 80˚C with continuous stirring to remove extra water and to form a gel. As the temperature increases, the solution become more viscous and after 4 hours a transparent gel was formed. Then put beaker in a dry place for 24 hours. Because, during aging polycondensation continues which increase the thickness and decrease porosity[13]. The gel was then dried in an oven at 120 ˚C for several hours for complete drying. After drying, the sample was ground using agate mortar to get a fine powder. The fine powder was than calcined at 600 ˚C for 4 h.

2.2. Co-precipitation method

The ceramic electrolyte with the formula of $Ce_{1-x}Gd_xO_{2-x/2}$ (x=0.15) was synthesized by co-precipitation method. The precursor of Cerium nitrate hexahydrate and gadolinium nitrate hexahydrate were used. Stoichiometric amounts of gadolinium nitrate hexahydrate and cerium nitrate hexahydrate were dissolved in de-ionized water separately. The

concentration of the precursor solution was 1M. Then mix both the solution in a separate beaker with continuous stirring at hot plate. After homogenizing mixing, added ammonium hydroxide drop wise in the solution with continuous stirring, until precipitation occurred. After precipitation raise the temperature to 200˚C to dry the slurry type sample with continuous stirring at hot plate. Pale yellow matter was obtained after complete drying. Then ground the sample by using agate mortar to obtain a fine powder. The fine powder was calcined at 600 ˚C for 4 hours.

Crystal structure and phase formation of the calcined samples were analyzed by X-ray Diffraction equipment (STOE Germany). X-ray powder diffractogram of the calcined sample was recorded using CuKα radiation (λ=1.5425Å) with 2θ values ranging from 20˚ to 80˚. The morphology of the samples was observed by scanning electron microscopy (JEOL Analytical SEM). The average grain size was measured from higher magnification SEM images. For conductivity measurement a pellet with a thickness of 2 mm and diameter of 10 mm was formed using a hydraulic press. The pellet was sintered at 1000 ˚C for 4 hours for conductivity measurement the pellet was sintered at 1050 ˚C for 4 hours. DC conductivity was measured by LCR meter (Wayne Kerr precision analyzer 6440B) in the temperature range of 200 – 600 ˚C.

3. Results and Discussion

3.1. XRD Patterns

Fig.1 shows the XRD pattern of Gadolinium doped Ceria (GDC) powder synthesized by two different methods, namely sol-gel and co-precipitation. The XRD pattern revealed the formation of cubic $Gd_{0.15}Ce_{0.85}O_{1.5}$ in all samples. All peaks are associated to cubic fluorite crystal structure with the space group Fm-3m (225) (PDF Card No. 75-0161). XRD peaks positioned at 2 theta values of 28.40˚, 32.95˚, 47.28˚, 56.16˚, 58.99˚, 69.32˚, 76.51˚, and 78.95˚ corresponding to (111), (200), (220), (311), (222), (400), (331) and

(420) crystallographic planes, matching well according to the pattern JCPDS 75-0161. There are no other phases formed in sol-gel and co-precipitation methods.

From diffractogram, it can be seen that the intensity of (111) peak is maximum in all samples. The interplaner spacing d and lattice parameter of all samples are calculated by JADE 6.0 software. The reflection from (111) plane is used to measure the crystallite size D, calculated from the Sherrer formula

$$D = 0.9 \times \lambda \ / B \times \cos(\theta)$$

Where 'θ' is the diffraction angle, 'λ' is the wavelength of X-rays, and B is the full width at half maximum intensity.

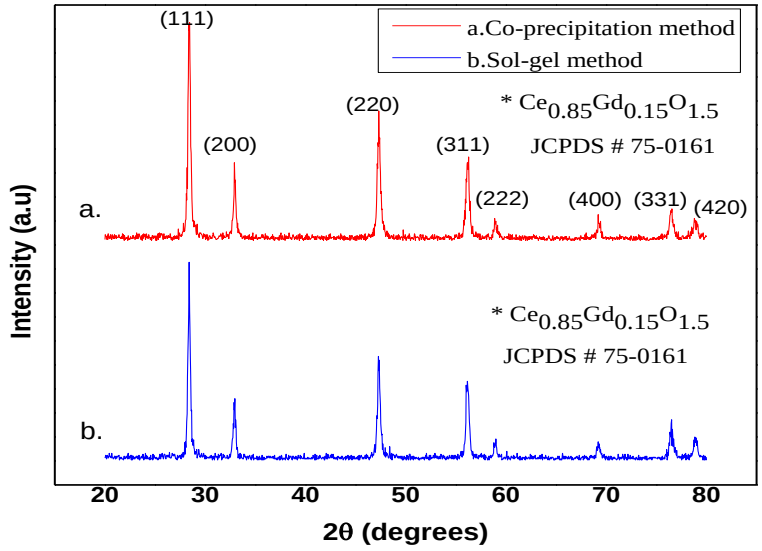

Fig.1. XRD patterns of 15 mol% GDC calcined at 600 ˚C for 4h prepared by sol-gel and co-precipitation methods.

Table 1 shows the crystallite size 'D' of GDC prepared by both methods. From table, it can be concluded that, GDC prepared from sol-gel method has crystallite size slightly

larger than that of GDC prepared by sol-gel method. There is a good agreement with SEM results of both the samples. The peaks of sample prepared by co-precipitation are relatively broad as compared to sample prepared by sol-gel, due to small crystallite size. The XRD pattern showed that GDC electrolyte prepared by two different methods have same phase and structure.

Table 1. Results based on XRD

Method	**Composition**	**Crystallite size (nm)**
Sol-gel	$Gd_{0.15}Ce_{0.85}O_{1.5}$	53
Co-precipitation	$Gd_{0.15}Ce_{0.85}O_{1.5}$	40

3.2. Surface Morphology

Fig. 2 shows the micrographs of GDC electrolyte synthesized by sol-gel and co-precipitation. SEM micrograph shows the particles are well dispersed and in a round shape. In fig. 2a the particles prepared via sol-gel method have nearly homogeneous size distribution without definite big agglomerate. The particles prepared by co-precipitation have high rate of agglomeration, but all the particles forming agglomeration are highly uniform. The particles size ranges from 50 to 70 nm by sol-gel and from 40 to 60 by co-precipitation. So by co-precipitation method, the particles are larger, fewer and denser then by sol-gel method[14].

(a) 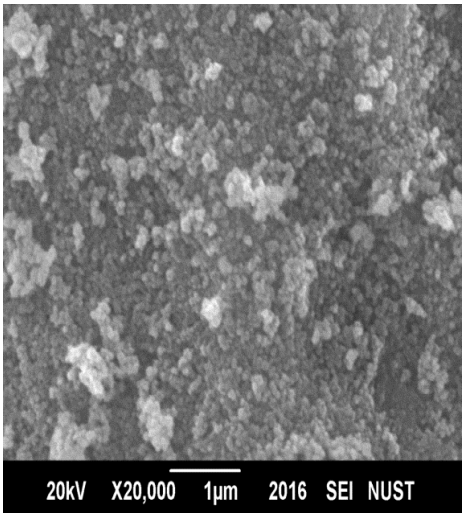

(b) 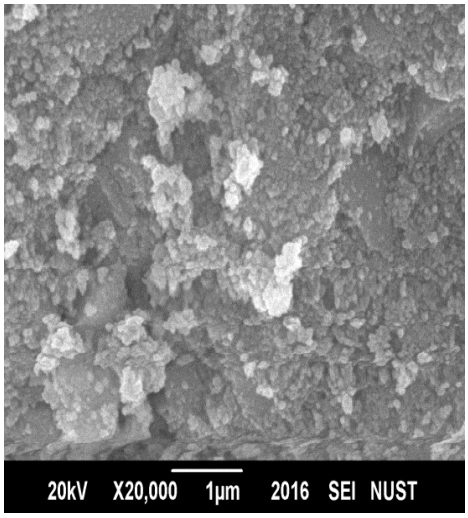

Fig.2. SEM Images of $Gd_{0.15}Ce_{0.85}O_{1.5}$ by sol-gel (a) and by co-precipitation (b)

It can also be concluded that the Ostwald's ripening is increased by increasing the pH of the solution[15]. Fig. 2 shows the EDS analysis of the prepared samples. There is no other element found in EDS analysis except O, Ce and Gd. The intense peaks of Gd, Ce and O are present, which confirms the purity of GDC powders. The atomic percentage of cerium and gadolinium are higher in the sample prepared by co-precipitation method as shown in Fig. 3(a, b).

3.3 DC Conductivity Measurement:

The DC conductivity was measured by two probe method with LCR meter (Wayne Kerr precision analyzer 6440B) in the temperature range of 200 – 600 ˚C. Fig.4. shows the typical Arrhenius plots of ln (σT) versus 1000/T. The changes in dc conductivity calculated from the bulk resistance and sample dimensions with temperature. The dc conductivity obeys the Arrhenius behaviour

$$\sigma_{dc} = \sigma_o \exp (- Ea / kT)$$

Where k is the Boltzmann's constant, T is the absolute temperature, σ_o is the pre-exponential factor and Ea is the activation energy [13].

4th International Conference on Energy, Environment and Sustainable Development 2016 (EESD 2016)

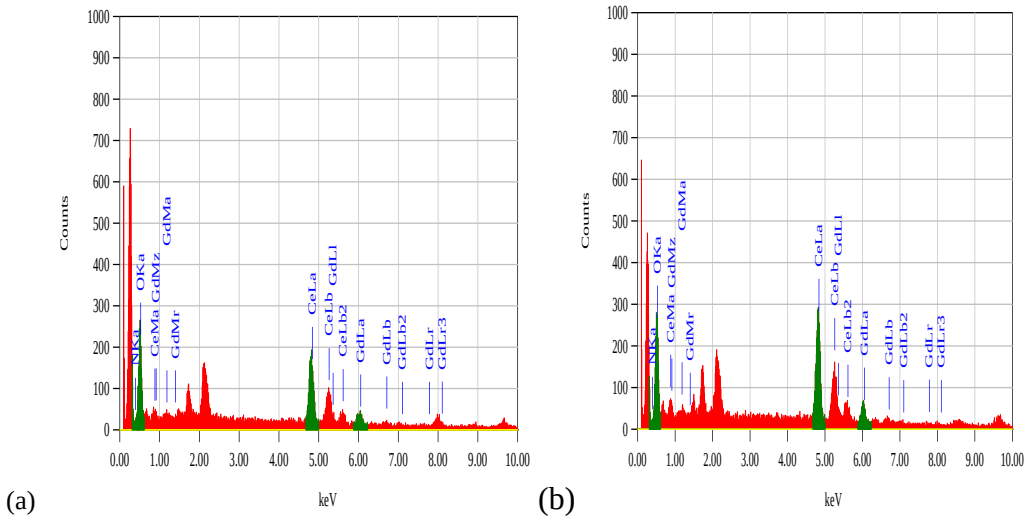

Fig.3. EDS spectra of $Gd_{0.15}Ce_{0.85}O_{1.5}$ by sol-gel (a) and by co-precipitation (b)

Conductivity curve of both the samples consist of two linear parts. Initially the

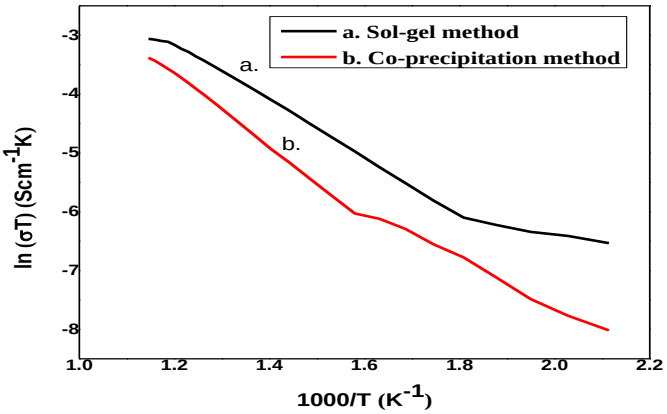

Fig.4. DC conductivity curves of $Gd_{0.15}Ce_{0.85}O_{1.5}$ by sol-gel (a) and by co-precipitation

conductivity value is very low form 200 to 280 ˚C in the sample prepared by co-precipitation method. At 280 ˚C, the conductivity value becomes higher because the electrons move fast due to low resistance. After 280 to 600 ˚C, the conductivity curve is almost linear and it increases with the temperature increases. Similarly, GDC prepared by

sol-gel method showed very low conductivity from 200 to 240 ˚C and from 240 to 600 ˚C the conductivity curve is almost linear. GDC prepared by sol-gel method showed the conductivity value of 2.17×10^{-4} (S/cm) at 600 ˚C with activation energy Ea value of 0.31 keV. And GDC prepared by co-precipitation showed the conductivity value of 1.03×10^{-4} (S/cm) at 600 ˚C with activation energy of 0.36 keV slightly lower than by sol-gel method.

4. Conclusion

GDC electrolyte was successfully synthesized by sol-gel and co-precipitation methods. It was found that both the prepared samples have single phase with cubic fluorite structure. The co-precipitation synthesis resulted in better control on crystallite size in comparison to that by sol-gel route. DC conductivity results showed that GDC prepared by sol-gel method has slightly higher value of conductivity and lower activation energy.

Acknowledgement:

The authors would like to thank School of Chemical and Materials Engineering (SCME), National University of Science and Technology (NUST) Islamabad and COMSATS for their support in carrying out the experiments.

Annexure I

4th International Conference on Energy, Environment and Sustainable Development 2016 (EESD 2016)

References

[1] N. Mahato, A. Banerjee, A. Gupta, S. Omar, and K. Balani, "Progress in material selection for solid oxide fuel cell technology: A review," Prog. Mater. Sci., vol. 72, pp. 141–337, 2015.

[2] M. Mogensen, N. M. Sammes, and G. A. Tompsett, "Physical, chemical and electrochemical properties of pure and doped ceria," Solid State Ionics, vol. 129, no. 1, pp. 63–94, 2000.

[3] V. V Kharton, "Ceria-based materials for solid oxide fuel cells," vol. 6, pp. 1105–1117, 2001.

[4] E. For, I. Temperature, S. Oxide, and F. Cells, ") and grain boundary (D," 2015.

[5] S. (Rob) Hui, J. Roller, S. Yick, X. Zhang, C. Decès-Petit, Y. Xie, R. Maric, and D. Ghosh, "A brief review of the ionic conductivity enhancement for selected oxide electrolytes," J. Power Sources, vol. 172, no. 2, pp. 493–502, 2007.

[6] S. Omar, E. D. Wachsman, and J. C. Nino, "A co-doping approach towards enhanced ionic conductivity in fluorite-based electrolytes," Solid State Ionics, vol. 177, no. 35–36, pp. 3199–3203, 2006.

[7] M. G. Chourashiya, J. Y. Patil, S. H. Pawar, and L. D. Jadhav, "Studies on structural, morphological and electrical properties of Ce1-xGdxO2-(x/2)," Mater. Chem. Phys., vol. 109, no. 1, pp. 39–44, 2008.

[8] X. Li, Z. Feng, J. Lu, F. Wang, M. Xue, and G. Shao, "Synthesis and electrical properties of Ce 1-xGd xO 2-x/2 (x = 0.05-0.3) solid solutions prepared by a citrate-nitrate combustion method," Ceram. Int., vol. 38, no. 4, pp. 3203–3207, 2012.

[9] C. Veranitisagul, A. Kaewvilai, W. Wattanathana, N. Koonsaeng, E. Traversa, and A. Laobuthee, "Electrolyte materials for solid oxide fuel cells derived from metal complexes: Gadolinia-doped ceria," Ceram. Int., vol. 38, no. 3, pp. 2403–2409, 2012.

Annexure I

4th International Conference on Energy, Environment and Sustainable Development 2016 (EESD 2016)

[10] F. Aydin, I. Demir, and M. Dursun, "Engineering Science and Technology , an International Journal Effect of grinding time of synthesized gadolinium doped ceria (GDC 10) powders on the performance of solid oxide fuel cell," Eng. Sci. Technol. an Int. J., vol. 17, no. 1, pp. 25–29, 2014.

[11] D. Wattanasiriwech and S. Wattanasiriwech, "Effects of Fuel Contents and Surface Modification on the Sol-gel Combustion Ce0.9 Gd0.1O1.95 Nanopowder," Energy Procedia, vol. 34, pp. 524–533, 2013.

[12] L. Fan, C. Wang, M. Chen, and B. Zhu, "Recent development of ceria-based (nano)composite materials for low temperature ceramic fuel cells and electrolyte-free fuel cells," J. Power Sources, vol. 234, pp. 154–174, 2013.

[13] L. L. Hench and J. K. West, "The sol-gel process," Chem. Rev., vol. 90, no. 1, pp. 33–72, 1990.

[14] C. Frayret, A. Villesuzanne, M. Pouchard, and S. Matar, "Density functional theory calculations on microscopic aspects of oxygen diffusion in ceria-based materials," Int. J. Quantum Chem., vol. 101, no. 6, pp. 826–839, 2005.

[15] J. L. M. Rupp, E. Fabbri, D. Marrocchelli, J. W. Han, D. Chen, E. Traversa, H. L. Tuller, and B. Yildiz, "Scalable oxygen-ion transport kinetics in metal-oxide films: Impact of thermally induced lattice compaction in acceptor doped ceria films," Adv. Funct. Mater., vol. 24, no. 11, pp. 1562–1574, 2014.

Annexure II

Under Review in Journal of Electroceramics

Effect of lutetium (Lu) as a co-dopant on structural and electrical properties of gadolinium doped ceria (GDC) electrolyte for IT-SOFC applications

Muzammal Zulfqar, Zuhair S. Khan*

US-Pakistan Center for Advance Studies in Energy (USPCAS-E) NUST, Islamabad 44000, Pakistan

---

Abstract

In the present study, the effect of lutetium (Lu) addition on structure, morphology and electrical properties of gadolinium doped ceria (GDC) electrolyte is investigated. Gd and Lu co-doped ceria $Ce_{0.85}Gd_{0.15-x}Lu_xO_{2-\delta}$ (at x = 0.00, 0.05, 0.075, 0.10 and 0.15) electrolytes were synthesized by solid state reaction method. The structural and morphological properties of the prepared co-doped samples were characterized by x-ray diffraction (XRD) and scanning electron microscopy (SEM). All the synthesized materials were found to be single phase with cubic fluorite structure. The most intense peak crystallite size was calculated by Scherrer equation for all samples. The elastic strain present in the $Ce_{0.85}Gd_{0.10}Lu_{0.05}O_{2-\delta}$ sample is found to be negligible as compared to singly doped Gd and Lu samples. The grain sizes were examined by SEM images and it is found to be in the range of 30-60 nm. The electrical conductivity as a function of temperature and compositions were measured in air in the temperature range of 200 to 600°C and found to be linearly rising with the increase in temperature. The electrical conductivity of samples varies with the increase in dopant (Lu) content. The maximum conductivity was observed to be 0.0217 S/cm at 600°C for $Ce_{0.85}Gd_{0.10}Lu_{0.05}O_{2-\delta}$ sample, which is slightly higher than that for pure gadolinium doped ceria $Ce_{0.85}Gd_{0.15}O_{2-\delta}$ and quite higher than for pure lutetium doped ceria $Ce_{0.85}Lu_{0.15}O_{2-\delta}$.

Keywords: IT SOFC; Conductivity; Ceria; Co-doping; Solid-state

1. Introduction

Annexure II

Under Review in Journal of Electroceramics

Solid oxide fuel cells (SOFCs) have attracted a great attention due to its higher conversion efficiency, high waste heat utilization, greater fuel flexibility and the ability of environmental friendship [1]. ZrO_2 based electrolyte mostly doped with Yttria (Y) is commonly used as an electrolyte material for SOFC, requires high operating temperature (i.e. ~ 1000°C), which causes various issues such as high cost of materials, long start up time and durability etc. [2]. By reducing the thickness of YSZ electrolyte the operating temperature of YSZ can be minimized. But, there are various practical issues and limitations to reducing the thickness of YSZ electrolyte, such as at a certain thickness YSZ works at best, but further reducing the layer gets no benefit [3]. Furthermore, at 1000°C the ionic conductivity of 8YSZ is 0.178 (S/cm), but at 800°C it reduces to 0.012 (S/cm) [4]. Instead of decreasing the thickness of an electrolyte, there are other materials available that are operated at low or intermediate temperatures (400 – 800°C) such as doped ceria, bismuth oxide and doped lanthanum gallate [2]. Various investigations have been made to analyze the pros and cons of these electrolyte materials, but among all doped ceria is one of the most promising electrolyte materials for low to intermediate temperature SOFCs [2], [3] and [5].

Pure ceria has low ionic conductivity and mechanical strength, but it can be increased when it is doped with some rare earth or alkaline earth materials [6]. Gadolinium doped ceria $Ce_{0.9}Gd_{0.1}O_{1.5}$ (GDC) synthesized by a citrate complexation method has the total conductivity of 0.0192 (S/cm) at 600°C, which is very high as compared to YSZ at this temperature [7]. Similarly, $Ce_{1-x}Nd_xO_{2-x}$ (NDC) [8], $Ce_{1-x}Sm_xO_{2-x}$ (SDC) [9], $Ce_{1-x}Y_xO_{2-x}$ (YDC) [10], $Ce_{1-x}Lu_xO_{2-x}$ (LDC) [11] and $Ce_{1-x}Er_xO_{2-x}$ (EDC) [12] etc. at various compositions have been studied and show high oxide ionic conductivity as compared to YSZ at the same temperature. Among various dopants have been studied, Gd^{3+} and Sm^{3+} are considered as most potential dopants for ceria based electrolytes for low to intermediate temperature (400 – 800°C) SOFCs.

A co-doping approach has also been conducted to further increase various key properties of ceria based electrolytes including conductivity and stability etc., and it showed very

promising results. Dikmen [13] synthesized $Ce_{0.8}Gd_{0.2-x}M_xO_{2-\delta}$ (where M = Sm, Nd and Bi) by hydrothermal method which showed significantly higher oxide ion conductivity than singly doped ceria electrolytes with single phase structure. Ramesh et al. [14] prepared praseodymium and gadolinium co-doped ceria electrolyte with a formula $Ce_{1-x}(Gd_{0.5}Pr_{0.5})_xO_2$ (where x = 0 - 0.24) by sol-gel method. The composition $Ce_{0.84}(Gd_{0.5}Pr_{0.5})_{0.16}O_2$ showed the 11.5 % higher oxide ionic conductivity at 500°C than singly prepared $Ce_{0.9}Gd_{0.1}O_2$ electrolyte. Omar et al. [15] investigated the effect of elastic strain on the ionic conductivity of Lu and Nd co-doped ceria $Lu_xNd_yCe_{1-x-y}O_{2-\delta}$ (where x+y = 0.05, 0.10, 0.15 and 0.20) electrolytes. It was found that positive strain which is produced by introducing of larger dopant ion Nd^{3+} was balanced with the negative elastic strain produced by smaller dopant ion Lu^{3+}, and hence the grain ionic conductivity of $Lu_xNd_yCe_{1-x-y}O_{2-\delta}$ is larger than either of singly doped ceria $Lu_xCe_{1-x}O_{2-\delta}$ and $Nd_xCe_{1-x}O_{2-\delta}$ electrolytes. Various attempts have been made on co-doping strategy, such as $Ce_{0.8}La_{0.2-x}Y_xO_{1.9}$ [16] ,$Ce_{0.8}Gd_{0.2-x}La_xO_{2-\delta}$ [17], $Ce_{0.8}Gd_{0.2-x}Nd_xO_{2-\delta}$ [13], $Ce_{1-a}Gd_{a-y}Sm_yO_{2-0.5x}$ [18], $Ce_{1-x}Gdx\text{-}yY_yO_{2-0.5x}$ [19] etc., the results demonstrated that co-doping is the effective way to improve electrical properties of ceria based electrolytes. Considering the elastic strain, conductivity and possible co-doping effect, Gd^{3+} and Lu^{3+} co-doped ceria materials might be better electrolytes for intermediate temperature solid oxide fuel cell.

It is interesting to know about the changes in electrical conductivity and activation energy of Gd^{3+} and Lu^{3+} co-doped ceria electrolyte materials with various compositions. However, to the best of our knowledge, there is a lack of systematic studies reported on these co-doped materials. Hence in this paper with the aim to develop new electrolyte materials for IT-SOFCs, Gd^{3+} and Lu^{3+} co-doped ceria electrolytes were synthesized by solid state reaction method. The effect on structure, morphology and electrical properties of co-doped ceria were investigated and also compared with singly doped $Ce_{0.85}Gd_{0.15}O_{2-\delta}$ and $Ce_{0.85}Lu_{0.15}O_{2-\delta}$ materials.

2. Experimental

Annexure II

Under Review in Journal of Electroceramics

2.1 Sample preparation

A series of samples with a chemical formula of $Ce_{0.85}\,Gd_{0.15-x}\,Lu_x\,O_{2-\delta}$ (x = 0.00, 0.05, 0.075, 0.10 and 0.15) were synthesized by solid state reaction method. Cerium oxide (CeO_2), Gadolinium oxide (Gd_2O_3) and Lutetium oxide (Lu_2O_3) were used as starting materials. The calculated amounts of all of these materials were ground using agate mortar and pestle. An appropriate amount of ethanol was also added for homogenizing mixture. After well mixing, the samples were dried at 120˚C for 8 hours. The dried samples were ground and then calcined at 1200˚C for 4 hours in a muffle furnace. The samples were allowed to cool at room temperature in the same muffle furnace. The samples were ground again to obtain a fine powder. The obtained fine powder was used for XRD and SEM analysis. For electrical properties the grinded powder of all the samples then pressed into cylindrical pellets (diameter = 10mm and thickness = 2mm) under a pressure of 20 MPa with the help of hydraulic press. The pellets were then sintered at 1400˚C for 4 hours.

2.2 Characterization

Crystal structure and phase formation of all the samples calcined at 1200˚C for 4 hours were analyzed by X-ray Diffraction equipment (STOE Germany). X-ray diffractogram of all the samples were recorded with computer interface using Cu Kα at λ = 1.5418 Å at scan angle ranging from 20˚ to 80˚ with step size 0.04 / sec. the reflection peaks were recorded using accelerated voltage of 20 kV and a current of 5 mA. The average and most intense peak crystallite size was calculated using Sherrer formula by measuring β (full width half maximum intensity). Scanning electron microscopy (JEOL Analytical SEM) was used to observe the morphology of all the samples. The average grain size was measured from higher magnification SEM images.

The surface of the sintered pellet was carefully cleaned and then two electrodes were attached on the surface of the pellet for conductivity measurements. The pellet along with two electrodes on both sides was then inserted into an evacuated ceramic rod attached with tube furnace. Then the variations of resistance were recorded in the temperature

range of 200 to 600˚C with the help of Wayne Kerr LCR meter (precision analyzer 6440B) at 1V applied voltage. By applying small DC voltage (1V) on the surface of one electrode, ions are pumped on the surface of another electrode. After recording the resistance values along temperature, the dimension of the pellet was measured. These dimensions and values of resistance were then used to measure the resistivity of the pellet and then from resistivity, dc conductivity was calculated.

3. Results and Discussions

3.1 X-ray diffraction analysis

Fig. 1 (a) shows the XRD patterns of the as prepared $Ce_{0.85}Gd_{0.15-x}Lu_xO_{2-\delta}$ samples (x = 0, 0.05, 0.075, 0.10 and 0.15) calcined at 1200˚C for 4 hours. All sample peaks are associated to cubic fluorite crystal structure with the space group Fm-3m (225). XRD peaks positioned at 2 theta values corresponding to crystallographic planes, matching well according to the pattern of pure ceria CeO_2 with JCPDS File No. 34-0394. There is no other phase found in all samples. From diffractogram, it can be seen that the intensity of (111) peak is maximum in all samples. The reflection from (111) plane is used to measure the most intense peak crystallite size $D_{(111)}$. The most intense peak crystallite size $D_{(111)}$ is calculated from Scherrer formula,

$$D = \frac{0.9 \times \lambda}{\beta \times \mathrm{Cos}\theta} \quad \ldots\ldots\ldots\ldots 2$$

where D is the crystallite size, λ is the wavelength of x-rays, θ is the diffraction angle and β is the full width at half maximum intensity in radians. The interplaner spacing d and lattice parameter of all the samples are calculated using JADE 6.0 software by fitting the peak data of ceria phase. The crystallite sizes relative to most intense peak are given in Table1.

Annexure II

Under Review in Journal of Electroceramics

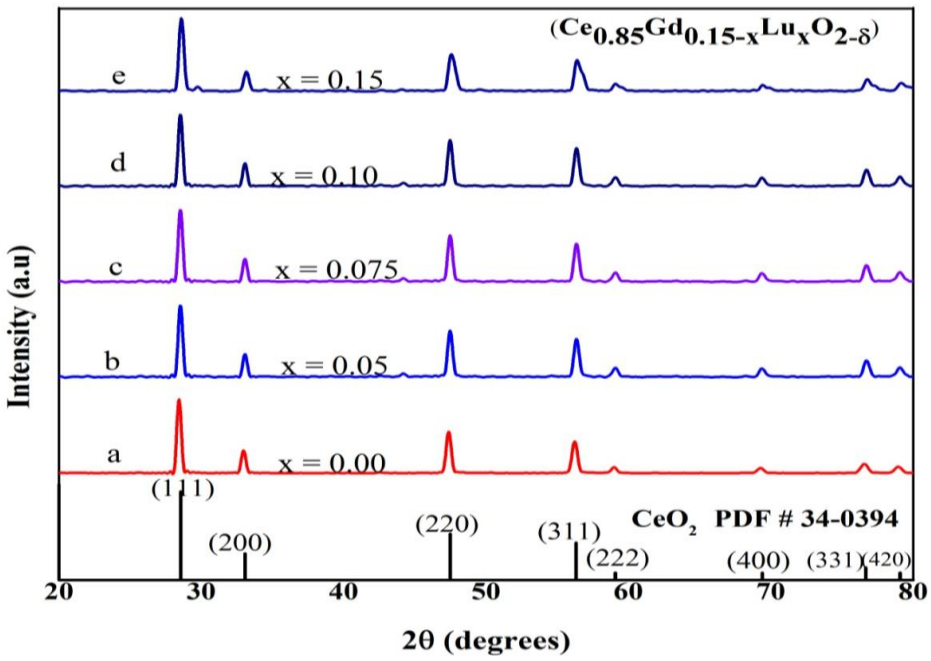

Figure 1.XRD patterns of $Ce_{0.85}Gd_{0.15-x}Lu_xO_{2-\delta}$ samples (x = 0, 0.05, 0.075, 0.10 and 0.15) calcined at 1200˚C for 4hours.

Table 1

The most intense peak crystallite size calculated by Scherrer formula and Elastic strain present in the lattice of doped ceria electrolytes.

Doping concentration	Sample ID	Crystallite size $D_{(111)}$ (nm)	Elastic strain (10^{-3})
x = 0.00	$Ce_{0.85}Gd_{0.15}O_{2-\delta}$	47	1.91
x = 0.05	$Ce_{0.85}Gd_{0.10}Lu_{0.05}O_{2-\delta}$	44	0.36
x = 0.075	$Ce_{0.85}Gd_{0.075}Lu_{0.075}O_{2-\delta}$	36	-1.21
x = 0.10	$Ce_{0.85}Gd_{0.05}Lu_{0.10}O_{2-\delta}$	31	-1.68
x = 0.15	$Ce_{0.85}Lu_{0.15}O_{2-\delta}$	37	-2.38

Annexure II

Under Review in Journal of Electroceramics

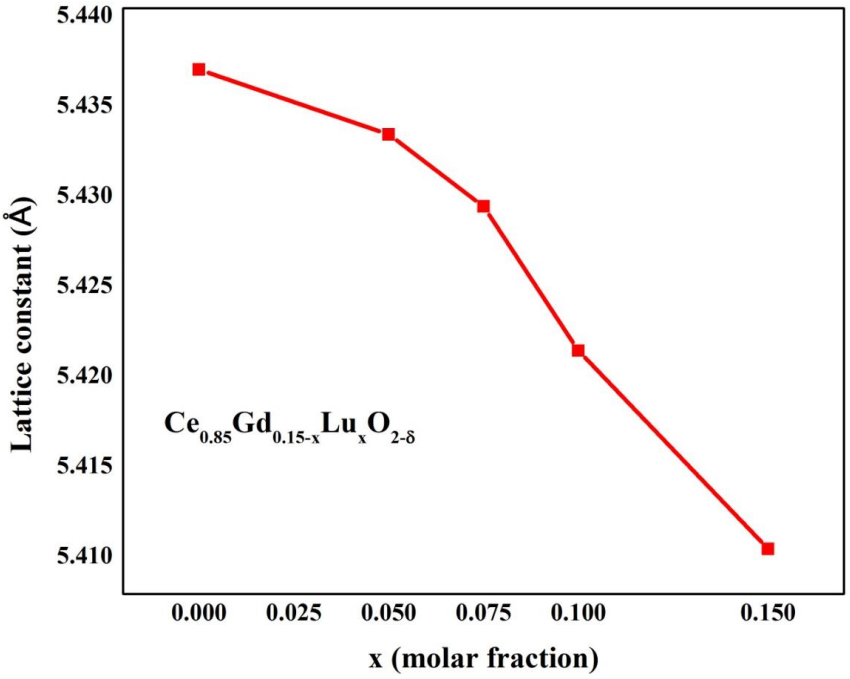

Figure 2. The dependence of lattice constant on the composition of as prepared doped ceria electrolytes.

It can be observed from Fig. 1 that the addition of Lu_2O_3 in GDC samples can cause a small shift in higher angles in ceria peaks which showed the change in lattice parameters. The 2θ values of doped ceria slightly shift towards right with x changes from 0 to 0.15. The relationship between dopant concentration and unit cell parameters is shown in Fig. 2. From Fig. 2 it can be seen that the cell parameter decreases with the increasing concentration of lutetium as x varies from 0 to 0.15.

As reported in literature, the critical ionic radius of ceria doping with trivalent metals is 0.1038 nm [15]. The ionic radius of Lu^{3+} (0.085 nm) is smaller whereas the ionic radius of Gd^{3+} (0.1053 nm) is larger than the critical ionic radius of ceria which is 0.1038 nm [23]. Therefore the cell parameter decreases with the increasing concentration of Lutetium as x varies from 0 to 0.15. From Fig. 2, it can be seen that the relationship is linear between lattice parameter and the concentration of lutetium, it means that lattice

parameter follows Vegard's rule [5], which further confirms that Gd and Lu are co-doped into crystal lattice of ceria.

The effect of dopant concentration on the elastic strain available in cubic fluorite crystal structure of doped ceria samples was calculated by using the following relation [20];

$$\text{Elastic strain} = (a_o - a) / a \quad \ldots\ldots\ldots\ldots\ldots(2)$$

where a_o is the lattice constant of $Ce_{0.85}Gd_{0.15-x}Lu_xO_{2-\delta}$ and a is the lattice constant of pure ceria CeO_2. Table 1 shows the different values of elastic strain present in doped ceria samples of $Ce_{0.85}Gd_{0.15-x}Lu_x O_{2-\delta}$ (x = 0.00, 0.05, 0.075, 0.10 and 0.15). Negative and positive elastic strain is seen as lutetium concentration varies from 0 to 0.15. There is a very small elastic strain present in $Ce_{0.85}Gd_{0.10}Lu_{0.05}O_{2-\delta}$ sample.

3.2 Microstructure / Morphology

Fig.3 shows the SEM micrographs of the as prepared $Ce_{0.85}Gd_{0.15-x}Lu_xO_{2-\delta}$ (x = 0.00, 0.05, 0.075, 0.10, 0.15) co-doped ceria samples calcined at 1200˚C for 4 hours. SEM images reveal that prepared composites consist of well separated particles without distinct agglomeration and have occasionally irregular shapes. The grain size was measured from higher magnification SEM images. The average grain size of each sample was found to be in the range of 30 to 60 nm which is in good agreement with the results of XRD. Samples a, b and c with low concentration of Lu^{3+} at x = 0, 0.05 and 0.075 respectively, have larger particle size as compared to samples d (x = 0.10) and e (x = 0.15) with higher concentration of Lu^{3+}. The addition of Lutetium in ceria impedes the crystallite growth of ceria as Lu^{3+} concentration increases from x = 0 to 0.15. This observation is well matched with literature data [11] and [21], and it also testifies with the results of XRD. It can also be clearly shown from SEM images d (x = 0.10) and e (x = 0.15) that the solubility decreases with the increasing concentration of Lutetium. According to Malgorzata et al. [20] lesser solubility of Lutetium in Ceria at higher concentration may be explained by the segregation of dopant ions at the surface of Ceria crystallites. All samples have dense particles with heterogeneous shapes and sizes. The

singly doped $Ce_{0.85}Gd_{0.15}O_{2-\delta}$ (a) and $Ce_{0.85}Lu_{0.15}O_{2-\delta}$ (e) materials have most heterogeneous as compared to co-doped ceria samples (b, c and d).

It is interesting to note that all the particles in the samples are heterogeneously distributed with irregular shapes and without large agglomeration, which further demonstrates that solid state route is the effective way to produced nano sized particles.

3.3 DC electrical properties

The dc electrical conductivity was measured as a function of temperature and compositions for as prepared $Ce_{0.85}Gd_{0.15-x}Lu_xO_{2-\delta}$ (x = 0.0, 0.05, 0.075, 0.10 and 0.15) samples. The changes in dc electrical conductivity were measured from the bulk resistance and sample dimensions with temperature. The relationship between the temperature and conductivity obeys the Arrhenius behavior of the form

$$\sigma_{dc} = \sigma_o \exp [- E_a / kT] \quad \ldots\ldots\ldots \quad 3$$

where σ_{dc} is the dc conductivity, k is the Boltzman constant, σ_o is the pre-exponential factor, E_a is the activation energy and T is the absolute temperature.

Fig.4 shows the typical Arrhenius plots of ln (σ_{dc}) versus 1000/T for $Ce_{0.85}Gd_{0.15-x}Lu_xO_{2-\delta}$ samples (x = 0.0, 0.05, 0.075, 0.10 and 0.15) sintered at 1400 °C for 4 hours. After measuring the resistance of pellets, the resistivity was calculated by using the formula,

$$\rho = RA / L \quad \ldots\ldots\ldots\ldots \quad (4)$$

where ρ is the resistivity, L is the thickness, A is the area of pellet and R is the resistance of pellet. The dc conductivity was calculated by using

$$\sigma_{dc} = 1 / \rho \quad \ldots\ldots\ldots\ldots\ldots \quad (5)$$

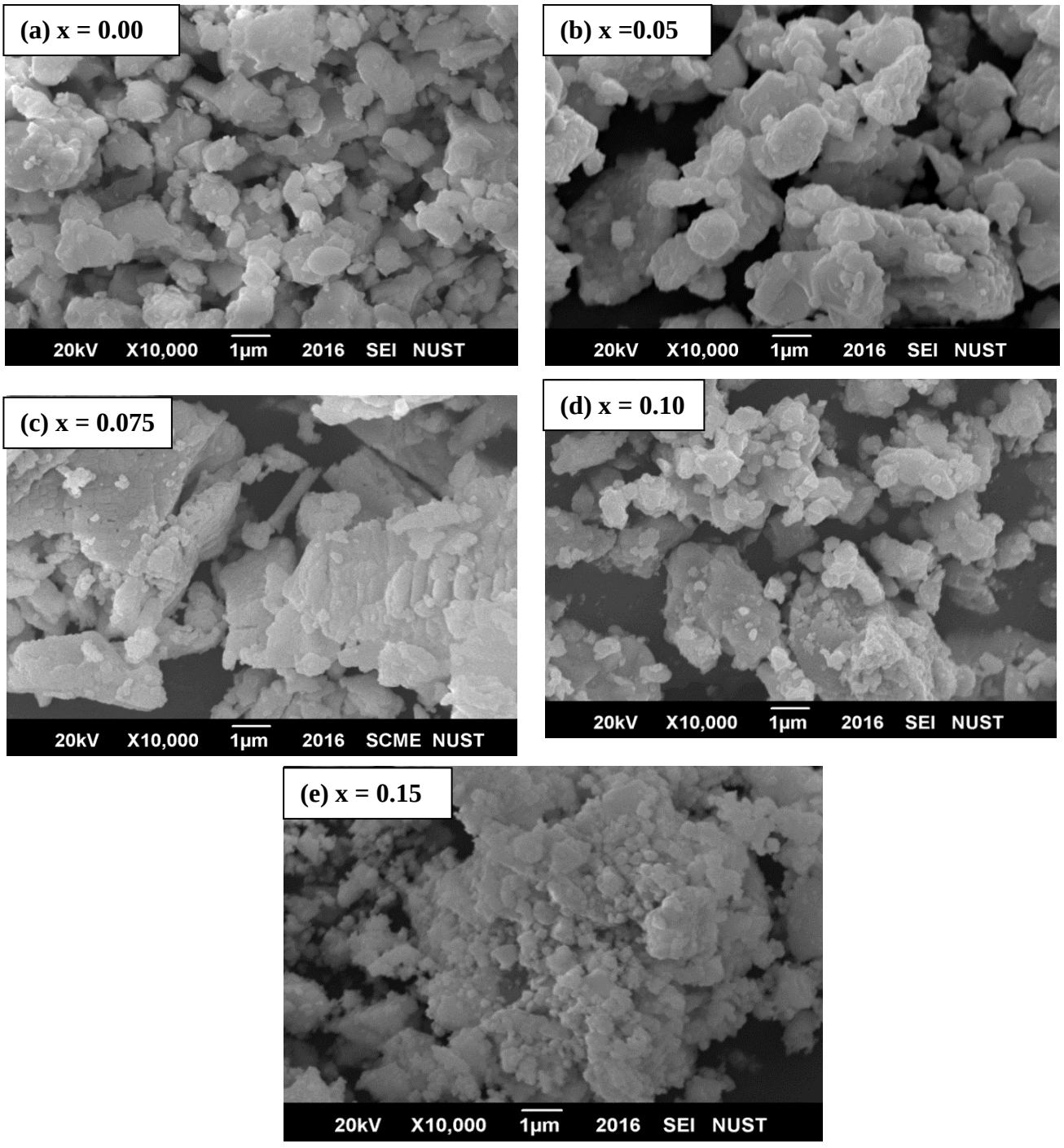

Figure 3.SEM Micrographs of $Ce_{0.85}Gd_{0.15-x}Lu_xO_{2-\delta:}$ (a) x = 0, (b) x = 0.05, (c) x = 0.075, (d) x = 0.10 and (e) x= 0.15 calcined at 1200˚C for 4h.

Annexure II

Under Review in Journal of Electroceramics

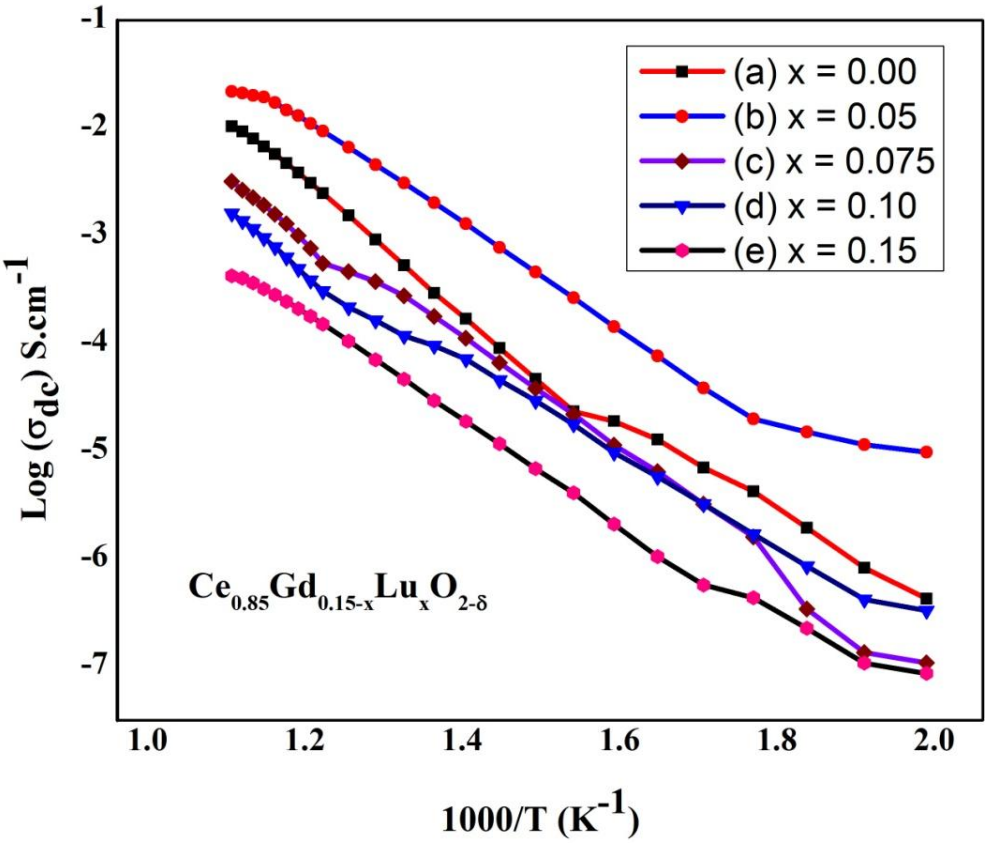

Figure 4. Arrhenius plots for dc electrical conductivities of $Ce_{0.85}Gd_{0.15-x}Lu_xO_{2-\delta}$ samples (x = 0, 0.05, 0.075, 0.10 and 0.15) sintered at 1400°C for 4 hours.

It is obvious form fig that dc conductivity increases with increasing temperature which is the normal characteristics of fluorite structured electrolytes. Initially, at low temperature range the dc conductivity value of all samples is very low and show little deviation from linearity, whereas, at high temperature range the dc conductivity value is high and show linear dependence, which implies that the dc conductivity is dependent on temperature and also follows Arrhenius behavior [22]. It can be seen that the sample $Ce_{0.85}Gd_{0.10}Lu_{0.05}O_{2-\delta}$ showed dc conductivity value of 0.0217 (S/cm) at 600°C, which is

slightly high than pure gadolinium doped ceria $Ce_{0.85}Gd_{0.15}O_{2-\delta}$ and very high than pure lutetium doped ceria $Ce_{0.85}Lu_{0.15}O_{2-\delta}$. The calculated values of dc conductivity as a function of temperature and compositions are given in Table 2.

For electrolyte materials it is important to analyze the value of ionic conductivity. Pure ceria has low ionic conductivity [5]. The oxide transference number (also called transport number) for pure ceria was found to be ~ 0.002 in the temperature range of 550-1200°C [23]. In pure ceria, the electronic conductivity is due to small polaron known as defects which is produced due to trapping of electron carrier in between atoms or ions hopping [24]. Gadolinium doped ceria (GDC) has the oxide transference number of 0.880 at 600°C which is very high as compared to pure ceria [25]. A co-doping strategy is used to increase the ionic conductivity and suppress the electronic conductivity of ceria. Various studies have been reported the value of oxide transference number in the range of 0.85 to 0.95 at 600°C for co-doped ceria [26] . So, if we consider the oxide transference number equal to 0.90 then the value of ionic conductivities for $Ce_{0.85}Gd_{0.15-x}Lu_xO_{2-\delta}$ samples (x = 0.00, 0.05, 0.075, 0.10 and 0.15) at 600°C are 9.2×10^{-3} (S/cm), 1.95×10^{-2} (S/cm), 2.86×10^{-3} (S/cm), 1.44×10^{-3} (S/cm) and 3.78×10^{-4} (S/cm) respectively.

The values of activation energies for the prepared samples were calculated from the slopes of the lines in Fig.4 and shown in Table 2. Activation energy is mainly due to defect association enthalpy (ΔH_a) and oxygen migration enthalpy (ΔH_m) [27]. (ΔH_m) is not depends on dopant concentration whereas (ΔH_a) is depends on elastic strain and dopant cation [15]. As there is very low elastic strain found in two samples $Ce_{0.85}Gd_{0.10}Lu_{0.05}O_{2-\delta}$ and $Ce_{0.85}Gd_{0.15}O_{2-\delta}$, so it may be reason for lower activation energy. The other samples have higher elastic strain and higher activation energy as compared to $Ce_{0.85}Gd_{1.0}Lu_{0.05}O_{2-\delta}$ and $Ce_{0.85}Gd_{0.15}O_{2-\delta}$ samples. These results are well matched with literature data [15] and [28]. From these results, it can be concluded that, the ionic conductivity is directly related to lattice distortion. Guan et al. [28] reported that, less distortion in pure ceria lattice causes decrease in activation energy and increased

Annexure II

Under Review in Journal of Electroceramics

Table 2

DC electrical conductivities and activation energies of $Ce_{0.85}Gd_{0.15-x}Lu_xO_{2-\delta}$ samples

Doping concentration	Sample ID	dc conductivity σ_{dc} ($S.cm^{-1}$) at 600 °C	Activation energy E_a (eV) (550 – 600°C)
x = 0	$Ce_{0.85}Gd_{0.15}O_{2-\delta}$	0.01033	0.89
x = 0.05	$Ce_{0.85}Gd_{0.10}Lu_{0.05}O_{2-\delta}$	0.02173	0.68
x = 0.075	$Ce_{0.85}Gd_{0.075}Lu_{0.075}O_{2-\delta}$	0.00318	1.12
x = 0.10	$Ce_{0.85}Gd_{0.05}Lu_{0.10}O_{2-\delta}$	0.00160	1.17
x = 0.15	$Ce_{0.85}Lu_{0.15}O_{2-\delta}$	0.00042	1.59

in electrical conductivity. Further, it demonstrates that, a co-dopant strategy can be used to increase electrical conductivity of ceria based electrolytes.

Conclusion

Gd^{3+} and Lu^{3+} co-doped ceria $Ce_{0.85}Gd_{0.15-x}Lu_xO_{2-\delta}$ samples (x = 0.00, 0.05, 0.075, 0.10 and 0.15) were synthesized by solid state reaction method. All the synthesized materials were found to be single phase with cubic fluorite structure. The reflection from (111) plane was used to measure the most intense peak crystallite sizes. The elastic strain present in the $Ce_{0.85}Gd_{0.10}Lu_{0.05}O_{2-\delta}$ sample is found to be negligible as compared to singly doped Gd^{3+} and Lu^{3+} samples. SEM images reveal that all the samples consist of well separated particles without large agglomeration. The electrical conductivity of co-doped ceria samples were found to be improved as compared to singly doped ceria. Among all, the sample co-doped with 5 mol% Lu^{3+} and 10 mol % Gd, showed the best conductivity performance. It suggests that the co-doping with Gd^{3+} and Lu^{3+} with a suitable ratio that is closed to critical ionic radius of ceria can further improve the conductivity performance.

Annexure II

Under Review in Journal of Electroceramics

References

[1] N. Mahato, A. Banerjee, A. Gupta, S. Omar, and K. Balani, "Progress in material selection for solid oxide fuel cell technology: A review," Prog. Mater. Sci., vol. 72, pp. 141–337, 2015.

[2] M. Rękas, "Electrolytes For Intermediate Temperature Solid Oxide Fuel Cells," Arch. Metall. Mater., vol. 60, no. 2, 2015.

[3] J. W. Fergus, "Electrolytes for solid oxide fuel cells," J. Power Sources, vol. 162, no. 1, pp. 30–40, 2006.

[4] S. P. S. Badwal and F. T. Ciacchi, "Oxygen-ion conducting electrolyte materials for solid oxide fuel cells," Ionics (Kiel)., vol. 6, no. 1–2, pp. 1–21, 2000.

[5] M. Mogensen, N. M. Sammes, and G. A. Tompsett, "Physical, chemical and electrochemical properties of pure and doped ceria," Solid State Ionics, vol. 129, no. 1, pp. 63–94, 2000.

[6] S. (Rob) Hui, J. Roller, S. Yick, X. Zhang, C. Decès-Petit, Y. Xie, R. Maric, and D. Ghosh, "A brief review of the ionic conductivity enhancement for selected oxide electrolytes," J. Power Sources, vol. 172, no. 2, pp. 493–502, 2007.

[7] R. O. Fuentes and R. T. Baker, "Structural, morphological and electrical properties of Gd0.1Ce0.9O1.95 prepared by a citrate complexation method," J. Power Sources, vol. 186, no. 2, pp. 268–277, 2009.

[8] G. Dönmez, V. Sarıboğa, T. Gürkaynak Altınçekiç, and M. A. F. Öksüzömer, "Polyol Synthesis and Investigation of $Ce_{1-x}RE_xO_{2-x/2}$ (RE = Sm, Gd, Nd, La, $0 \leq x \leq 0.25$) Electrolytes for IT-SOFCs," J. Am. Ceram. Soc., vol. 98, no. 2, pp. 501–509, 2015.

[9] M. R. Kosinski and R. T. Baker, "Preparation and property-performance relationships in samarium-doped ceria nanopowders for solid oxide fuel cell electrolytes," J. Power Sources, vol. 196, no. 5, pp. 2498–2512, 2011.

[10] M. Jamshidijam, R. V. Mangalaraja, A. Akbari-Fakhrabadi, S. Ananthakumar, and S. H. Chan, "Effect of rare earth dopants on structural characteristics of nanoceria

synthesized by combustion method," Powder Technol., vol. 253, pp. 304–310, 2014.

[11] M. A. Małecka, L. Kepiński, and M. Maczka, "Structure and phase composition of nanocrystalline Ce1-xLuxO2-y," J. Solid State Chem., vol. 181, no. 9, pp. 2306–2312, 2008.

[12] M. Stojmenović, S. Bošković, M. Žunić, B. Babić, B. Matović, D. Bajuk-Bogdanović, and S. Mentus, "Studies on structural, morphological and electrical properties of Ce1-xErxO2-?? (x = 0.05-0.20) as solid electrolyte for IT - SOFC," Mater. Chem. Phys., vol. 153, pp. 422–431, 2015.

[13] S. Dikmen, "Effect of co-doping with Sm3+, Bi3+, La3+, and Nd3+ on the electrochemical properties of hydrothermally prepared gadolinium-doped ceria ceramics," J. Alloys Compd., vol. 491, no. 1–2, pp. 106–112, 2010.

[14] S. Ramesh and K. C. J. Raju, "Preparation and characterization of Ce 1-x(Gd 0.5Pr 0.5) xO 2 electrolyte for IT-SOFCs," Int. J. Hydrogen Energy, vol. 37, no. 13, pp. 10311–10317, 2012.

[15] S. Omar, E. D. Wachsman, and J. C. Nino, "A co-doping approach towards enhanced ionic conductivity in fluorite-based electrolytes," Solid State Ionics, vol. 177, no. 35–36, pp. 3199–3203, 2006.

[16] X. Sha, Z. Lü, X. Huang, J. Miao, Z. Ding, X. Xin, and W. Su, "Study on La and Y co-doped ceria-based electrolyte materials," J. Alloys Compd., vol. 428, no. 1–2, pp. 59–64, 2007.

[17] N. Kim, B. H. Kim, and D. Lee, "Effect of co-dopant addition on properties of gadolinia-doped ceria electrolyte," J. Power Sources, vol. 90, no. 2, pp. 139–143, 2000.

[18] F.-Y. Wang, S. Chen, and S. Cheng, "Gd3+ and Sm3+ co-doped ceria based electrolytes for intermediate temperature solid oxide fuel cells," Electrochem. commun., vol. 6, no. 8, pp. 743–746, 2004.

[19] X. Guan, H. Zhou, Z. Liu, Y. Wang, and J. Zhang, "High performance Gd3+ and Y3+ co-doped ceria-based electrolytes for intermediate temperature solid oxide

fuel cells," Mater. Res. Bull., vol. 43, no. 4, pp. 1046–1054, 2008.

[20] Y. Tsur and C. a Randall, "Maximum Likelihood Estimation Method," vol. 66, no. 189376, pp. 2062–2066, 2000.

[21] M. A. Małecka, L. Kepiński, and W. Miśta, "Synthesis, structure and morphology of CeO2 and CeLnOx mixed oxides (Ln = Pr, Tb, Lu) prepared by microemulsion method," J. Alloys Compd., vol. 451, no. 1–2, pp. 567–570, 2008.

[22] A. Tschope and R. Birringer, "Grain Size Dependence of Electrical Conductivity in Polycrystalline Cerium Oxide," J. Electroceramics, vol. 7, pp. 169–177, 2001.

[23] M. Anwar, Z. S. Khan, K. Mustafa, and A. Rana, "Effects of some rare earth and carbonate-based co-dopants on structural and electrical properties of samarium doped ceria (SDC) electrolytes for solid oxide fuel cells," Int. J. Mod. Phys. B, vol. 29, no. 24, p. 1550179, 2015.

[24] L. Zhang, L. Zhu, and A. V Virkar, "Electronic conductivity measurement of yttria-stabilized zirconia solid electrolytes by a transient technique," J. Power Sources, vol. 302, pp. 98–106, 2016.

[25] C. Milliken, "Properties and Performance of Cationâ€ • Doped Ceria Electrolyte Materials in Solid Oxide Fuel Cell Applications," J. Am. Ceram.Soc., vol. 86, no. 189049, pp. 2479–2486, 2005.

[26] M. Dudek, "Some Structural Aspects of Ionic Conductivity in Co-Doped Ceria-Based Electrolytes," Arch. Metall. Mater., vol. 58, no. 4, pp. 1355–1359, 2013.

[27] X. W. Wang, J. G. Chen, Y. W. Tian, X. E. Wang, B. H. Zhang, and X. H. Chang, "Lattice strain dependent on ionic conductivity of Ce0.8+xY0.2−2xSrxO1.9 (x=0–0.08) electrolyte," Solid State Ionics, vol. 296, pp. 85–89, 2016.

[28] X. Guan, H. Zhou, Y. Wang, and J. Zhang, "Preparation and properties of Gd3+ and Y3+ co-doped ceria-based electrolytes for intermediate temperature solid oxide fuel cells," J. Alloys Compd., vol. 464, no. 1–2, pp. 310–316, 2008.